THE UNIVERSITY OF QUEENSLAND

AUSTRALIA

Predicting long term coal seam gas concentrations from

Multi-component sorption

By

Hla Shwe

Master of Science

A thesis submitted for the degree of Master of Philosophy at

The University of Queensland in 2018

School of Chemical Engineering

ABSTRACT

During a last decade also, the coal seam gas (CSG) industry in Australia, particular in Queensland has grown rapidly due to large export-oriented LNG projects. Consequently, many CSG fields were developed to meet the necessary gas demand for these LNG plants as well as to supply domestic need. A key requirement in gas supply from the CSG reservoirs, important for conditioning the feed and operating conditions of the LNG plants is the correct forecasting of the gas quality variation with time. In particular, CO2 concentration in the produced gas is likely to trend upwards in the long term. The impact of this dictates the LNG plant gas pre-conditioning and may also raise environmental concerns. Because of these investment sensitive and environmentally crucial reasons, it is important to predict how this is likely to play out.

The main objective of this study is to find a method to enable prediction of gas concentration profile as it evolves with time. Most of the previous methods in the literature roughly predict future gas concentrations, but the models are subject to considerable uncertainties, and are not underpinned by solid experimental data on multi-component gas sorption in real coals. This study seeks to utilized both experimental (single and binary components) data and available field observed data to provide further insight into this issue.

Adsorption is the main storage mechanism whereas desorption, diffusion and Darcy flow are key production and transport processes in coals investigated in this study using experimental methods and numerical simulation.

For diffusion and desorption, coals from different areas were utilized and the single component isotherms for CH_4 and CO_2 were measured. These isotherms were used with existing theory, namely Ideal Adsorption Solution and correlations to validate measured binary component Isotherms. Using the methodology and workflow, the attempt was made to predict binary component isotherms with different feed ratios of adsorbed initial CH_4:CO_2. The resultant binary isotherms with different CH_4:CO_2 ratios were used in the numerical model as input to model to predict of long term CH_4:CO_2 production profiles.

As part of coal characterisation, coal physical properties serve as input to the mathematical modelling. experimental coal physical properties and sorption

characteristics are used to generate the coal Diffusivity coefficient. The intention is to compare the results from the numerical model using Diffusivity coefficient against the alternative input, namely the desorption time constant (measured as desorption days in a canister test). Two types of coals used in this study originated from Surat Basin. Unsurprisingly, the results of the using Diffusivity coefficient provide much more accurate results.

In the simulation study, the results from numerical model matched reasonable well with actual production data and the forecast gas concentration production trends for long term are taken to be reasonably accurate.

There are some limitations in the method used to obtain the binary component Isotherm machine (using a BG Belsorp), which can be improved in future study similar to this work.

The current study can be extended to multicomponent version with more accurate experimental measurements. However, the outcome from the present study provides a useful reservoir monitoring tool to understand the long term binary gas production trends (CH_4:CO_2) and the relation with coal physical properties as well as coal seam gas transport mechanism due to pressure and saturation changes during production life span.

Declaration by author

This thesis *is composed of my original work, and contains* no material previously published or written by another person except where due reference has been made in the text. I have clearly stated the contribution by others to jointly-authored works, if any, that I have included in my thesis.

I have clearly stated the contribution of others to my thesis as a whole, including data interpretation, statistical analysis, significant technical procedures, professional editorial advice, and any other original research work presented or utilized in my thesis. The content of my thesis is the result of work I have carried out since the commencement of my research higher degree candidature and does not include a substantial part of work that has been submitted *to qualify for the award of any* other degree or diploma in any university or other tertiary institution. I have clearly stated which parts of my thesis, if any, have been submitted to qualify for another award.

I acknowledge that an electronic copy of my thesis must be lodged with the University Library and, subject to the policy and procedures of The University of Queensland, the thesis be made available for research and study in accordance with the Copyright Act 1968 unless a period of embargo has been approved by the Dean of the Graduate School.

I acknowledge that copyright of all materials contained in my thesis resides with the copyright holder(s) of that material. Where appropriate I have obtained copyright permission from the copyright holder to reproduce material in this thesis.

Publications during candidature

"No publications".

Publications included in this thesis

"No publications included".

Contributions by others to the thesis

"Dr Pradeep Shukla has contributed in MATALB codes writing for the program."

Statement of parts of the thesis submitted to qualify for the award of another degree

"None".

Research Involving Human or Animal Subjects

"None".

Acknowledgements

First of all, I would like to express my sincere gratitude to my principal advisor, Professor Victor Rudolph, for his invaluable advice and extreme patience during my graduate study. I would like to thank Dr Paul Massarotto, my associate supervisor, for his encouragement and helpful discussions. Most importantly, I would like to thank Dr Pradeep Shukla for his practical insights and tireless passion which coerces me going even when I was down. Never forget his generous help and everlasting friendship. I wish to thank my parents, U Nu Daw Than Kyi and my beloved wife, Cho-Mar Lay Shwe, for their everlasting love and support; especially, for my wife endless support, encouragement love and partnership. Last but not the least, I am sincerely grateful to some laboratory staff from UQ Chemical Engineering Laboratory. Finally, I would like to acknowledge the support from Australia Government Research Higher Degree Education department, without which this work would not have been possible.

Financial support

"'No financial support was provided to fund this research".

Keywords

Adsorption, Isotherm, Equilibria, Unipore, Bidisperse pore, Simulation, History Matching, Coal seam gas

Australian and New Zealand Standard Research Classifications (ANZSRC)

ANZSRC code: 090404, Membrane and Separation Technology, 50%

ANZSRC code: 090409, Chemical Engineering not elsewhere classified, 50%

Fields of Research (FoR) Classification

FoR code: 0904, Chemical Engineering, 100%

Contents

Table of Tables

Table of Figures

Nomenclature

CSG = Coal seam gas

ASAP =

CMG= Computer modelling group

IAS = Ideal Adsorption Solution Theory

RAST = Real Adsorption Solution Theory

P = Pressure in equilibrium

b = constant in the model isotherms

c = constant in the Sips model

t = constant in the Toth model

θ = fractional saturation

Q_t = amount of total gas per mass of coal (as received)

Q_l = lost gas volume;

Q_d = desorbed portion gas;

Qr = residual gas; gas amount

R_{omax} = vitrinite reflectance

V_d = dead volume

V_s = sample cell volume

P_i = initial pressure at the sample cell

P_e = equilibrium pressure at the sample cell

P_{ix}, P_{iy} = initial pressure for components x, y

P_{ex}, P_{ey} = equilibrium pressure for components, x, y

SEM = Scanning Electron Microscope

V_L = Langmuir volume constant

P_L = Langmuir pressure constant

D_{eff} = the effective diffusivity in the coal particle

C_{init} = initial gas concentration in the centre of the matrix

C_{bulk} = bulk gas concentration in the centre of the matrix

P_{init} = the initial cell pressure at time zero

M = the mass of the sample in the cell

R = the gas constant

T = temperature in the cell

Z = the gas compressibility factor

V_e = the dead volume of the cell;

Chapter 1. INTRODUCTION

1.1 Background

A clear understanding of the storage capacity of a coal seam gas field and its associated transport properties is necessary to predict long term output and the concentration profile of the produced gas. This provides the basis for a field development plan and associated downstream plant design. Most of the gas, typically more than 95%, is stored as adsorbed gas in coal matrix and is produced through a complicated dynamic fluid mechanism which consists of desorption, diffusion and finally Darcy flow [1–3].

The fluid release mechanisms such as desorption and diffusion are governed not only by coal characteristics but also local environmental changes, notably pressure and saturation which change continuously during production making the prediction of long term gas concentration profile in the product gas difficult to predict with a reasonable degree of accuracy.

There are many previous works available in prediction of gas production profile using different methods, equations and simulation models [4–6]. However, most of the models and theories have limitations in prediction of mixed gas production profile, especially from real coal seams.

The main objective of this research is to come up with the most reliable method to predict long term gas concentration production profiles by applying existing methodologies, theories and equations, for application in the industry.

The first part of this study is primarily based on experimental measurements of single and binary components adsorption isotherms that are fitted to theoretically derived isotherms using the most suitable equations, methods and models. Thjs is then extended to allow the future gas concentration profiles from coal seams to be predicted accurately and reliably.

The unipore and bi-dispersed models including consideration of coal heterogeneity in micropore, mesopore and macropore ranges) are tested with experimental data from coal samples from different locations to investigate nature of adsorption as well as diffusive and desorption fluid transport processes).

Finally, applying the insights and knowledge gained from this and previous research works, as a final goal of this study, CH4, CO2 and total gas product.

ction trends are predicted for a case study for long term. Observed data (CH4, CO2 percentages from pre-selected wells) from Surat Basin coal seam gas fields are compared to the model prediction trend [7,8].

1.1.1 Scope and Research Questions

The scope of this study covers an initial investigation on relevant work from previous researchers, summarising their findings and highlighting controversial or discrepant results or methods. An important focus is how this work can be employed in such a way that the outcome will benefit to the industry and community.

The key goal of this work is to enable prediction of gas concentration profiles from coal seam reservoirs over long term production. Since experimental methods to determine multicomponent isotherms are extremely tedious, the main issue to be addressed is to establish a best practice approach and establish whether prediction of multicomponent gas-coal adsorption may be done with sufficient accuracy using single component adsorption equilibrium isotherms.

Once a reliable method to determine multicomponent isotherm is established based on comparison with experimental data, a numerical approach using existing theory could provide a suitable means to obtain isotherms for different gas composition ratios. These could then be plugged into readily available simulation software to predict long term gas concentration profiles [9,10]

Experimental adsorption equilibrium data of the two systems (gas and coal) were compared with results calculated from the model and three other correlations to obtain matched parameters. Then the model derived parameters were used in combination with: the ideal adsorbed solution (IAS) theory to determine adsorbed quantity of pure adsorbates and mixture. The results indicated that the IAS theory with Langmuir correlation used for single component adsorption isotherms (methane) predicted the results better

1.2 Research Objectives

There are two main objectives of this research:

Firstly, to obtain experimental results for isotherms on preselected coal powdered samples for both pure CH_4 and CO_2 gases and binary mixtures of these. The types of coals selected for this study possess different chemical and physical properties so that the findings can be generalised and extended to a wider regional application.

Secondly, appropriate equations, methods and theories are used to generate adsorption isotherms that are then matched with the experimental data, to provide a mathematical representation of the adsorption results. Once acceptable isotherms derived from a theory or an empirical correlation [3,11–13] for both pure and binary gas systems are obtained, and parametrised the adsorbed gas mole profiles with corresponding pressure are used in a simulator to predict a long term gas concentration profile.

1.2.1 Contributions from this study

Contributions from this study directly will be beneficial not only to the CSG industry also to the environment and community directly related to the industry [14].

These extend to social and environmental benefits including prior or predicted information regarding quantities of gases including CH_4, CO_2, H_2S, and water, will be produced. This enables proper planning cleaning methods and handling facilities can be put in place and implemented to manage the products, protect the environment and properly inform concerned stakeholders. As an example, properly treated water may be distributed to resident farmers for agricultural works and plantations usage which would benefit them regarding water supply and security.

It is imperative that CSG operators follow proper procedures and regulations to comply with environmental requirements and government rules and regulations. At the same time, proper planning with informed decision can only be made if the accurate information is available. An objective of this study is to assist the prediction of how CH_4, CO_2 gas quantities and qualities would be produced and the variation with time of the concentrations of these constituents. This kind of information will assist the industry to plan ahead for downstream processing and to avoid potential contamination to the environment and community [15].

1.3 Thesis Outlines

The thesis contains five chapters with all References and Appendices attached at the end of thesis.

Chapter 1 is the “Introduction” of Thesis and mainly consists of general information related to current research project. The main objectives and potential benefits of this research project are provided, along with a brief description of previous work in this area, its issues and limitations.

Chapter 2 covers theories related to fluid transport mechanism in coal seam reservoirs, explained using theory widely accepted in the industry. Also, it summarizes popular theories and equations directly related to the current research project, including a summary of theories pertaining to particle models (unipore, bidisperse diffusion models). A brief discussion is included on gas transport mechanisms and the controlling factors.

Chapter 3 mainly consists of experimental works including detailed description of experimental setup, procedures and sample preparation. Subsequently, detail methodology is provided in acquiring adsorption Isotherms and calculation of adsorbed quantity of individual components using 2^{nd} virial coefficients. Interpretation and application of laboratory data uses existing models, theories and equations to determine binary sorption and equilibria. Equipment limitations and laboratory data accuracy are discussed in this chapter including methods applied to mitigate problems mainly associated with the limitations of the BG Belsorp adsorption apparatus to obtain binary component isotherms at higher pressure.

Chapter 4 presents the adsorption kinetic transport mechanism in coals which is mainly composed of two parts; namely unipore and bi-disperse model. Mass transfer and mass balance occurring in pores and grains are presented to account for the diffusion process between coals and surrounding bulk gases. The model generated data were tested against laboratory measured data (ASAP adsorption and kinetic data), and diffusivity coefficients for different models were determined.

Chapter 5 combines all the data from experiments and models, and integrates them into commercial simulator to enable prediction of the evolving gas concentration profiles. The simulator used was from the Computer Modelling Group.

To validate the model prediction of gas concentrations, available collected well data which included CO_2, CH_4 mole percent from selected wells were used for comparison. Attempts were made to compare the traditional way of predicting gas concentration profile with. the use of an appropriate binary adsorption isotherm with correct ratios and adsorbed amount for the corresponding pressure. Also, the point is made that the use of desorption time is not adequate to predict the future gas production profile.

Chapter 2. INVESTIGATING GAS TRANSPORT MECHANISMS AND CONTROLLED PARAMETERS, AVAILABLE MODELS AND THEIR APPLICATION

This chapter commences with the conceptual theory on fluid transport in coals and elaborates on how adsorption capacity and transport processes in coals are governed by coal physical and petrophysical properties. Also it continues with discussion on some relevant theories and equations related to desorption and diffusion processes and their applications to determine multi-component adsorption equilibrium. Multicomponent Isotherms were determined using measured single component adsorption Isotherms as input in combination with IAS theory. The unipore and bi-dispersed diffusion models from previous research works are related with experimental data from different pore sizes were also presented.

2.0 THEORIES RELATED TO SORPTION AND DIFFUSION, FLUID TRANSPORT IN COALS

2.1 Conceptual Models showing gas movement in coal seams

The nature of coal seam gas transport mechanism is illustrated in a conceptual model shown in

Figure 2-1. In general, coal seam gas desorbs in micropores and diffuses into macropores and mesopores. Mesopores and macropores provide spaces for the released gases subsequently flow to cleats and eventually stream into the wellbore [16–19].

The whole gas movement from adsorbate in the form of adsorbed phase (methane) to free gas can be defined as three-step desorption, diffusional and viscous flow processes. Gas flow in the cleats obeys Darcy's law. These transport mechanisms are elaborated below:

(i) Desorption: If the temperature increases or pressure declines, rebalancing the equilibrium causes the gas molecules to escape from the surface of the coal matrix, thereby being released as free gas. This phenomenon is known as "desorption" [1] and the reverse of this process is adsorption.

(ii) Diffusion flow: Molecules move as a result of concentration gradient, with three types of mechanisms included under the general heading of diffusion, namely molecular,

Knudsen and surface diffusions. These three diffusion types are linked with particle pore sizes. The flow through the matrix is usually modelled using Fick's Law [1].

(iii) Darcy flow: This part of gas transport is mainly pressure-driven flow. The desorbed gases flow by (mostly) diffusion from micropores, enter the mesopores and macropores and then into the cleat system where Darcy flow predominates, eventually find their way into wellbore before flowing up to the surface. Typically, the flow is laminar in the cleats because the size of the flow channels is rather small (typically micron scale). However, in some cases turbulent flow in larger fractures.

The transport mechanism may be influenced by many other factors which include coal properties (physical and petrographic) to constantly changing operational environment and reservoir conditions (from near wellbore to surface, wellhead, separator and pipeline; the surface network system).

Most gases stored in coal seams exist in an adsorbed state rather than free gas [2].The amount of adsorbed gas on the coal is governed by the adsorption isotherm, if the system is in equilibrium [2, 3]. The pressure drops in the cleat system triggers gas to desorb from the micropore surfaces and to diffuse into the macropores. However, if the coal seam is under-saturated a substantial initial pressure reduction must be achieved before large amount of gas production can occur [20–22].

This is done by extracting water from the coal seam and may take several months before gas is released from the coal matrix. On the other hand, it is possible to see wells that produce gas from day one because is significant pressure drop is achieved and caused by dewatering and production from the near well region. In this case, the fluid movement consists of two-phases flowing simultaneously rather than (more commonly) initial single-phase water flow.

In nature, coals are very heterogeneous due to physical and chemical properties that result from the nature of the original plant materials and the coalification processes which may vary from area to area. Because of this variability it is difficult to establish general rules regarding the behaviour of coal and how it interacts with fluids.

Taking into account all the changing conditions (pressure, temperature changes and coal properties due to diagenesis) during coal forming process, gas transports from coal seams to well bore can be described in a three-step conceptual model as follows:

Figure 2-1.

1. Desorption followed by diffusion into the micropores, whereafter the evolved gases flow into the macropores, microfractures and cleats [4].
2. Dual mechanism of desorption-diffusion and flow through the microfractures and macro-cleats [4].
3. Flow through fractures. If the cleats are much greater than 0.20 microns, then the pressure driven flow will be dominated. The cleat system is the primary avenue for gas and water flow during gas production [5]. This stage of gas movement would involve Darcy's flow in conjunction with the diffusion process which feeds gas to it.

eventually flowing into the wellbore before going up through pipeline and to the separator on the surface [23–27]

4. open cleats as a laminar flow, the gas would flow into the wellbore before going up through pipeline and to the separator on the surface [23–27]

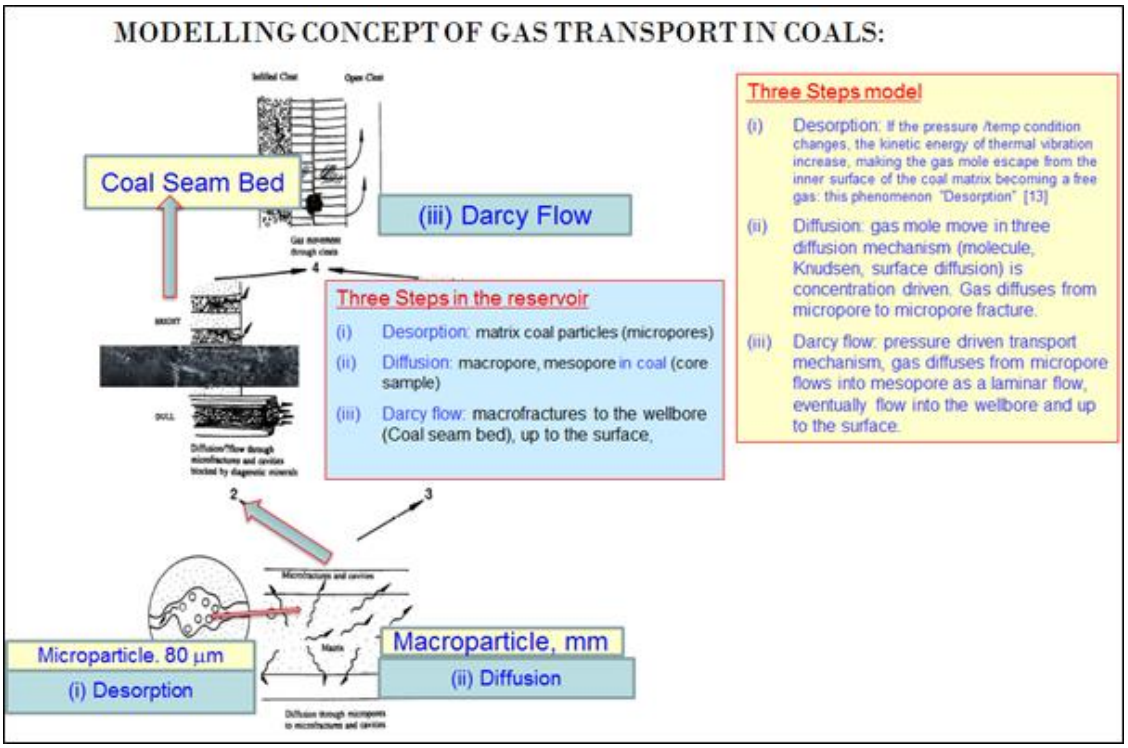

Figure 2-1. The gas transport conceptual model showing diffusion and desorption process from micropore, macropore to cleats [4]

With growing interest in coal seam gas and trying to understand the production mechanism from coals, there is a huge industry demand to obtain more accurate and reliable description of transport modes in coals. Many new research works related to this field have been carried out recently [28–31].

As a methodology workflow, unipore and bi-pore models were employed to match against the experimental data. The model were utilized in conjunction with some readily available theories and correlations. [3,32,33]. However, it is a challenge to find which pore types is suitable for the existing models during implementing the workflow

Due to the fact that coal has a complex heterogeneous structure and vast variation of chemical or petrophysical properties, it is extremely difficult to achieve a complete general solution using a single model, theory or correlation.

As a result, many model variants claim that they are suitable for coals, although they are tested for only particular locations and conditions, and may not necessarily be adequate if the conditions are different [10,11,25,35]. The solution becomes localized, not applicable to every coal.

It is an intention here to establish some models and associated theories suitable for for Australia coals from specific locations, so as to predict future gas concentration profiles for those particular gas fields and locations.

One of the important parameters controlling gas transport in coals, is the accumulated amount of coal seam gas in a particular coal seam, the storage capacity and stored gas in place. It is critical to understand how these numbers (particularly gas in place (GIP) in coal seams) are obtained and their limitations and uncertainties. Normally, calculation of GIP is provided as a volumetric expression eg cubic ft of gas per ton of rock). If ash free gas content is used in the calculation an appropriate correction is needed.

Hence, some fundamentals of coal storage process and the methods and procedures used to measure gas content from coal seams are presented so that the importance of getting accurate gas content measurement in the first place can be recognized.

2.1.1 Gas Content measurements

It is a well-known fact and widely accepted that gas storage mechanism in coals is totally different from conventional gas reservoir and also coal seams are not only reservoir rocks but also source rocks. Yee et al [23] described the gas in coal as existing primarily in a "condensed, near liquid-like state because of physical sorption". Because of this unique nature of the gas storage mechanism in coal, the conventional method to determine the volume of gas in place cannot be applied. Thus gas content determination methods have been developed to measure the volume of gas sorbed on coal seams.

The most commonly used gas content determination methods generally were subdivided the total initial gas content into three parts: lost, desorbed and residual gas. Each of these parts is measured or determined by different procedures and then combined to yield the total gas content of the sample [8].

Corresponding these portions of gas contents measured at different stages from initial core retrieving stage to a final stage where the last piece of the coal sample is crushed to determine residual gas content in the very coal sample.

The middle stage where desorbed gas amount is measured using a temperature controlled canister will be the most time consuming. The product from this stage can tell a lot about how the gases in a coal diffuse, desorb in relation to pressure changes, indirectly saturation change. Details of the definition of three collected gases at different stages can be found in [8].

The brief description of total gas content, Q_t is provided as below.

After three parts of gas contents are obtained, the amount of total gas contents, Q_t in a particular coal sample can be summed up [8]. The total amount here is defined as received, no ash content, no moisture correction is applied.

$$Q_t = Q_l + Q_d + Q_r \qquad (2-1)$$

Where

Q_t = amount of total gas per mass of coal (as received)

Q_l = lost gas volume; based on several early direct measurements of desorbed gas after the sample is sealed into the canister

Q_d = desorbed portion gas; total gas is measured periodically; daily emissions 0.05 cc/g used as a cut off limit to stop measurement

Qr = residual gas; gas amount measured by crushing desorption sample as possible to a powder ~ 200 mesh to release the remaining in-situ gas

All of the measurements in the above equation are from a coal sample as received and gas volumes are measured at Standard Temperature and Pressure from compositional analysis of the gas collected during the course of desorption test, the compositions of individual gases (CH_4, CO_2, and N_2) may be obtained.

The USBM method with measurement technique is used to determine the component parts of the total gas content. Two alternate approaches were proposed to estimate time zero and cumulative lost gas time; (t_{lg}).[35–37]
If the core was acquired using water or drilling mud, desorption is assumed to begin when the sample was halfway to the surface. The cumulative lost gas time (t_{lg}) would be [8].

$$t_{lg} = (t_4 - t_3) + \frac{(t_3 - t_2)}{2} \qquad (2-2)$$

Where:
t_2 = time core interval began
t_3 = time core reached surface
t_4 = time core sealed in desorption canister
and $\frac{t_3 - t_2}{2}$

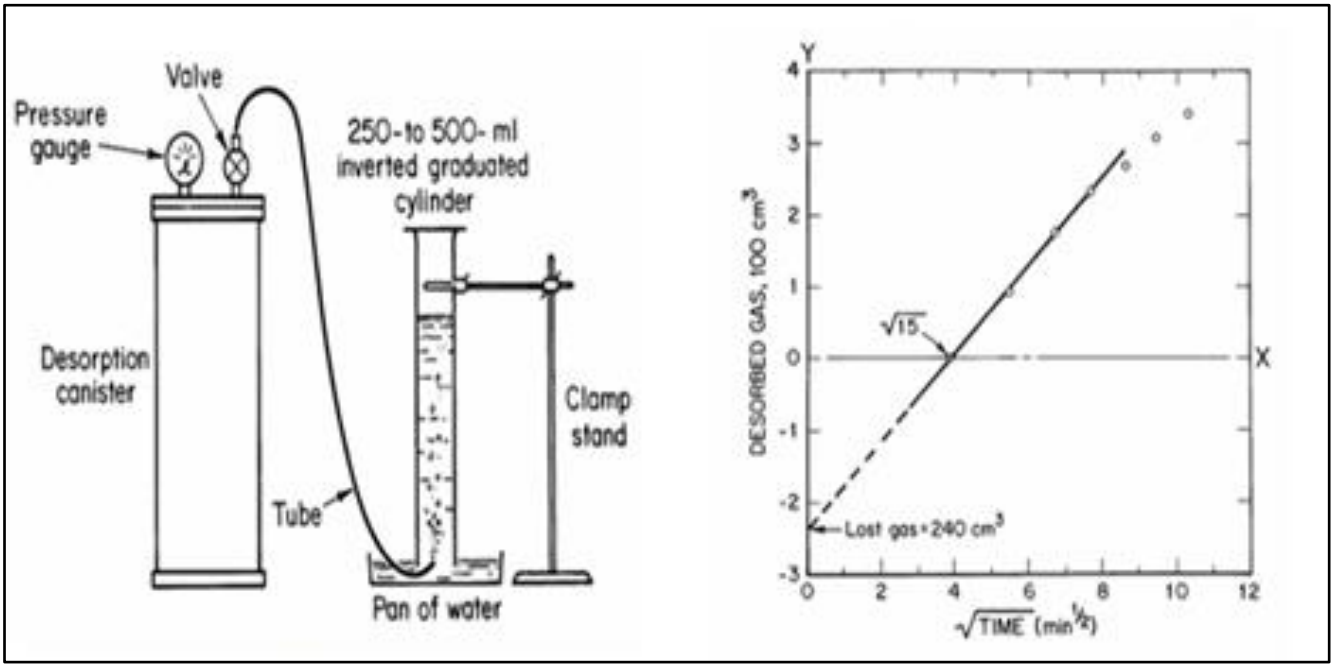

Figure 2-2. USBM Direct method gas content estimate from collected coal sample (Left) and the calculation of loss gas (extrapolated from measured gas content estimate from data points measured in canister test) (Right) [8]

If the hole was cored by air or mist, pressure release and gas desorption were assumed to begin at the first penetration of the coalbed by the core barrel. In this case, cumulative lost gas time (t_{lg}) would be

$$t_{lg} = t_4 - t_1 \qquad (2-3)$$

t_1 = time coal bed first penetrated (t_1 *is* $t = 0$)

Figure 2-2 USBM direct method was proposed to estimate the lost gas volume (Q_l) based on several early direct measurements of desorbed gas after the sample was sealed into the canister. As soon as the sample is sealed into desorption canister, several early measurements of desorbed gas readings are recorded every 15 to 20 minutes for the first several hours.

The initial linear portion of desorption curve is extrapolated through the point on the x-axis representing the lost-gas time (e.g. $\sqrt{15}$ Minute in

Figure 2-2 to estimate the lost gas volume). By extrapolating these early readings, the lost gas volume (in this example; 240 cm^3lost gas volume) is determined as illustrated in

Figure 2-2 USBM direct method [5].

2.1.2 Gas Desorption measurement and some related issues

In this section, some gas content measurements from several coal samples will be presented with discussions on the relations between coal seams locations (Basins), depths of coal seams and gas content variations.

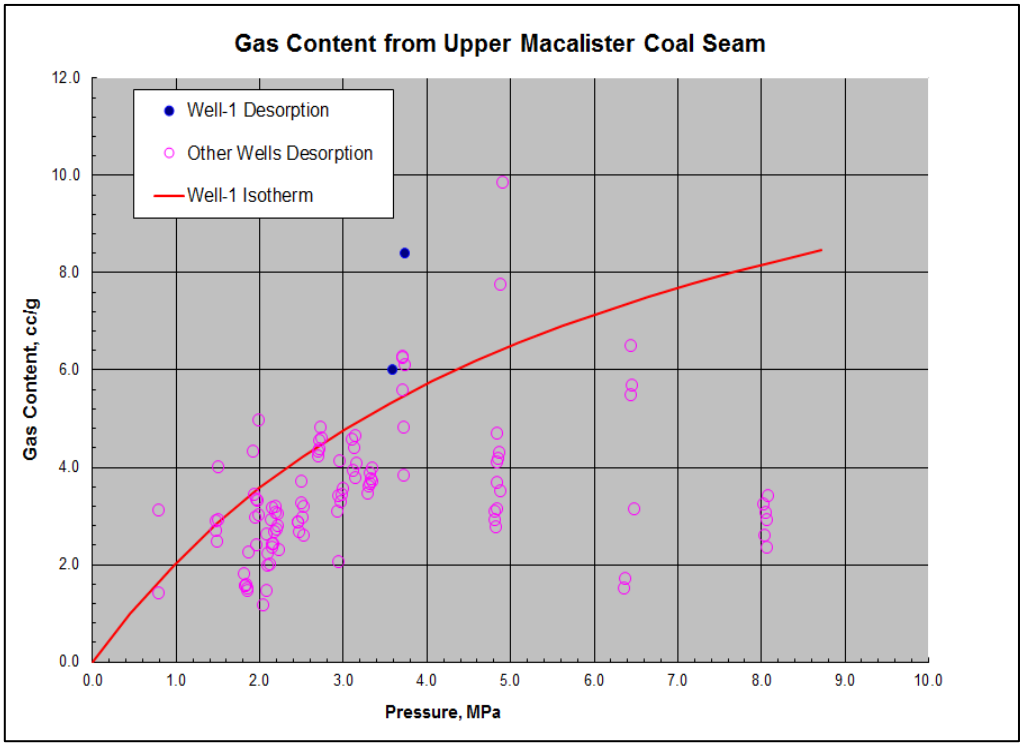

Figure 2-3 Gas content measurements from coals from well A1, other wells in different fields and Isotherms generated from A1 data [9]

Coal samples from different depths from Surat Basin were acquired during the coring procedures, then some portions of selected coals (normally 1meter length) from particular depths were preserved in canisters where gas contents were measured (initially hourly and later less frequently) under reservoir conditions.

An example of the outcome is presented in

Figure 2-3. For the Well-1, the gas content is approximately ~ 6 – 8.4 cc/g of coal at ~ 3.5 MPa (blue dots on the plot). The sum of all gas in place (GIP) in different coal seams represents field gas in place. The accuracy of GIP heavily relies on the gas content measurement of coals from many coal seams from many wells. The data for equilibrium adsorption pressure of methane are usually defined using the following Langmuir equation;

For the isotherm, a representative coal sample was collected and sealed in a canister to measure the gas content constant, V_L and Langmuir Adsorption Pressure constant, P_L.

Prior to detail discussion on gas content variation with depth, location etc. it is worthwhile to consider the Langmuir Isotherm curve and Langmuir volumes, $V_{L;}$ and the Langmuir Adsorption Pressure constant, P_L

Langmuir isotherm (Langmuir, 1918)

$$V = \frac{V_L P}{P_L + P} \qquad (2-4)$$

Where V_L is the Langmuir volume, and P_L is the Equilibrium adsorption pressure

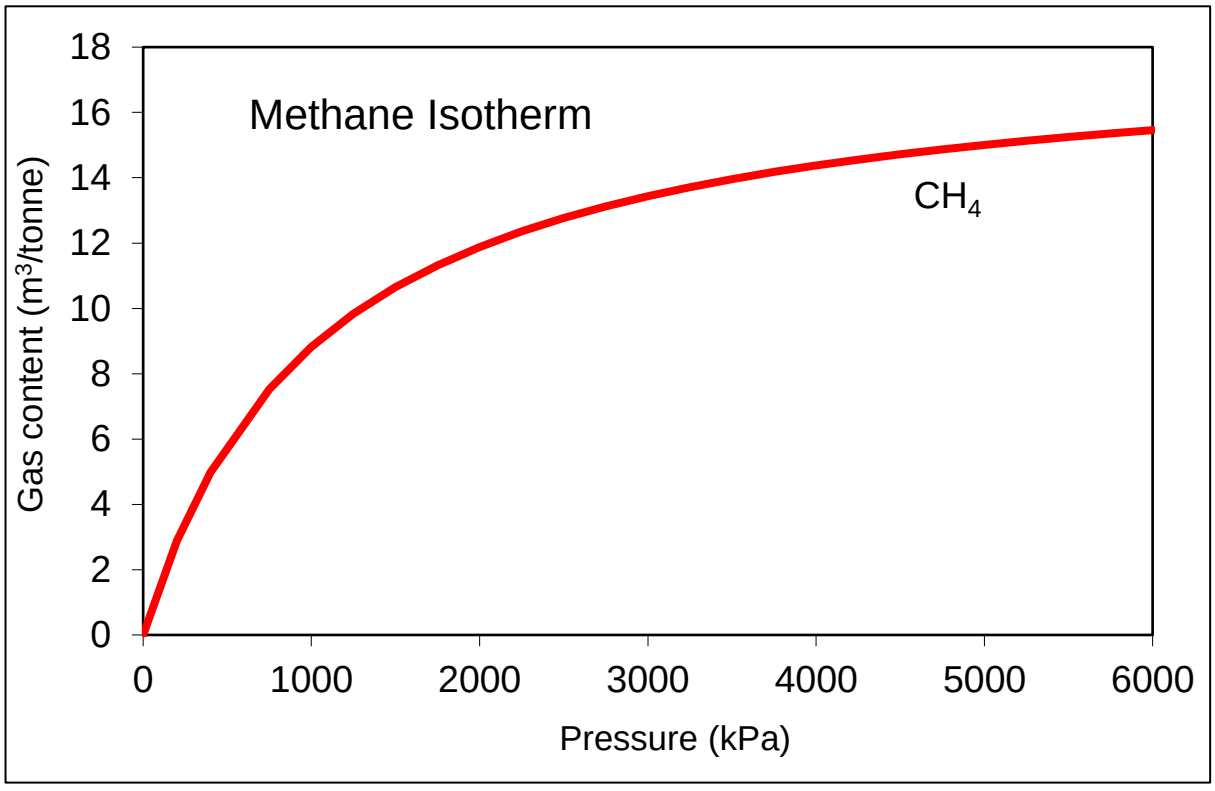

Figure 2-4 Methane Isotherm showing Gas Content relationship with pressure

Figure 2-3 depicts that there is a subtle relationship between increasing reservoir pressure and gas content. The gas content in 5-6 MPa (shallower coal seam measures, Iona, Argyle) is relatively less than the one at 8-9 MPa (deeper coal seam measures, Taroon) in Surat basin coals, although in many cases there is severe under-saturation.[38]

In Figure 2-5, gas contents from various fields in Surat Basin plotted vs depth including BWS (Berwyndale South) gas content varies from 6 - 8.4cc/g. This plot clearly shows the gas content increases with depth in all of the fields. However, some fields (for example, Andrew field has ~ 3 – 6.5 cc/g) shows scattered data with large gas content variations whereas other fields show relatively narrow range of gas content variation (for example Berwyndale and Mamdal fields). The scattered data basically show the coal properties variation laterally in coal seams in the same area. The data is considered to be reliable and the scatter may be interpreted as arising from gas migration or microbiological recharge.

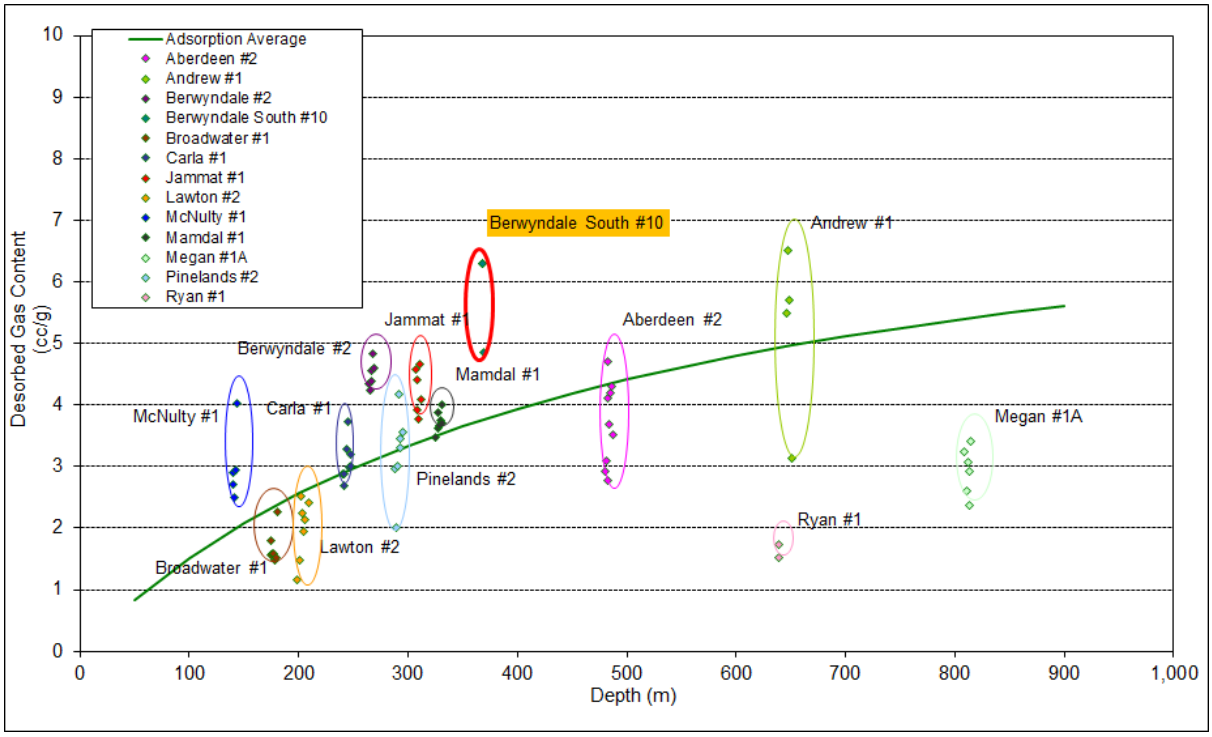

Figure 2-5 Gas contents increasing with depth in different fields in Surat Basin [9]

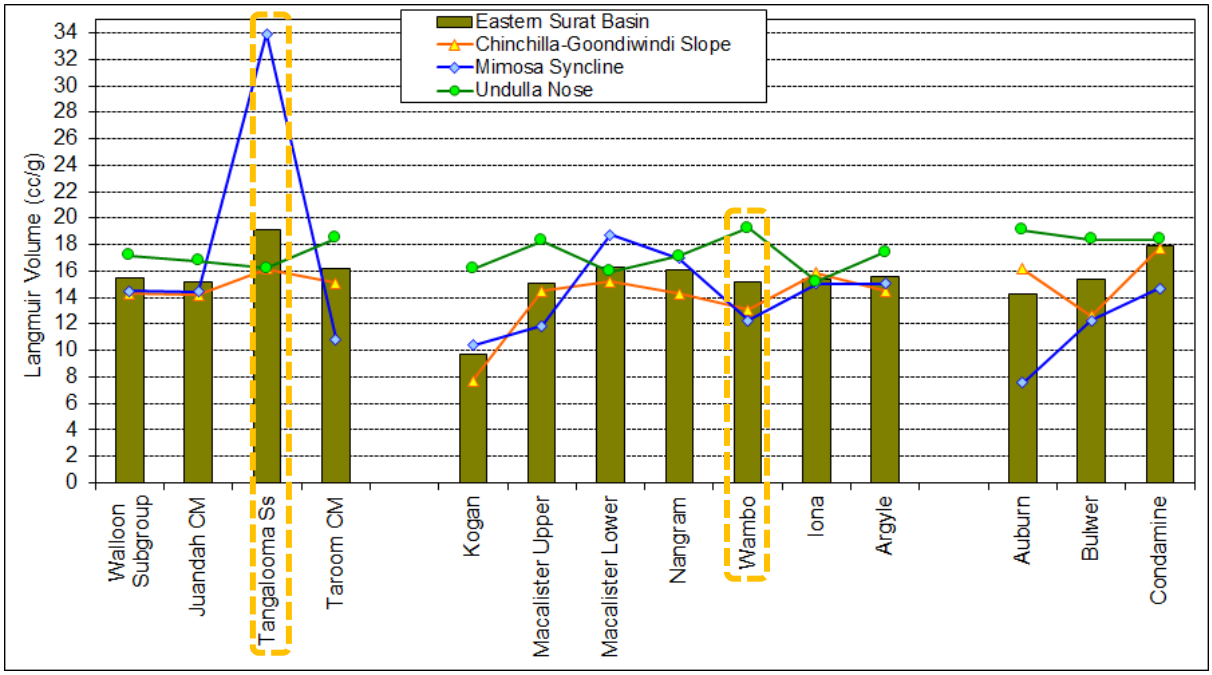

Figure 2-6 Langmuir Volume (V_L) from different coal seams at different Basin locations [9]

The previous section discusses the gas content vs. depth; it is worth also considering the variation of Langmuir volume, V_L in different Basins.

The plot in the Figure 2-6 illustrates the Langmuir volumes, V_L measured from coal samples collected from different coal seams from different basins. It showed that the V_L values from coal seams from different coal seam measures had significantly different V_L values. The most significant one could be observed in Tanglooma Sandstone where V_L in the Mimosa basin had extremely high V_L 34 cc/g whereas Undulla Nose and Chinchilla Goondiwindi had V_L ~16 cc/g. Another example is Wambo coal seam where Undulla Nose had V_L ~19 cc/g whereas Mimosa and Chinchilla Wambo coals have similar V_L ~ 12-13 cc/g.

Across these two locations, V_L variations in different coals are noticeable, it is expected the gas production and deliverability will be as significant accordingly [9].

The differences between as analysed (a.a) vs. dried ash free (d.a.f) Langmuir Volume, V_L from different coal seam measures in the Surat Basin ONLY are plotted and presented in Figure 2-7. Langmuir volumes, V_L for as analysed (a.a) for all coal seams in Surat Basin are less than 10 cc/g except Tangalooma Sandstone. It is worth noting that gas content (d.a.f) from all of the coal seams are much greater (to the extent of 30-40%) than as analysed (as received) V_L values, reflecting relatively high ash and water contents in situ.

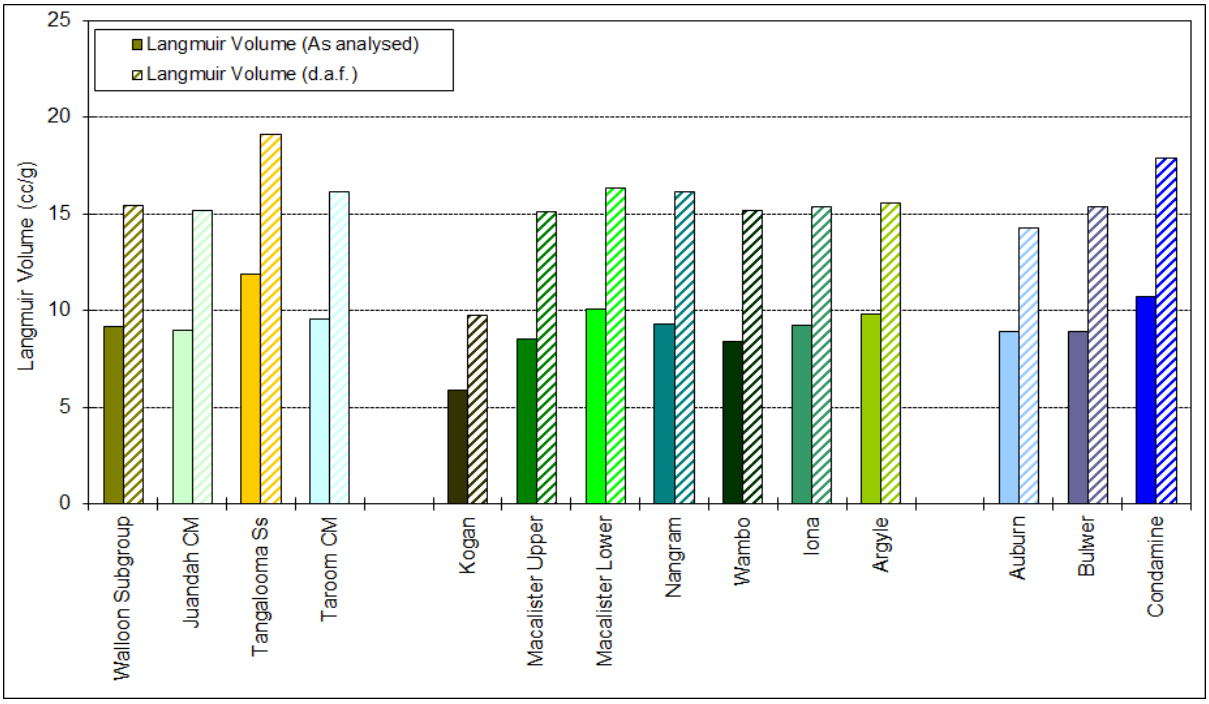

Figure 2-7 Comparison of Langmuir Volume (V_L) (a.a) and (daf) at different depth and Surat Basin [9]

In summary, gas content can according to depth and also by location within the same fields. For Langmuir V_L values, there is a significant difference between the different basins and different coal seam measures.

2.2 Coal physical and chemical properties controlling fluid transport in coals

Coal is a unique material with complicated structure as well as very complex chemical and petrographic compositions.

There were many research works conducted to understand the relationship between adsorption capacity and gas storage capacity and coal petrographic properties; vitrinite, inertinite, liptinite and rank of coals [4,24–27].

Bright vitrinite rich coals usually have the slowest desorption rates whereas some dull, inertinite coals may rapidly desorb. Similarly, mineral rich coals may be associated with rapid desorption [4]. Arguably, vitrinite rich coals have greater methane adsorption capacity than inertinite rich rank-equivalent coals [4].

Here the relationship between coal types and coal petrography is discussed. Some studies of gas adsorption from Surat basin coals indicate that bright coals have significantly higher methane adsorption than their dull coal equivalents from the same seams.

The evidence is that bright coals with high vitrinite content may have high gas content and provide a longer well deliverability, based on research conducted on many coal samples from Surat Basin by Scott et al. [10, 11].

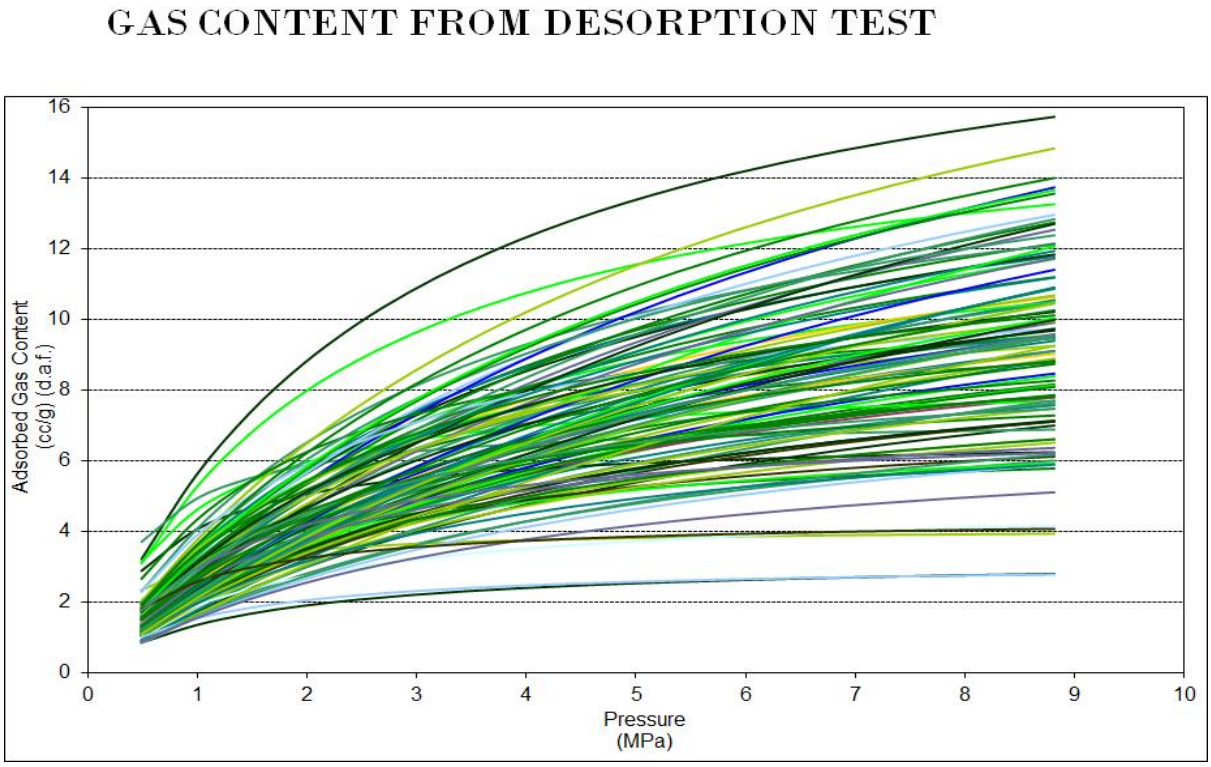

Figure 2-8 A suite of individual methane adsorption isotherms for the Walloon Subgroup (increase in gas content relationship with increasing pressure) [10]

These data presented here are from Lauren#66 coal sample, the same coal sample from which powdered coal samples were prepared and utilized for Adsorption experimental works and the data from the coal samples were used as input data for numerical modelling and simulation works.

Table 2-1 Coal Properties (vitrinite, proximate and ultimate analysis, porosity, pore size) and coal rank relationship

LAUREN#66 COAL CHARACTERISATION

Petrographic Analysis

Sample	UQ#1	UQ#4	UQ#8
Vitrinite reflectance			
Romax, % (avg)	0.48	0.53	0.51
Romax, % (range)	0.41-0.57	0.44-0.59	0.41-0.58

Correlate UQ Coal with coal in Liaohe and Xinjiang with R_{omax} (0.43%) Low rank coal with adsorption time (3 days)

Chemical Analysis

Sample #	UQ#1	UQ#4	UQ#8
Proximate analysis (a.d.)			
Moisture, %	3.2	4.1	1.7
Ash yield, %	51.5	18	63.5
Volatile matter, %	26.6	37.2	22.7
Fixed carbon, %	18.7	40.7	12.1
Total sulphur, %	0.3	0.63	0.17
Carbonate carbon, %	<0.01	0.01	0.01
Ultimate analysis (daf)			
Carbon %	71.1	78.9	67.1
Hydrogen %	7.85	6.27	8.92
Nitrogen %	1.05	1.35	1.29
Sulfur %	0.66	0.81	0.49
Oxygen %	19.3	12.7	22.2

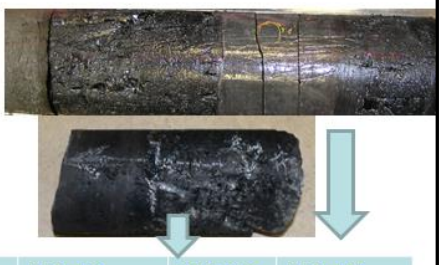

Coal	UQ#1	UQ#4	UQ#8
Total Porosity	4.2	10.2	13.6
MPD*, μm	162	1476	14.1
Pore size	**Intermediate**	**Large mean**	**smallest**
Kaolinite Quartz	High Peak	No Peak	High Peak

* Mean Pore Diameter (Hg injection)

The dull and bright coal samples from Lauren#66 well from the Lauren field were tested for petrographical analysis and basic rock properties to understand the relationship between coal sorption capacities and its physical and chemical properties. The results from three replicate samples are presented in Table 2-1.

From the petrographic analysis, coal samples (UQ#1, #4 and #8 have R_{omax} (vitrinite reflectance) 0.48, 0.53 and 0.51 % respectively. Therefore, vitrinite reflectance values from all coal samples are taken to be not significantly different.

Ultimate tests (dry ash free) for the Lauren#66 [12] coal samples (UQ#1, 4 and 8) show that coal rank could be subbituminous to bituminous coals from the carbon % determined from the test. Ash contents % from Proximate Analysis seem are unexpected, the values are high and based on other comparative information considered unreliable (51.5 % UQ#1 and 63.5 % UQ#8 in particular) Table 2-1.

Mean Pore diameter (MPD) values for three coal samples are significantly different. For UQ#8, MPD value of 14.1 μm; smallest pore size (20-50 nm range) with highest total porosity of 13.6% among three. Total porosity in coal is defined the sum of fracture and matrix porosity. It is apparent that micropores make up a big contribution to porosity and hence gas storage capacity. UQ#4 has the largest pore size and highest MPD at1476 μm. Interestingly, UQ#8 does not have kaolinite type clay whereas UQ#1 and UQ#8 have high kaolinite content and low MPD (162, 14.1 μm). Perhaps high kaolinite fills more pores and causes porosity reduction.

Among three coal samples selected to conduct a series of tests (Petrographic analysis, Proximate and Ultimate analysis and porosity, pore size distribution and SEM for clay morphology), two samples (UQ#4 and UQ#8) show a clear coal rank or type (dark, bright and dull coals) evidenced from visual inspection and description of coal samples.

From the data obtained from aforementioned tests, UQ#4 coal is fitted into a category as bright, vitrinite rich coal (R_{omax} values 0.44 to 0.59). In addition, UQ#4 contains low ash content, high fixed carbon (18% and 40.7%). The coal also has a better MPD to accumulate more gases in comparison with UQ#8 and UQ#1 (Table 2-1 Coal Properties (vitrinite, proximate and ultimate analysis, porosity, pore size) and coal rank relationship)

The comparison of core photos from UQ#4 and UQ#8 samples is presented in Figure 2-9. The nature of cleats in bright and dull coals is observed in Figure 2-9. The nature of cleats in coals reflects the permeability of the coals. The desorption rate or deliverability of fluid transport can be inferred.

According to the research papers conducted in two areas in Canada, it is clearly evident from their works that the difference in absolute coal permeability which is likely the cause of higher in-situ stress in the deeper coals has had an effect on both gas and water production rates from these particular coals[42–44]. From our experimental data, UQ#4 coal sample has 7.4 mD absolute permeability whereas UQ#8 sample has only 3.9 mD absolute permeability [12]. The coal characters from these two coals show a good relationship between permeability differences between two types of coals.

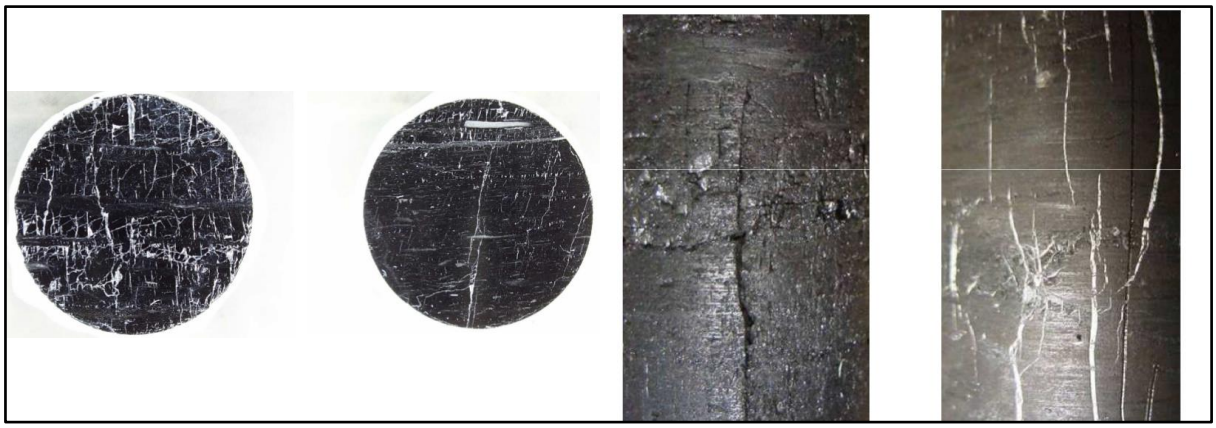

Figure 2-9 UQ#4 (bright densely cleated) and UQ#8 dull (poorly cleated) (on the right) and UQ#4 (clean open cleats) and UQ#8 (mineral infilled cleats) [12]

2.3 Model and Theories related to Multicomponent Adsorption equilibria

It is important to know multicomponent adsorption equilibrium as base information for predicting gas concentration profiles delivered from coal seam gas wells.

In a practical way, multicomponent adsorption equilibrium of mixed gases isotherms is predicted from the single solute (pure gas) isotherm. It is difficult to obtain multicomponent adsorption equilibrium experimentally because it is a tedious and time-consuming process. Using the approach that includes single component isotherms with suitable models to predict binary component adsorption isotherms presents a much easier and workable alternative.

Many models have been used to fit the experimentally determined pure gas isotherms (CH_4 and CO_2). These include the Langmuir, Dubinin-Radushkevich (D-R), Dubinin-Astakhov (D-A), Toth, and Sips models [13].

In this research work, three models (Langmuir, Toth and Sips) were considered suitable to predict pure gas isotherms by matching experimental data (pure gas CO_2 and CH_4 isotherms).

These models were used in combination with Ideal Adsorption Solution (IAS) Theory in this study. However, there were many options to select a suitable model (for example, Real Adsorption Solution Theory (RAST); the Extended Langmuir model, Multicomponent potential adsorption theory and others).

The pros and cons of using these models to predict multicomponent adsorption equilibrium can be found in previous research works [13]. Detail discussion will not be presented in this work except some relevant discussion on models as tey relate to this study.

Extended Langmuir is a popular choice of many researchers to model adsorption for binary mixtures (CH_4-CO_2, CH_4-N_2) whereas Langmuir model is extensively used for its simplicity and provides close fit to experimental data [7,40-41]. The Langmuir model is one of the models selected to use with the combination of matched parameters from single isotherm to predict binary adsorption data (chosen in this study as an alternate model option).

The most widely used thermodynamic model namely Ideal Adsorption Solution Theory (IAS) [47] is considered as an adequate model here to predict adsorption isotherms of binary components (CH_4:CO_2) with different ratios or feed compositions (varying from 98:2 to 80:20) [47,48].

In general, most of the methods using single component isotherms are considered to provide a less accurate determination of composition of mixed adsorbates (adsorbed phase) due to the non-ideal nature of some binary mixtures. The IAS theory can be extended to Real Adsorption Solution theory by adding an activity coefficient to deal with the adsorbed phase deviating from the ideal behaviour [8].

Recently, there is an efficient method for the simulation of packed bed adsorbers with implicit adsorption isotherms. It is shown that real and positive eigenvalues of the Jacobian of the underlying conservation equations will lead to a differential index of one. It is further shown that these eigenvalues of the Jacobian related to the IAS theory can be guaranteed for binary mixtures or for multicomponent mixtures. The new method is compared with alternative solution approaches using the modified FastIAS method by Do and Myers and semi-analytical solutions from equilibrium theory [49] It will be a good research project similar to this study and worth to investigate the outcome of this method used for coals.

2.3.1 Common Issues related to Binary adsorption equilibria determination from this study

The main obstacle facing an attempt to determine binary adsorption equilibria is not being able to measure the composition of adsorbed mixture directly and accurately. Although there are various methods to determine the composition of adsorbed mixture, using experimentally available single component isotherms with an assumption of ideal solution for the adsorbed mixture, they are still many questions on the practical applicability of the available theories.

The assumption of IAS theory, i.e. there is thermodynamic equilibrium between the adsorbate and adsorbent is not correct all the time.

IAS model was found to be adequate for predicting binary gas adsorption on dry coal which is similar to the coal used for the experiment. However, the IAS theory predictions are strongly dependent upon the choice of the single gas isotherm equations [7] whereas some models (IAS or RAST) still have limitations to predict the composition of adsorbed phase.

IAS theory has its assumption of ideal nature of mixed gas which is not always true and the outcome from using this model is somewhat erroneous, in some coals with high degree of heterogeneity.

In our study, it is not required to make any correction, since ideal solution assumption is shown to match the binary adsorption equilibrium data reasonably with the combination of single gas isotherms from the experiment.

Here in this study, IAS theory was applied with the combination of some selected isotherm models (Toth, Sips and Langmuir) to determine binary adsorption equilibrium. The matched results from this study seems to be reasonable, especially from Toth model, as demonstrated later.

2.3.2 The Approach to predict multicomponent adsorption equilibrium

Since a goal of this study is to enable prediction of gas concentration (CH_4 and CO_2) profiles over time a numerical simulator was used using experimental binary adsorption Isotherms as a key input. The GEM model suite from Computer Modelling Group was selected as a suitable simulator.

The experimental works produce single component Isotherms for the pure gas CH_4 and CO_2 and mixed gas isotherms for mixtures of these

Then a number of models were used to match these isotherms and tested to see which fitted the experimental data best [40,49,50].

The models used for matching experimental data and later applied in the simulations are presented here.

Langmuir isotherm (Langmuir, 1918)

$$\theta = \frac{bP}{1 + bP} \qquad (2-1)$$

Sips isotherm (Sips, 1950)

$$\theta = \frac{(bP)^c}{1 + (bP)^c} \qquad (2-2)$$

Toth isotherm (Toth, 1971)

$$\theta = \frac{bP}{(1 + (\mathrm{bP})^{\mathrm{t}})^{\frac{1}{\mathrm{t}}}} \qquad (2-3)$$

Where P = Pressure in equilibrium

b = constant in the model isotherms

c = constant in the Sips model

t = constant in the Toth model

θ = fractional saturation

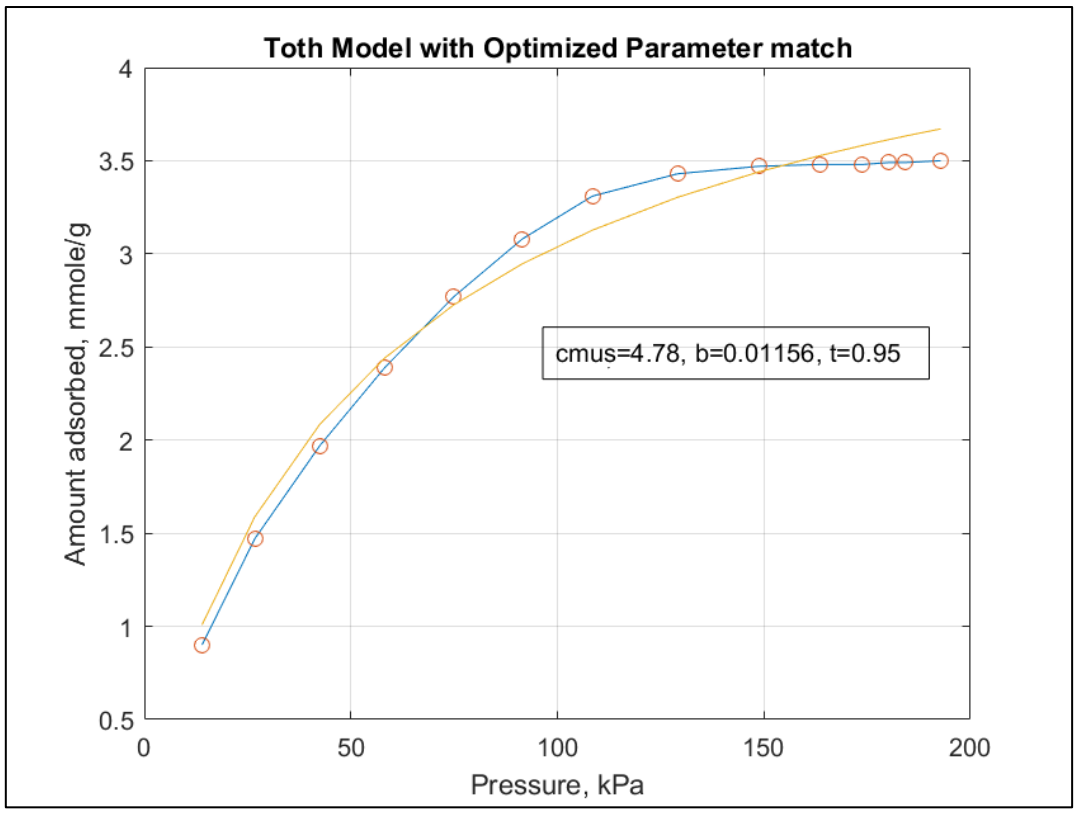

Figure 2-10 Selected model (Toth) with matched parameters against measured CH4 Isotherm using Newton Raphson Iteration method

The plots in Figures 2-10 to 2-12 the yellow line represents the model data trend and blue line with round symbols show the experimental data.

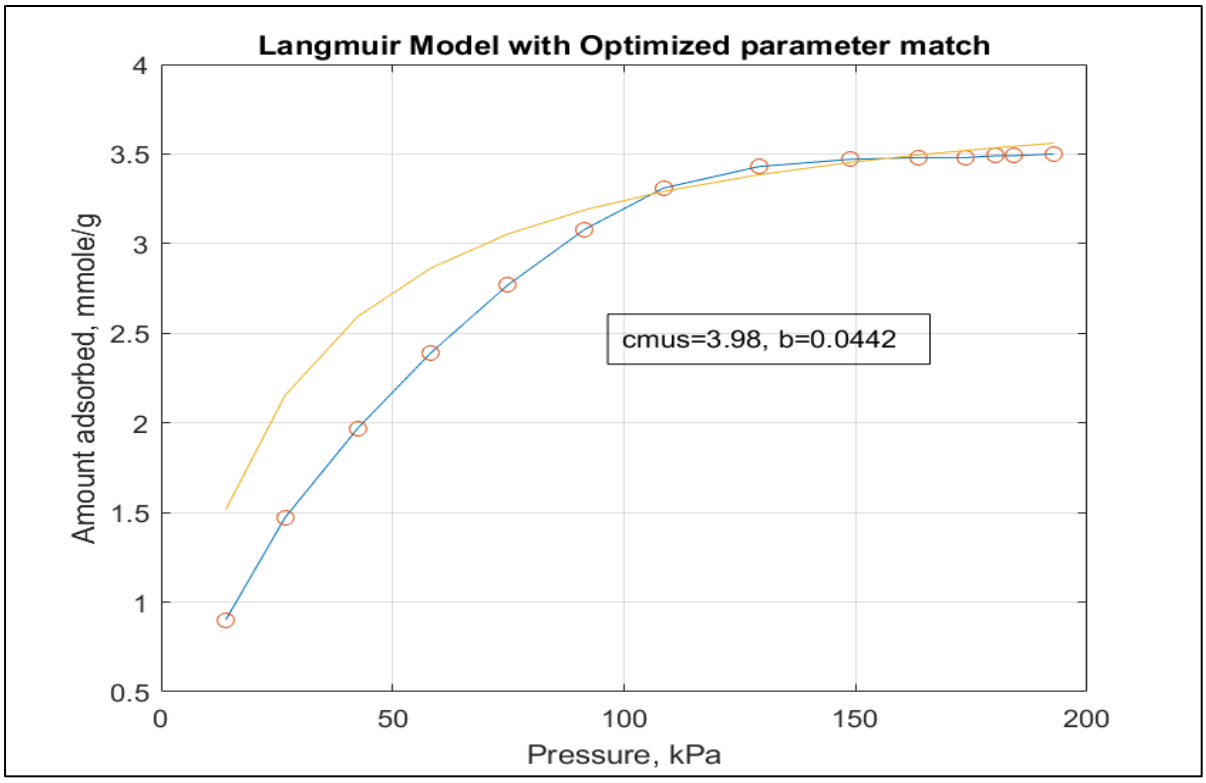

Figure 2-11 Langmuir model with optimized parameters for measured CH4 Isotherm

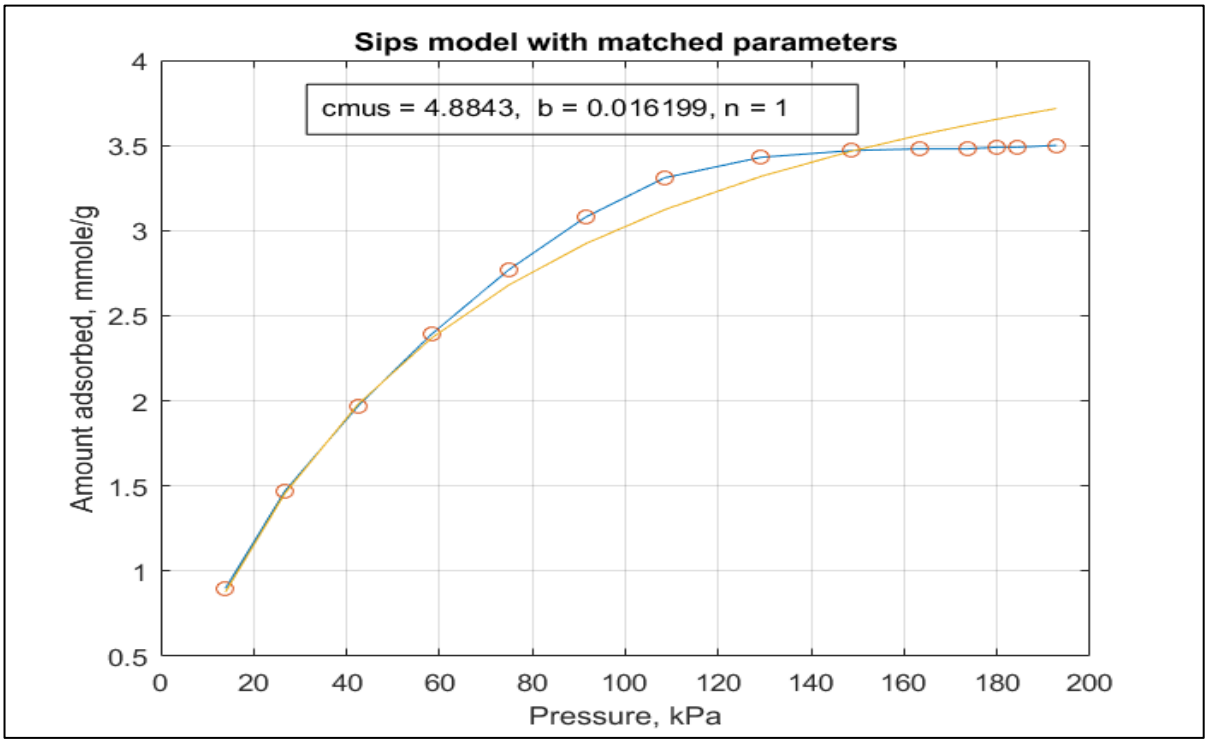

Figure 2-12 Sips model with optimized parameters for measured CO_2 Isotherm

From the pure component isotherms for example, Langmuir model was employed to fit experimental data from CO2 pure component isotherm and was used to obtain parameters because the model suits better for CO2 isotherms and to obtain parameters (cmus, b) that were utilized in the IAS model to generate Total adsorbed concentration, mole fraction and

concentration of adsorbed phase (example of the calculation from IAS model is shown in screen print below).

In this particular case, adsorbed phase mole fraction (CO_2 0.1461, CH_4 0.8540 with partial pressures of 649.95kPa and 7.10kPa for CH_4 and CO_2 respectively) and adsorbed concentration for CH_4 and CO_2 predicted from the model is 0.0034 mmole/g and 0.0199 mmole/g at total pressure of ~ 657kPa.

```
SPREADING PRESSURE: Initial guess = 0.019353;    Converged solution = 0.02706
PURE COMPONENT PRESSURE:

p0 =

  649.9492    7.0961

TOTAL ADSORBED CONCENTRATION = 0.023325
ADSORBED PHASE MOLE FRACTION:

x =

    0.1461    0.8540

ADSORBED CONCENTRATION:

cmu =

    0.0034    0.0199
```

As a final product, among the three binary adsorption data from three models, the Toth model generated Binary isotherm data is used in the dynamic simulation model since it is more accurate in comparison with Langmuir and Sips.

The remaining of this chapter presents the summary of how mole fractions of the adsorbed phase, pure component adsorbed concentration and total adsorbed concentration are calculated [7].

Step 1. The match parameters; cmus, b and n or t for (Sips and Toth models) were obtained from single isotherm match against experimental pure component isotherm

Step 2. Total adsorbed concentration; cmuT was calculated from cmus, b and P (n or t for Sips or Toth model)

Step 3. If not converged, new loop started again. If the results were acceptable (using convergence test), go next step.

Step 4. All the answers, mole fractions of the adsorbed phase, pure component adsorbed concentration and total adsorbed concentration were printed out from the program (see the screen print above).

$c_{\mu s}$ = cmus; adsorbed amount for a pure component CH_4 or CO_2); mmole/g

b, n, t = Langmuir constant, Sips constant and Toth constant respectively

$c_{\mu T}$ = cmuT; total adsorbed amount; mmole/g

Table 2-2 Parameters of CH4 and CO2 for corresponding models

Single Component	Model	Fitted Parameter Values (T = 293K)		
		Cμs (mmole/g)	b (kPa^{-1})	t
CH_4	Sips	4.88	0.016	n = 1.4
CH_4	Toth	4.78	0.01156	t = 0.9
CO_2	Langmuir	3.98	0.0442	

Some equations used in IAS model calculations and the algorithm are presented.

First of all, the parameters such as total gas pressure, pure component isotherm and the mole fractions in the pure gas phase are required to provide for calculations. Then,

The following steps are used in the algorithm:

First, to estimate the reduced spreading pressure, Z as the molar average of the following integral with total pressure P as the upper limit of the integral

$$Z = \frac{\pi A}{R_g T} = \sum_{j=1}^{N} y_j \int_0^P \frac{C\mu j}{P_j} dP_j \qquad (2-4)$$

Where,

Z = reduced spreading pressure = $\frac{\pi A}{R_g T}$

π = spreading pressure
A = crossectional area of the particle
R_g = gas constant
T = temperature
P = total pressure
y_j = mole fraction of gas phase
$C_{\mu j}$ = adsorbed amount of pure component j
P_j = pressure of component j

Since all variables (P, y and $C\mu j$, the single component isotherm) are provided, the RHS of the equation can be evaluated.

If the pure component isotherm can be determined by a Langmuir equation, the initial estimate of the spreading pressure can be taken as:

$$Z = C_{\mu s} \ln\left(1 + \sum_{i=1}^{N} b_i P_i\right) \qquad (2-5)$$

$C_{\mu s}$ can be considered as the weighted average of the maximum adsorbed concentration of all species.

Since the estimated reduced spreading pressure can be known from equation 2.1, evaluate the pure component pressure P_j that provides that *reduced pressure* using equation 2.3 [4].

$$\frac{A\pi}{R_g T} = \int_0^{P_1} \frac{C\mu_1}{P_1} dP_1 = \int_0^{P_2} \frac{C\mu_2}{P_2} dP_2 \quad \ldots = \quad \int_0^{P_N} \frac{C\mu_N}{P_N} dP_N \qquad (2-6)$$

Then the *amount adsorbed of the single component is evaluated* from the single component isotherm at that hypothetical pressure P_j^o

The pure component pressure P_j to be evaluated from the hypothetical pressure, P_j^o

Since the spreading pressure for the pure component isotherm of Langmuir from is:

$$Z = C_{\mu s} \ln\left(1 + b_j P_j^o\right) \qquad (2-7)$$

$Z =$ spreading pressure for the pure component;

$C_{\mu s} =$ the weighted average of maximum adsorbed concentrations of all species

$$P_j^o = \frac{\exp\left(\frac{z}{C_{\mu s,j}}\right) - 1}{b_j} \qquad (2-8)$$

When the pure component isotherm takes a general form, the pure component pressure P_J as a function of Z must be obtained iteratively.

Flow chart for calculation of adsorbed phase concentration using single isotherms as input with suitable model to determine matched parameters.

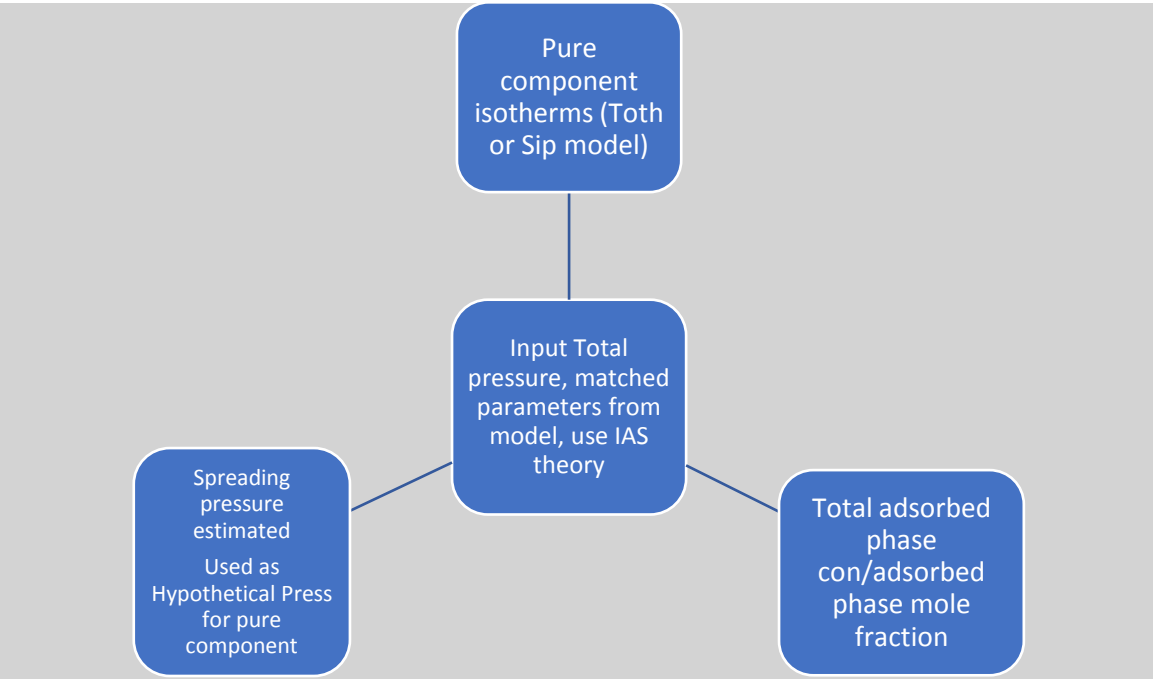

2.4 Unipore and bi-dispersed model for diffusion process in coals

Gas transport in coal matrix can be modelled with the application of the unipore diffusion model. The model employs transient volumetric or gravimetric adsorption or desorption data.

The unipore model is based on the solution to Fick's second law for spherically symmetric flow:

$$\frac{D}{r^2}\frac{\partial}{\partial r}\left(r^2\frac{\partial C}{\partial r}\right)=\left(\frac{\partial C}{\partial t}\right) \qquad (2-9)$$

Where

$$\begin{aligned} r &= radius\ of\ the\ particle, \\ C &= concentration\ of\ the\ adsorbate\ in\ the\ surroundings \\ D &= diffusion\ coefficient\ and \\ t &= time \end{aligned}$$

In this form of the equation, Diffusion coefficient; *D* is independent of concentration and location.

As a result, a more appropriate form of the conservation equation was proposed to account for a concentration-dependent diffusion coefficient. Now *D* is a function of concentration.

$$\frac{1}{r^2}\frac{\partial}{\partial r}\left(r^2 D\frac{\partial C}{\partial r}\right)=\left(\frac{\partial C}{\partial t}\right) \qquad (2-10)$$

The effects of non-linear adsorption become more pronounced when the large step changes in concentration were used, particularly in the gravimetric adsorption rate measurements. Therefore, the unipore model was not suitable for describing diffusional fluxes from coal over the entire period of desorption.

In addition, the magnitude of kinetic parameters change for the linear and non-linear adsorption cases was expected to be different, even though the adsorption rate curve shape may be similar [14].

There are some works that demonstrate that the unipore model is often not adequate for coals (because of the heterogeneous pore structure) [8, 15].

The bi-dispersed model was formulated considering the adsorbent to be a spherical particle (macrosphere) made up of an aggregate of microspheres of uniform size. Ruckenstein assumed (i) a step change in concentration of the adsorptive external to the particle and (ii) a linear isotherm [14].

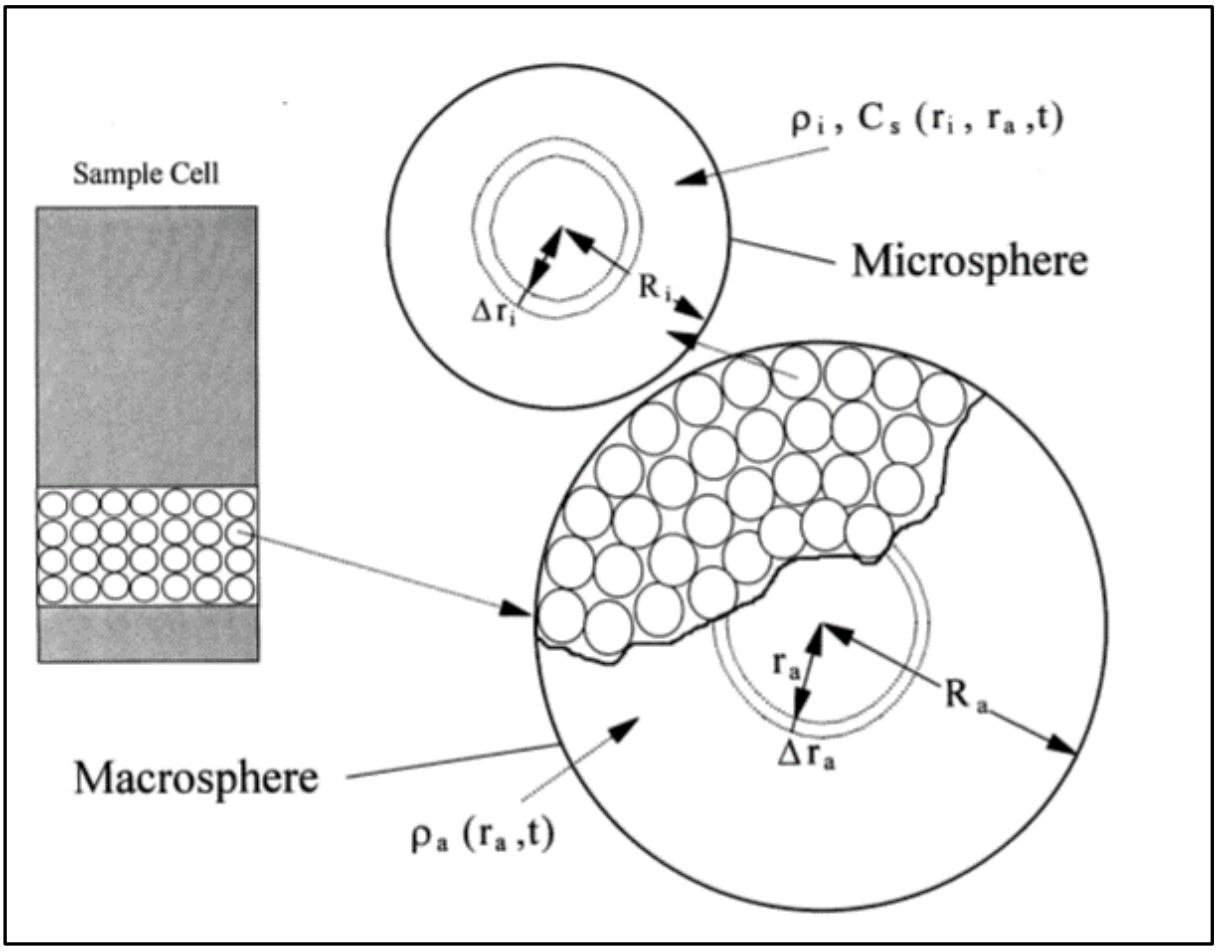

Figure 2-13 Conceptual model for bidisperse pore structure [14]

As illustrated in Figure 2-13, there are many macrospheres in the coal sample placed in the sample cell. A macro-particle has a gas density of ρ_a at time 't" and radius while microsphere has gas concentration of C_S .

As part of requirement for calculation of mass balance equations the macro-particle was subdivided into many shells, for example: $\Delta r_a = r_{a1} - r_{a2}; r_{a2} - r_{a3}; r_{a3} - r_{a4} \ldots . r_{an-1} - r_{an})$

Where $R_a = \sum_1^n r_{a1} + r_{a2} + r_{a3} + \cdots . r_{an}.$

Similarly, the micro-particle is subdivided into many shells: $\Delta r_i = r_{i1} - r_{i2}; r_{i2} - r_{i3}; r_{i3} - r_{i4} \ldots . r_{in-1} - r_{in})$ Δ ri= ri1 – ri2; ri2 – ri3; ri3 – ri4 …….. rin-1 – rin);

Where $R_i = \sum_1^n r_{i1} + r_{i2} + r_{i3} + \cdots . r_{in}.$

The mass balance and concentration change in unipore and bi-disperse models and formulations can be found in the works of previous researchers [14, 51,52].

Smith and Williams found the bidisperse model described the whole period of adsorption rate curve [15] better than the unipore model.

The Ruckenstein model may be inadequate for application of high-pressure volumetric adsorption/desorption experiments firstly because the model assumes a step change in external (to sorbent particles, coals) concentration of the diffusing species at time zero and

this concentration change remain unchanged with time [14] This assumption is not true for constant volume, variable pressure adsorption rate as utilized here [14]. Secondly, methane and carbon dioxide adsorption isotherms used for bituminous coal are known to be non-linear and the application of linear models, is inadequate for most coals.

Just to demonstrate the unipore, bi-dispersed modelling, the sketch below illustrates the process. A small spherical macroporous particle consists of many microporous particles (uniform size). Considering how the adsorption process takes place, the sorbate (methane) in the surrounding (bulk gas) diffuses into the macropores and adsorbs on the macropore walls and diffuses into micropores and adsorbs on the micropore wall. As shown in the sketch, the diffusion process advances towards the centre of the macroporous sorbent.

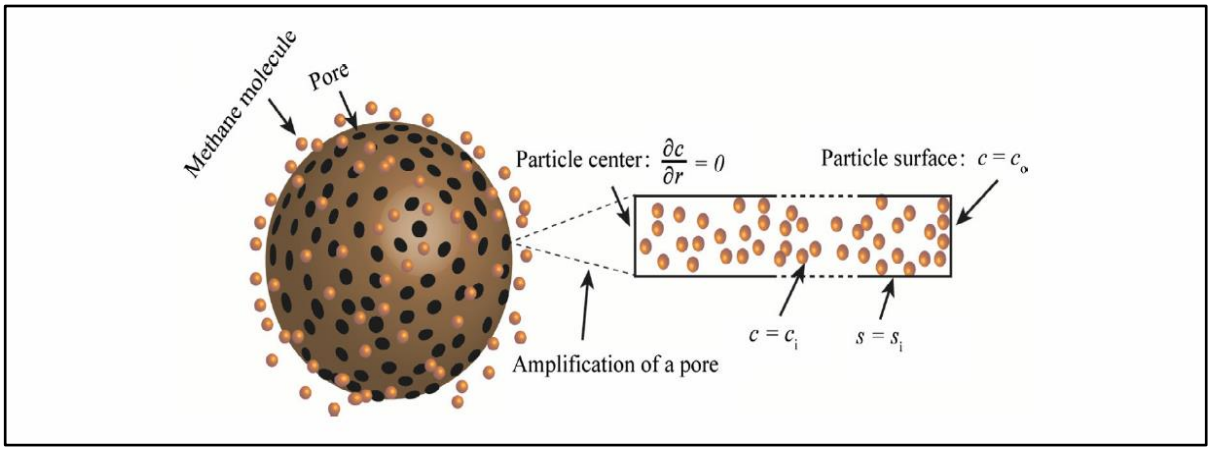

Figure 2-14. Sketch showing the process of desorption and diffusion from the centre of a coal particle towards outside with much higher concentration than the coal concentration

Due to the heterogeneity of coals (coal rank, type, pore size distribution etc.) the transport process becomes even more complicated. A great deal of works related to modelling heterogeneity using various adsorbates (corresponding in principle to various ranges of coals) can be found in works of many researchers. There are many similar works done in real coals conducted elsewhere (mainly US and Canada), and the present study will be based on selected previous works as well as current study from Surat basin coals [13, 14, 16].

Some of the important works done to understand coal heterogeneity and bidisperse models is presented here. Gan et al. studied the structure of various coals from Eastern US using mercury porosimetry and nitrogen adsorption [17]. The results indicate that many coal exhibits a bidisperse pore structure with majority of pores are found in size greater than 30nm and less than 1.2nm [16]. Similarly, Smith and Williams reported bidisperse pore structures in Pittsburgh bituminous and New Mexico Anthracite coals. They present their evidence that the unipore is not suitable for describing diffusional fluxes from coal over the entire period of desorption [13]. The majority of gas adsorbed on coals is stored in micropores within the matrix portion coals (as high as 90%) and the remaining gas may adsorb in meso pores and macro pores. It is realistic to model coal seam reservoirs as bi-pore model that consists of both micropores and mesopores with some cleats or fracture networks initially filled with water. The surface area in coal matrix is a parameter controlling how much gas amount should be adsorbed initially in coals. It is even suggested that methane and carbon dioxide adsorption rate behaviour of bituminous (dull or banded) coals

with a multimodal pore volume distribution are captured accurately with the numerical model [14].

2.5 Conclusions

The Conceptual model with desorption, diffusion and Darcy flow was presented. Desorption and diffusion processes in coals were related to micropores, mesopores and macropores. The physical and petrographic properties of coals, are important controlling parameters in gas transport mechanism. Example analysis data from samples taken from core of the Lauren#66 well were presented and the significance of vitrinite, pore size, cleat nature and types, carbon and ash contents from some coal samples were discussed. In this particular study, coals type and rank are not vastly spread out, are in the range of sub bituminous and bituminous coals and include dull and bright coals as indicated from collected coal samples.

Fluid transport process and behaviour in coals is governed by many factors from inherent coal properties to operation conditions. Here as discussed earlier, we are concerned only with coal heterogeneity, and adsorption equilibrium and kinetics of gas in the coal matrix and cleats. Our work attempts to model fluid movement in coals due to concentration change and pressure change in relation to bulk gas concentration.

Diffusion and desorption are two main transport processes in coals until the gases enter larger flow channels where the flow becomes a pressure driven laminar flow. It is fair to say that getting diffusion parameters for unipore or bi-dispersed model and its importance cannot be underestimated because some coals may have behaviour that is described by a unipore structure while the other have bi-pore structure. Among many models and correlations, Toth, Langmuir and Sips models are investigated and matched to experimental data. Applying resultant coefficients from the model, matched in conjunction with IAS theory model, binary isotherms are determined to obtain desired binary isotherms with different binary ratios. This information is utilized in numerical simulation for different cases with different binary ratios (CH_4:CO_2)

As part of the investigation on how heterogeneity influence on the transport process, the application of unipore and bidisperse pore models will be further discussed in Chapter 4.

Chapter 3. EXPERIMENTAL WORK AND RELATED INFORMATION

This chapter contains methodology, procedures and descriptions of the apparatus used to measure relevant coal characteristics. It also includes a summary of some results (especially for Binary component sorption data), with comments on the limitations of the Belsorp BG machine. A detailed description of the Belsorp BG apparatus and related functions are presented and discussed. A discussion on recalculation of adsorbed amounts for binary adsorption isotherms were properly presented. The consideration of buoyancy correction with virial coefficients in recalculation is discussed in detail with experimental data. The binary experimental data with different binary ratios (methane and carbon dioxide) is then presented, and a comparison is made with data available from literature, highlighting the validity of current study. After confirmation of binary data with different ratios, calculations then determine Binary component isotherms, combined with Ideal Adsorption Solution theory.

3.0 PROCEDURE TO MEASURE SINGLE AND BINARY ISOTHERMS USING BELSORP BG MACHINE

Belsorp BG is a unit the can measure both single component and Binary component sorption isotherms at high pressure and high temperature. The adsorption unit measurement system is made up of a combination a weight and constant volume methods. Detailed schematic of the machine is illustrated in

Figure 3-1. The operation procedure can be found in the Belsorp BG manual [18].

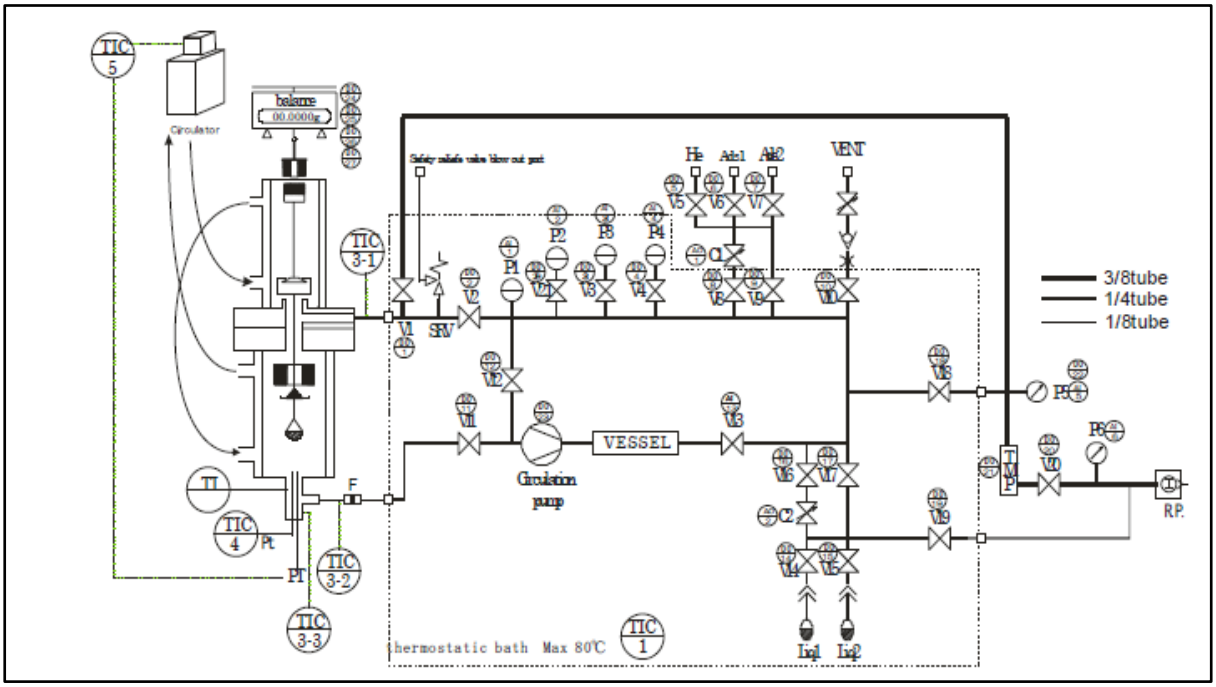

Figure 3-1 High Pressure Binary Gas Adsorption Measuring Unit (BELSORP BG) [18]

3.1 Sample Selection preparation

The coal samples used in this study originate from Surat Basin coals. The samples used for Belsorp analysis were collected from different locations, namely the Lauren and Berwyndale South fields in Queensland, Australia. There are bright coal and dull banded coal with some variations in coal properties as may be observed from the coal physical and petrophysical properties tests (Table 2-1). The impact of coal heterogeneity on the lab results and integration of coal heterogeneity in modelling will be presented in Kinetic Sorption (unipore and bi-dispersed) models.

Figure 3-2 Coal powdered samples for Adsorption test using Belsorp Machine for Binary Gas Adsorption measurement

Coal samples were ground to approximately 40-60 mesh sized powders. Not precise size is not important, but smaller particles speed up the attainment of equilibrium in the adsorption tests.

3.2 Experimental Setup

The simplified schematic diagram of the experimental set up is shown in Figure 3-3 and for convenience is divided into two main components labelled as PART1 and PART2.

The first component shown as PART1 is the weight change measurement system, and the second component named as PART2 is the volume change measurement system.

These two components are housed as a single unit. Outside the main unit, there are rotary pump, standalone desktop computer, and gas cylinders which are connected through tubing to the main unit.

PART1 is composed of balance, magnetic coupling system, and sample basket and sinker, tubing and wire connections.

PART2 contains all the tubing and wire connections, normal actuated valves, safety relief valve (SRV), pressure gauges whose functions are to supply required gas, so as to reach and maintain pressure equilibrium, to perform degassing and to maintain isothermal conditions. Also, a special pre-treatment heater (up to 400ºC) and a vessel connected to a circulationr pump to supply the hydraulic system to the sample cell.

There are four pressure sensors with pressure ranges to 15 MPa, 2 MPa, 133.3 kPa and 1.33 kPa. The function of all these sensors is to provide accurate pressure measurement, which is necessary to calcyulate changes in gas quantities when making volumetric measurements. In addition, there is a safety relief valve which set to the maximum use pressure of 15 MPa.

Rotary pump performs degassing and also evacuates the system once the test is completed. Degassing is normally aimed to achieve an ultimate vacuum of 1.0e-15 Torr or lower for 12 hours [19] and is part of the sample preparation procedure.

There is a circulation pump (shown in

Figure 3-1) which circulates heating fluid to maintain an isothermal condition in the measurement vessel.

There are three ports available to connect cylinders which for this study were Helium, Methane nad Carbon dioxide. The cylinder pressures range from 8000 MPa to 5000 MPa.

Once the experiment is finished, the gases in the sample cell will be released through V_{10} to vent to the atmosphere.

There are tubing connections between PART1 and PART2 allowing either (or both simultaneously) to be used.

The temperature of Vs is maintained throughout the entire test as per the information entered to the software. Also, the temperature of the balance and magnetic coupling system is maintained according to the thermostatic bath temperature 80ºC. During pre-treatment, most likely the temperature will be kept 150ºC. It is worth to mention that the experimental temperature is kept constant in the sample cell during the entire testing period.

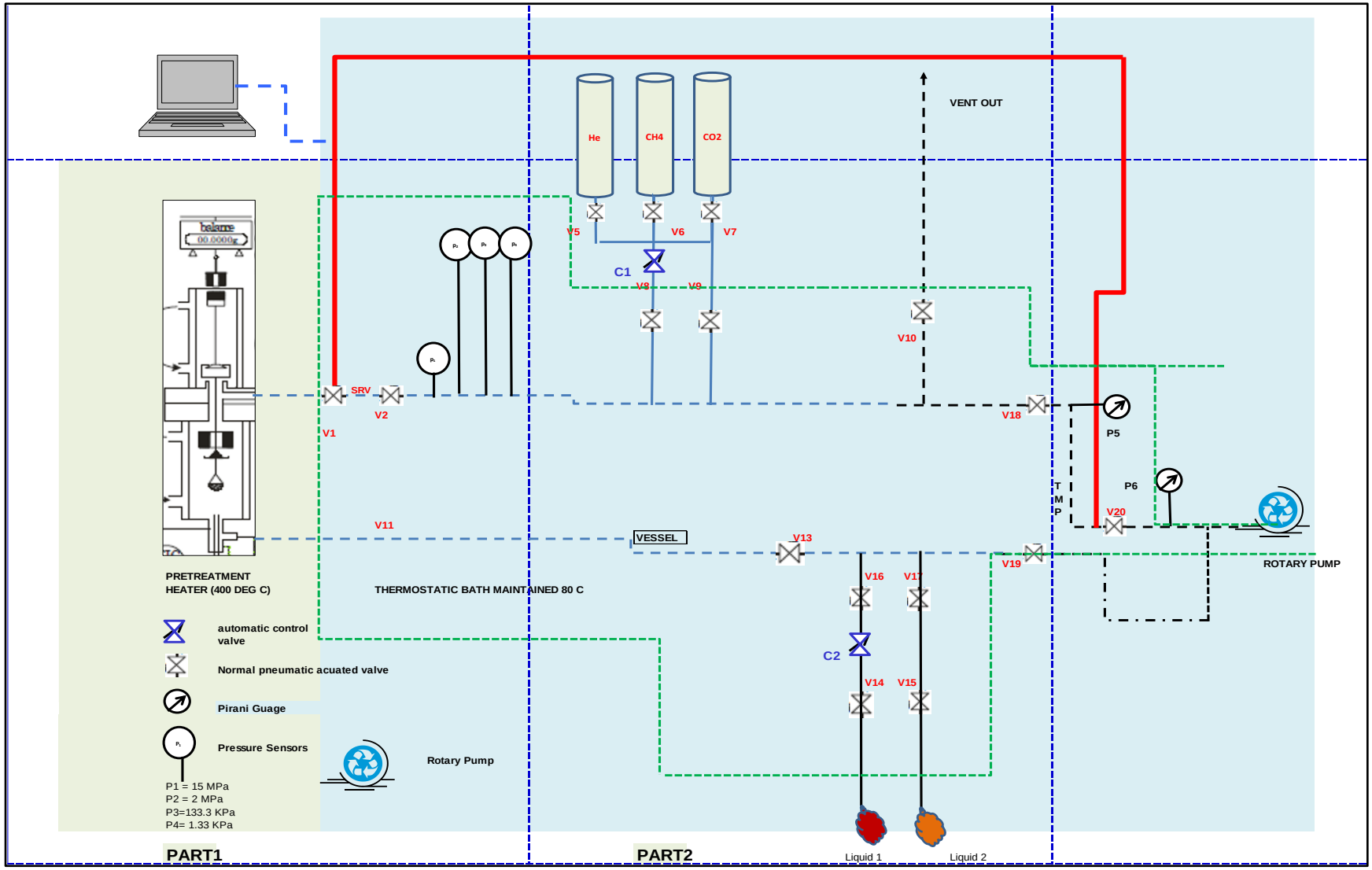

Figure 3-3. Schematic Diagram of Experimental Setup for Single and Binary Components Sorption

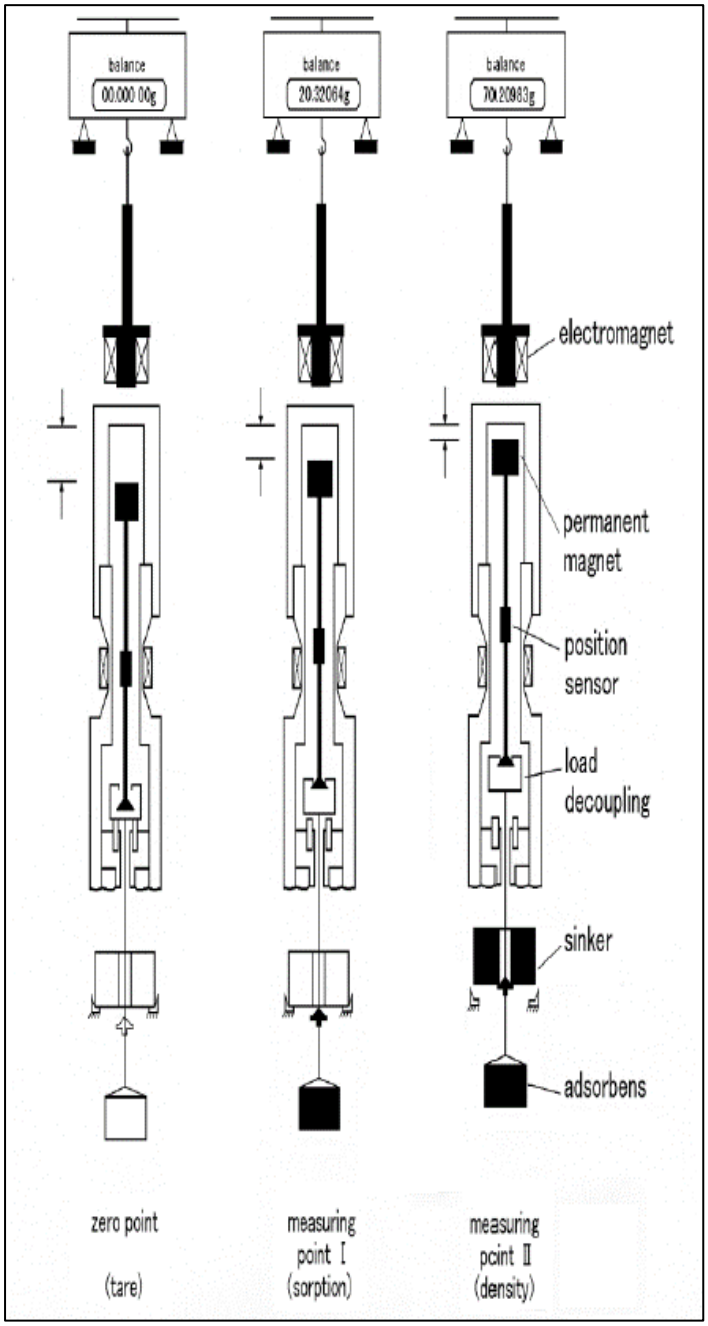

Figure 3-4 Floating Magnetic Balance in the Unit (BELSORP BG) [18]

The weight measurement system, comprising the main elements of balance and magnetic coupling system, is separated from the sample cell and the balance components themselves are not exposed to the experimental conditions. As illustrated in **Error! Reference source n ot found.**, a floating magnetic balance is part of weight change measurement system. The floating balance consists of permanent magnet, position sensor, load coupling and sinker with the sample. The bottom of the balance is attached with electromagnet which has a role to couple with permanent magnet during the measurement.

In **Error! Reference source not found.**4, the first picture (zero point) shows how to obtain t are weight after a correction on any drift in the balance. The second picture (measuring points) shows the total weight change and records the balance location during the

measurement. The last picture (measuring point II) shows the system in equilibrium showing the final balance position with respect to the position when the sinker is lifted. This data is used to determine the fluid density [19]. Basically, the sinker whose weight and volume are precisely known is lifted using load coupling and position sensor and the buoyancy at the given temperature and pressure provides an accurate measure of the gas density in the adsorption cell.

3.3 Experimental Procedure

Belsorp BG a provides contactless magnetic weight change measurement system from RUBOTHERM, Germany. The sample mass is measured continuously during the experiment. The sample basket is connected to the permanent magnet and the weight change in the sample due to adsorption will be accounted for by the balance.

Before measuring adsorption equilibrium for a binary mixture the procedure is:,

Check all the connections (from the gas cylinders, liquid reservoir). Set the supply pressure at the gas cylinder to 14 MPa and driving pressure to 5050 kPa.

Open V5, 6 and 7 (He, CH_4 and CO_2) (

Figure 3-1)

Start the PC and launch the software while all the valves are closed. Turn on Rotary Pump.

The weighed powdered coal sample is put in the sample basket. Then the sample cell is wrapped with thermal insulator and the desired temperature set on the PC controller for the heated oil bath.

V10 was used to vent out the system to the atmosphere and V17, V19 open to evacuate the system. Flushing to atmosphere with the desired gas followed by another evacuation cycle and then closed all V5, V6 and V7 (from gas cylinders).

Once the sample cell was securely placed, make sure there was no leak.

One important check before degassing is to ensure the reservoir liquid is warm (labelled as liquid 1, liquid 2 in the **Error! Reference source not found.**). Then close V20 and open V 19. Often V14 or 15 needs to open to clean up adsorbed degas. This process was repeated until degassing was completed. Degassing took 10-12 hours under vacuum of $1X10^{-5}$ Torr or lower [19].

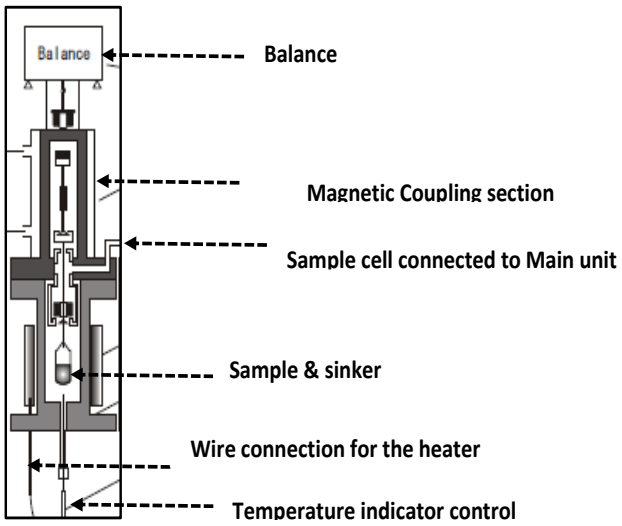

Figure 3-5 PART1 of BG Machine

In the next step, a certain amount of gas filled in the reference cell from the reservoir by opening C1 (automatic valve) (Figure 3 3). At every pressure step, the initial pressure, Pi and volume Vi were recorded, equilibrium pressure Pe and volume Ve were recorded similarly. The procedures above were repeated for several pressure steps (in this study 7 pressure steps),

One very important step is to make sure the value of balance is stabilized. If not stabilized, the position of electromagnetic must be adjusted (for details refer to the Manual [18].)

3.3.1 Adsorption measurement

Before actual sorption isotherm measurement, the dead volume Vd needs to be measured. This is done using He gas, which does not adsorb on the sample.

P_i, was measured when He gas was introduced into the sample cell of known volume V_S.

Then, by opening valve 2 gas is introduced into the dead volume of sample cell f V_d, and pressure P_e, was recorded after an equilibrium had been achieved. V_S is the known volume of sample cell including sinker.

V_d, was calculated from V_S, P_i and P_e (refer to Belsorp BG for detail calculations and formula) [1]

$V_d =$ dead volume
$V_s =$ sample cell volume
$P_i =$ Initial pressure at the sample cell
$P_e =$ Equilibrium pressure at the sample cell
$P_{ix}, P_{iy} =$ Initial pressures for components x, y
$P_{ex}, P_{ey} =$ Equilibrium pressure for components x, y

The table below is provided to discuss how the Belsorp machine measure pressures (initial and equilibrium) throughout the experiment. Also, the table contains sample cell volume, Vs and dead volume, Vd that were measured and recorded accordingly.

First initial adsorption pressure, P_i was measured when the gas was introduced to the sample cell (see below excel sheet from a binary adsorption measurement data). At every pressure step, the software calculated pressures for individual components (initial pressure and equilibrium pressure; P_{ix}, P_{iy} and P_{ex}, P_{ey} and they were recorded throughout the entire experiment.

Sample cell temperature (43^0C) was controlled at a constant value during the whole time of the experiment presented in column 3, Table 3.1, with the oil temperature shown in column 2. .

Table 3-1. Belsorp Measurements

No.	Julabo_Te	Vs temp	Pi	Pix	Piy	Pi open	Pix open	Piy open	Pe	Pex	Pey	Pe2	Vd	Vs
	(°C)	(°C)	(kPa)	(kPa)	(kPa)	(kPa)	(kPa)	(kPa)	(kPa)	(kPa)	(kPa)	(kPa)	(cm3)	(cm3)
1	42.8	43	709.337	72.699	644.056	252.706	25.631	227.075	248.416	23.602	224.814	248.416	158.1974	86.161
2	42.8	43	958.692	99.991	867.529	501.972	50.537	451.436	495.882	49.549	446.332	496.004	158.17579	86.161
3	42.8	43	2041.053	203.876	1826.999	1001.665	100.4	901.264	1011.001	96.908	914.092	1010.543	158.13081	77.732
4	42.9	43	2516.523	259.612	2240.144	1501.641	150.53	1351.112	1510.979	147.885	1363.094	1510.979	158.08716	77.732
5	43	43	3024.483	306.93	2688.782	2000.385	200.31	1800.074	2015.426	195.968	1819.458	2014.969	158.04311	77.732
6	43.1	43	3527.41	360.881	3126.772	2500.8	250.338	2250.462	2516.523	246.599	2269.923	2519.726	157.99936	77.732
7	43	43	4027.591	409.114	3565.945	2997.473	300.189	2697.285	3022.195	290.388	2731.808	3022.653	157.9552	77.732

In a case with a large binary ratio (CH_4: CO_2, 90:10) the; adsorbed amounts of individual adsorbates were less accurate at pressures below 1000 and above 2500 kPa (Figure 3-5). The plot in the Figure 3-5 is provided to illustrate this issue, details of which will be discussed in section 3-4 “Limitation of Belsorp HCPV”. The plot contains 3 sets of data, blue dots; total adsorbed amount; red dots represent the adsorbed amount of CO_2 and green dots are for CH_4 adsorbed amount (all in units; g/g adsorbate). Table 3.2 provides the numerical values from the same experiment.

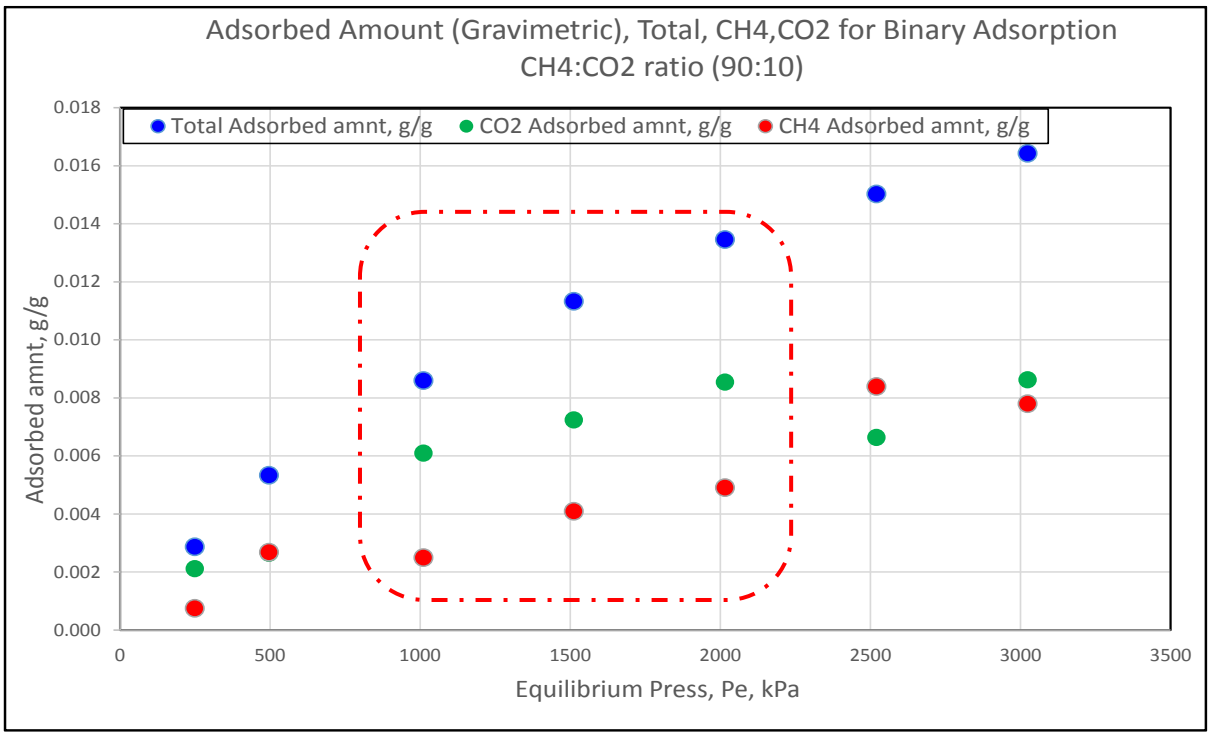

Figure 3-5 The Plot shows Total adsorbed amount, adsorbed amounts of CH4 and CO2 with increasing equilibrium pressures, Pe (for CH4:CO2, 90:10)

The experiment data show an issue with CH_4 and CO_2 adsorbed amount at pressure higher than 2500 kPa. Even though total adsorbed amount from Gravimetric method is equal to the sum of the adsorbed amount of CH_4 and CO_2 (refer to the Table 3-2 column 3 to 5). The adsorbed amounts of CH_4 and CO_2 do not show a linear increasing trend for the entire pressure range (500 -3500 kPa). However, for the data set between pressures 1000 kPa and 2500 kPa, the trend is almost linear for CH_4 adsorbed amount and CO_2 adsorbed amount (referring to data in the box in Figure 3-5 . The cause of this irregular trend in adsorbed amounts of individual components is unclear. Also this trend is not consistent for different CH_4:CO_2 ratios. To understand this inconsistency, more experimental works are required, since this is not the main purpose of the research. The cause may relate to selective adsorption of CH_4 and CO_2 or some limitation of the machine

Table 3-2 The basic measurements from CH_4:CO_2 (90:10) sorption experiment

Pi (kPa)	Pe (kPa)	Gravimetric (g/g)	Wx (g/g)	Wy (g/g)	Fluid density (g/cm3)	z=PV/RT
709.337	248.416	0.00287	0.00211	0.00076	*0.00176*	1.0122501
958.692	495.882	0.00534	0.00266	0.00269	*0.00357*	0.9961645
2041.053	1011.001	0.0086	0.0061	0.0025	*0.0073*	0.9932296
2516.523	1510.979	0.01133	0.00724	0.00409	*0.011*	0.9848028
3024.483	2015.426	0.01346	0.00854	0.00491	*0.0149*	0.9694529
3527.41	2516.523	0.01503	0.00664	0.00839	*0.0186*	0.969386

The following section includes some discussions on how adsorbed amount for individual components, CH4 and CO2 in this case, determined from the experimental data.

3.3.2 Recalculation of adsorbed amount

The main uncertainty in adsorbed amount calculation is in the Z value for the mixture and, its variation with pressure during the binary adsorption measurement, which affects the fluid density calculated from the mass change during the experiment. From the experimentally known fluid density (see in the table 3.2, column 6), the relationship between the Z value and pressure is established.

The $Z_{mixture}$ vs. Pressure relation was utilized to calculate adsorbed amount for pure components in the mixture (W_x, W_y,). Using this relationship to correct pressures and volumes (P_i, P_e, V_s, V_d) provided the main input for this recalculation.

In addition, total adsorbed amount using the constant volume method required the buoyancy correction and with the pressure and volume corrections, accurate total volumetric adsorbed amounts were determined.

Step by Step calculation of adsorbed amount during the adsorption test for CH_4:CO_2 (90:10)

The minor correction for Vd (dead volume) (column 5 in the Table 3-3) is made using Vd slope from the measured Vd data set. Virial_mix (in column 6 in Table 3-3) shows the deviation in Vs for the different points in the test.,

Table 3-3 Calculations to obtain 2nd Virial Coefficients VsBp1, VsBp2, VsBp3

				Vd CORRECT	Vd*2Virial+		Vs,Vd, Pi,Pe, Bp1, Bp2, Bp3 Bp4 coefficients			
CONVERSION OF P TO PASCAL				using slope,	Vs*2Virial correction		PiVs,2ndVir	Pe, Vd,Vs	Pe2,Vs	Pe,Vs,Vd, Virmix
Pi	Pe	Pe2	Vs	Vd	Virial_mix	Vs temp	VsBp	VsBp	VsBp	VsBp
Pascal	Pascal	Pascal	(cm3)	(cm3)		(˚C)	1	2	3	4
				5	6		7	8	9	10
709,337	248416	248,416	86.161	1.58E+02	-1.54E-08	43	6.18E+07	0	0	*60935045.04*
958692	495882	496004	86.161	158.1758	-1.536E-08	43	83836395.01	6.09E+07	21485753.5	*122092165.9*
2041053	1011001	1010543	77.732	158.13083	-1.536E-08	43	1.64E+08	122092165.9	43064291.2	*242218968.7*
2516523	1510979	1510979	77.732	158.08718	-1.536E-08	43	203479625.2	242218968.7	79790024.5	*364783969.5*
3024483	2015426	2014969	77.732	158.04314	-1.536E-08	43	246552992.9	364783969.5	120242074	*490367636.5*
3527410	2516523	2519726	77.732	157.9994	-1.536E-08	43	289899694.6	490367636.5	161630007	*617075803.5*
4027591	3022195	3022653	77.732	157.95525	-1.536E-08	43	333717751.1	617075803.5	203749039	*746967761.9*
0	0	0	0	158.21909	-1.536E-08	0	0	746967761.9	246396550	0

Explanation: During binary adsorption isotherm measurement, Vd, dead volume slightly changes at every pressure steps (Table 3-1). This was corrected in the adsorbed amount volume calculation using Vd (differential dVd). In addition, the adsorbed volume of pure components and mixture measurements are not accurate due to the dosing procedure.

Individual pure gas cylinders (CO2 and CH4) were used to dose the gas separately. Between the pressure step changes, there is no degassing to clear the mixture of the gas in the sample cell. Therefore, the desired binary ratio after every pressure interval may not be exactly as planned.

In addition, there is some limitation of cylinder pressure for CO2. Due to the small percent of CO2 dosing is required for the test, the cylinder pressure requires 8000 – 9000 psi. At one point the cylinder pressure is not strong enough to dose correct CO2 ratio which may cause in accurate adsorbed volume of mixture at higher pressure.

The virial coefficients Bp1, Bp2, Bp3 and Bp4 were used to calculate adsorbed volume and moles of CH_4 and CO_2. Using Virial coefficient, Temperature, unit conversion, the adsorbed amount (volumetric), V in ml was calculated using the equation below:

$$V = 7.29 + \frac{V_s B_{p1} + V_s B_{p2} - V_s B_{p3} - V_s B_{p4}}{101325 \times (T(°C) + 273.15) \times 273.15} = 17.47\ ml$$

$$V = 7.29 + \frac{V_s B_{p1} + V_s B_{p2} - V_s B_{p3} - V_s B_{p4}}{101325 \times (T(°C) + 273.15) \times 273.15} = 17.47\ ml$$

The first column in the Table 3-44 shows all total volumetric adsorbed amount for individual pressure steps. Gravimetric adsorbed amount (in g) is shown in the second column. The third and fourth columns show the change of adsorbed amount in mass (dW) and moles (dV_mol). The 5th column (Snx) presents the amount of CO_2 adsorbed moles.

dV_mol was calculated using the formula provided below where 'A' and 'D' were sample weight (Gravimetric and Volumetric) after pre-treatment.

$$dV_{mol} = \frac{V_s B_{p1} + V_s B_{p2} - V_s B_{p3} - V_s B_{p4}}{101325 \times 1000 \times 0.082057 \times (T(°C) + 273.15) \times (A + D)}$$

Once dW and dV_mol was determined,

$$Snx = \frac{dW - Mw_{CH_4} \times dV_{mol}}{Mw_{CH_4} + Mw_{CO_2}}$$

Snx was calculated using molecular weights of CH_4 and CO_2 incorporated into the formula above. After Snx was obtained, Wx was calculated using MW of CO_2 providing the total gravimetric adsorbed amount in g. This is the adsorbed amount of CO_2 for this binary ratio.

Table 3-4 Calculations of total adsorbed amount and adsorbed amount and numbers of moles for CO_2.

	Gravi Mas	g	mol	mol		g	g	g/g
V	Ads Mass	dW	dV_mol	Snx		Wx	Wx	Wx/g
ml	g			1		1	3	Gravi wt
			11			13		
7.29	0.00982	0.00982	9.50904E-05	0.000296632		0.01305477	0.0098214	0.00287
17.47	0.01827	0.00845	0.000132682	0.000226123		0.01977312	0.018274	0.00534
22.58	0.02943	0.01116	6.65843E-05	0.000360705		0.03414869	0.0294301	0.00860
32.17	0.03877	0.00934	0.00012502	0.000262332		0.04097535	0.0387724	0.01133
38.37	0.04606	0.00729	8.08474E-05	0.000214254		0.04820178	0.0460615	0.01346
51.68	0.05143	0.00537	0.000173592	9.25295E-05		0.05013375	0.0501338	0.01465
52.34	0.05623	0.00479	8.53261E-06	0.000166412		0.05745757	0.0562252	0.01643

Next steps show similar steps to calculate CH_4 adsorbed amount, Sny and number of moles; dV_mol. But there were some major corrections on Vd changes and V1, V2, V3 were calculated to obtain new volumetric adsorbed amount.

Pi	Pe	Pe2	Pi	Pe	Pe2	Vs	V1	V2	V3	V
Pa	Pa	Pa	Pa	Pa	Pa	(cm3)				ml
		MAJOR CORRECTION FOR Pi and Pe, Pe2								V1+V2+V3+R1
							PiVs Corr	Pe,Pe2Vs	eVs Vdslope	
709,337	248,416	248,416	734,251	251,809	251,809	86.161	0.024067	0	0.02341	14.74273
958,692	495,882	496,004	1,001,731	508,662	508,790	86.161	0.032835	0.015156	0.047288	30.48718
2,041,053	1,011,001	1,010,543	2,199,684	1,058,317	1,057,821	77.732	0.065048	0.030611	0.094993	45.40822
2,516,523	1,510,979	1,510,979	2,744,645	1,606,216	1,606,216	77.732	0.081163	0.063712	0.144172	61.16351
3,024,483	2,015,426	2,014,969	3,346,562	2,170,685	2,170,168	77.732	0.098963	0.096674	0.194838	79.056
3,527,410	2,516,523	2,519,726	3,974,708	2,744,645	2,748,367	77.732	0.117538	0.130664	0.246357	120.404
4,027,591	3,022,195	3,022,653	4,650,269	3,343,789	3,344,344	77.732	0.137515	0.165083	0.300135	175.6177

After new adsorbed amount for volumetric unit (column 1 in the Table 3-5 below), V ml is determined, then calculate CH_4 adsorbed amount, Sny (in number of moles) followed by the calculations of Wy and gravimetric mass for Wy/g (g/g)

Table 3-5 Calculation of total adsorbed amount (volumetric and gravimetric) and individual adsorbed amounts and numbers of moles for CO_2 and CH_4

V	Ads vol	Ads Mass	g	mol	mol	mol	g	g/g
ml	ml	g	dW	dV_mol	Sny	Sny	Wy	Wy/g
+V2+V3+R186					1	2	2	Gravimass
14.74273	14.7	0.00982	0.00982	0.000658	0.000684	0.000612	0.009821	0.00287
30.48718	30.5	0.01827	0.00845	0.000702	0.000803	0.000527	0.018274	0.00534
45.40822	45.4	0.02943	0.01116	0.000666	0.000649	0.000649	0.028681	0.00838
61.16351	61.2	0.03877	0.00934	0.000703	0.000772	0.000629	0.038772	0.01133
79.056	79.1	0.04606	0.00729	0.000798	0.000996	0.000454	0.046062	0.01346
120.404	120.4	0.05143	0.00537	0.001845	0.002711	0.000335	0.051434	0.01503
175.6177	175.6	0.05623	0.00479	0.002463	0.003705	0.000299	0.056225	0.01643

Using volumetric adsorbed amount in total and Gravimetric adsorbed amount, weight and molecule changes at every pressure steps are obtained. Then using molecular weights of CH_4 and CO_2, adsorbed amount of CH_4 and CO_2 in moles were determined. Finally, Gravimetric adsorbed amount in g/g was estimated (Table 3-5 column 9).

As the final numbers for both Volumetric and Gravimetric adsorbed amount in total and for CH4 and CO2 were determined and presented in the Table 3-6.

Table 3-6 Calculated results of total adsorbed amount (Volumetric) and measured total adsorbed amount (Gravimetric). Individual adsorbed amount in ml for CO_2 and CH_4 (calculated)

						Recal	Recal
Ads vol	Ads Mass	Ads_X	Ads_Y	Ads_X	Ads_Y	Wx	Wy
ml	g	ml	ml	ml/g	ml/g	g/g	g/g
		CO2	CH4	CO2	CH4	CO2	CH4
7.3	0.00982	3.69	3.6	1.1	1.1	0.00212	0.00075
17.5	0.01827	4.62	12.8	1.4	3.8	0.00265	0.00269
22.6	0.02943	10.63	12.0	3.1	3.5	0.00610	0.00250
32.2	0.03877	12.62	19.6	3.7	5.7	0.00724	0.00409
38.4	0.04606	14.90	23.5	4.4	6.9	0.00855	0.00491
51.7	0.05143	11.57	40.1	3.4	11.7	0.00664	0.00839
52.3	0.05623	15.03	37.3	4.4	10.9	0.00863	0.00780

The last two columns present recalculated adsorbed amount of CH_4 and CO_2 in gravimetric method. Obviously, total adsorbed volume (measured and calculated) from two methods (Gravimetric and Volumetric methods) are significantly different due to different methods used.

The reason for significant difference is individual adsorbed amount of CH_4 and CO_2 in moles is the two values are calculated from two total adsorbed amount (Volumetric in column 1 of Table3-6) This adsorbed amount is calculated from Virial coefficient temperature and unit conversion to obtain volumetric adsorbed amount (Table 3-4). The other is total adsorbed amount (Gravimetric method) is calculated from pressure and volume changes (using P_i, P_e, V_1 V_2 V_3 etc). The volume is shown in the column 1 of table 3-5. Obviously, these total adsorbed volumes from different calculations are significantly different. As a result, the measured values presented in the final individual adsorbed amount of CO2 and CH4 are much different (Table 3-6).

In summary, there are some actions taken in the recalculation to correct initial machine measurement and calculations.

Basically, (sample cell and dead volumes) Vs, Vd, Pressures (Pi, Pe etc.) needed to be more accurate than initial software calculated value since the Vs, Vd values were slightly varied throughout the entire test. Then 2_{nd} virial coefficient was used to determine, more accurate $Z_{mixture}$.

In addition, initial volumetric adsorbed amount required buoyancy correction and also the update pressure and volume from the correction so that accurate total volumetric adsorbed amount could be determined before individual component adsorbed volume in mass and in numbers of moles.

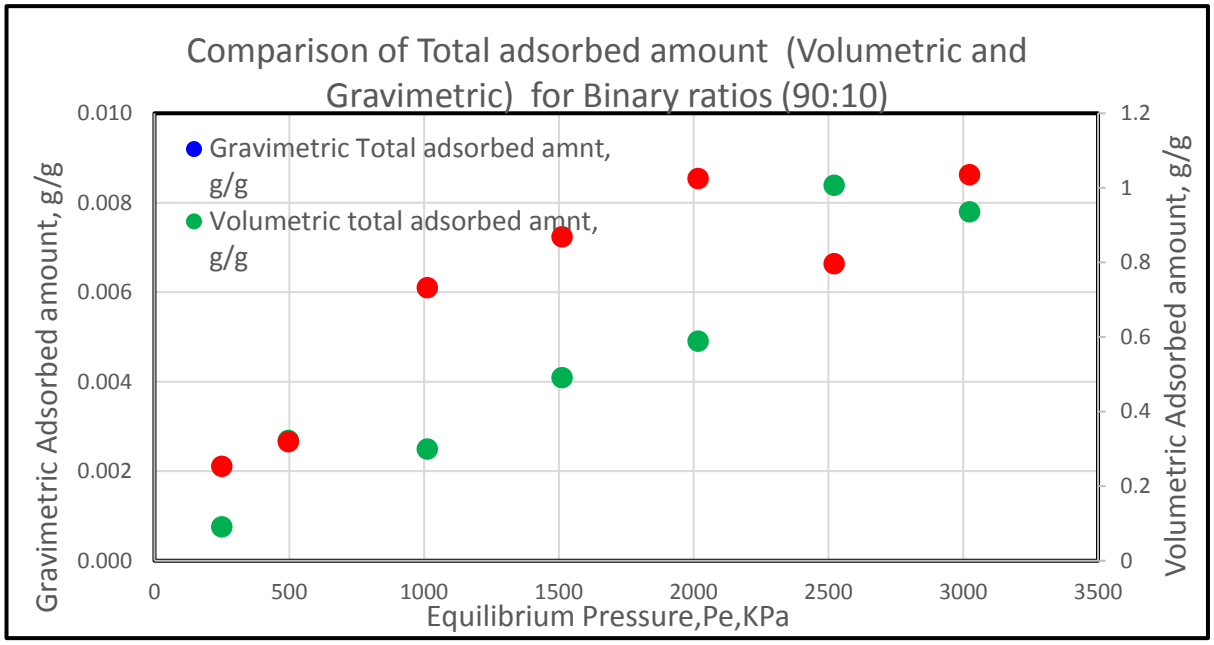

Figure 3-6 The Plot shows Total adsorbed amount (in Gravimetric and Volumetric) and adsorbed amounts of CH_4 and CO_2

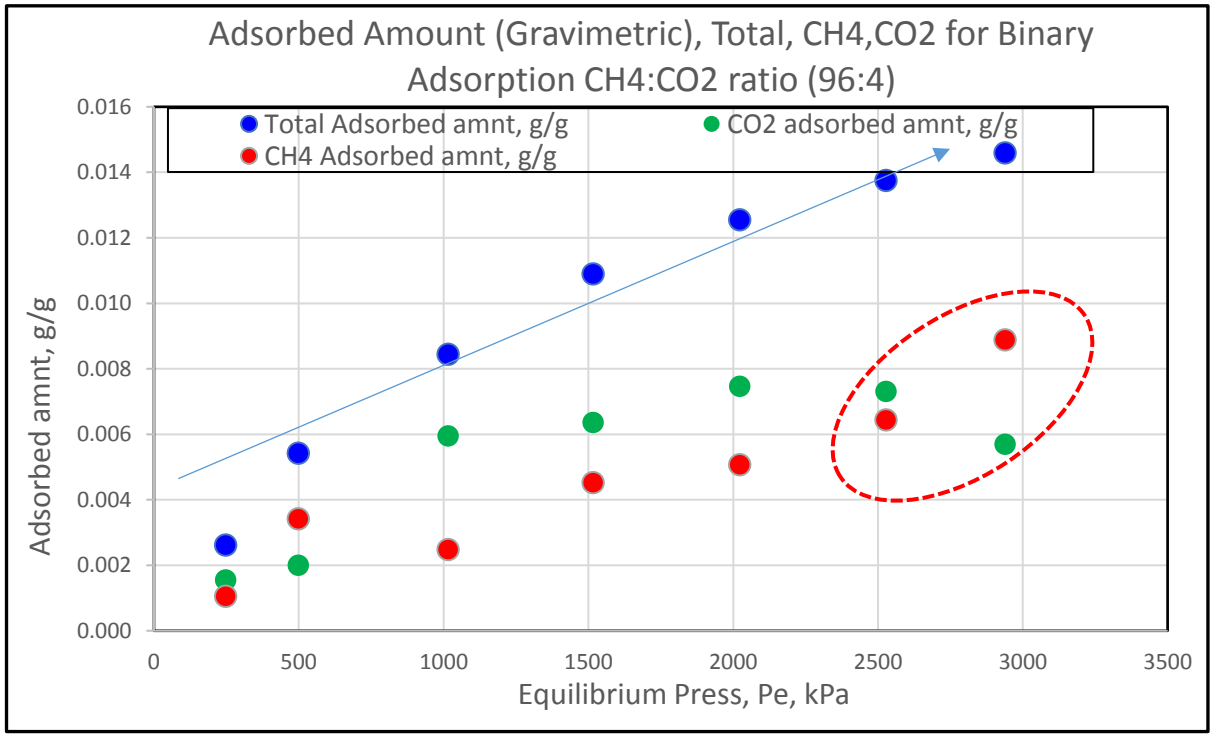

Figure 3-7 CH_4 and CO_2 adsorbed amounts with not proper trend of increasing (scattered)

The explanation for this irregular trend may have some possible reasons: Pre-determined binary ratio (for example CH_4:CO_2 96:4) were entered as the input data requirement before the test commenced (Figure 3 7). At the first pressure step; correct CH_4 and CO_2 ratio (96% and 4%) would be dosed from the corresponding cylinders. Hence, the adsorbent would

receive accurate binary ratio (96:4). The sorption equilibrium would be reached, once some gas components (both CH_4 and CO_2) were adsorbed in the coal sample. The gas mixture remaining in the sample cell may not be exactly CH_4:CO_2 (96:4).

According to Belsorp algorithm, CO_2 would be injected into the sample cell to build up next pressure (which was higher than current pressure). Then CH_4 would be subsequently injected into the sample cell. In this process, CO_2 would have an earlier advantage (priority) over CH_4 since part of the sample cell was filled with CO_2 first. That might give CO_2 molecules a preferred or favourable chance to adsorb the remaining pores in comparison with CH_4 molecules. This may be one reason the irregularity or abnormal adsorbed amount of CH_4 and CO_2 in the early pressure steps. Also, supercritical situations and CO_2 affinity may play an important role of adsorption to coal.

It is fair to say that we know the ratio of CH_4:CO_2; the starting feed compositions at each step. For example, we dosed 96% CH_4 and CO_2 4 % at the beginning of each pressure step.

But there was some amount of earlier batch of dose left in the sample cell after adsorption was in equilibrium, we do not know (96:4? 95:5? 97:3?). But it would not be 96:4.

Then new dose 96:4 gas mixture was injected. The composition of gas mixture at every pressure step.

The suggestion was proposed to collect the gas mixture sample after each equilibrium so we would know exact composition of the gas mixture from the analysis of collected gas mixture. But this did not materialize since there was a safety concern and restrictions imposed on the modification of the machine.

After 1st step of pressure when an equilibrium was achieved, the procedure to measure binary adsorption equilibria at next pressure interval was continued. There was no process/sensor to ensure/detect the dosing mixed gas ratios in the sample cell had in fact at desired ratio (96:4). Ideally there should be a vacuuming step to clean up the sample cell before continuing the experiment at next pressure interval. If vacuuming were carried out at the end of each pressure step, it may take several hours to complete one binary adsorption test, it was not practically feasible to do so. In addition, during vacuuming process the sample integrity and mass may alter, the impact would affect on the results.

During the process of measuring binary isotherms, CH_4 and CO_2 were dosed according to the pre-determined ratio (for example 80:20; CH_4:CO_2).

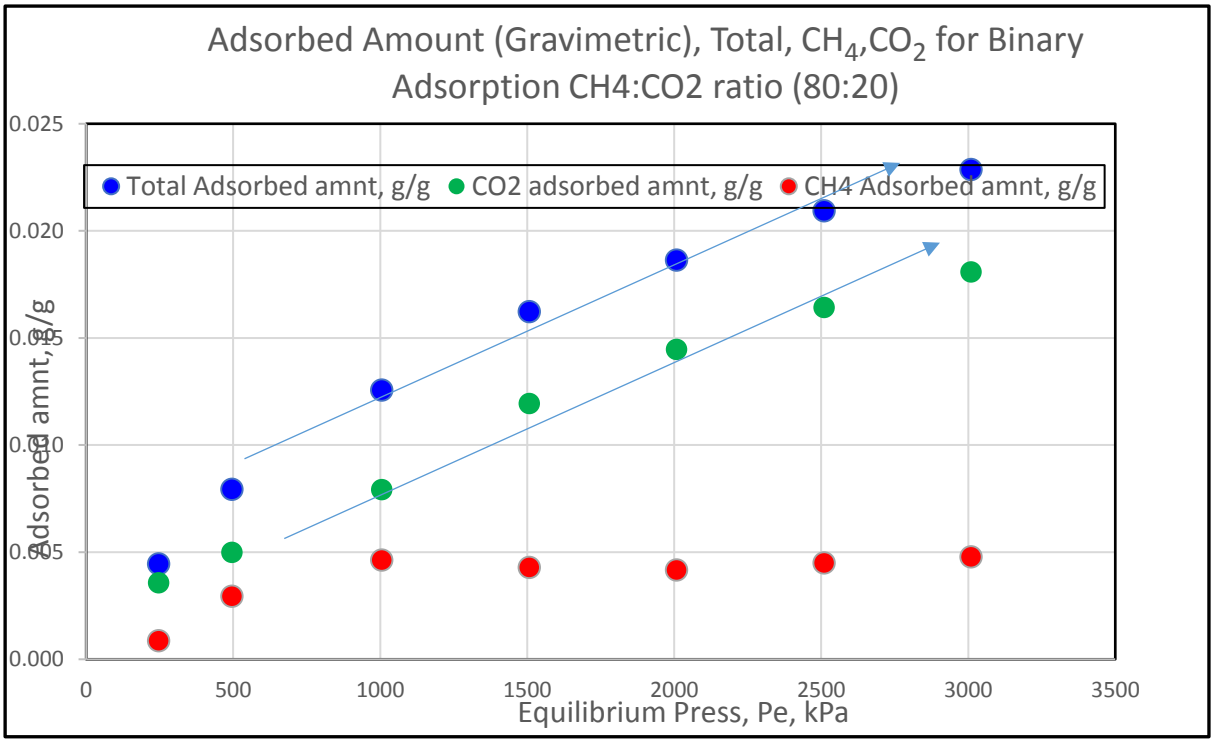

Figure 3-8 Gravimetric Adsorbed amount (Total, CH_4 and CO_2) for Binary mixture (80:20)

However, it is noteworthy that the (80:20) ratio of (CH_4:CO_2) binary measurement data in Figure 3-8 showed a reasonable trend of adsorbed amount (for both total, individual component gases (CO_2) for the entire testing pressure range (Figure 3 8). But the methane (CH_4) adsorbed amount was found remained almost unchanged after 1000 kPa.

Some plots with large contrast ratios of CH_4:CO_2 cases are presented here for comparison purposes and also to point out the limitation of Belsorp machine to measure Binary adsorption with great contrast (98:2, 96:4, 94:6 and 90:10).

In this section, the quality control and validation works on adsorption measurement using Belsorp machine will be discussed with the example data measured for CH_4:CO_2 (98:2).

In Figure 3-9 the comparison of total adsorbed amounts from two different methods (Gravimetric and Volumetric) for binary ratio (98:2) (CH_4:CO_2). As mentioned in previous discussion, two sets of data were in a good agreement within the testing pressures ranging from 500-3000 kPa and showed a good tracking trend.

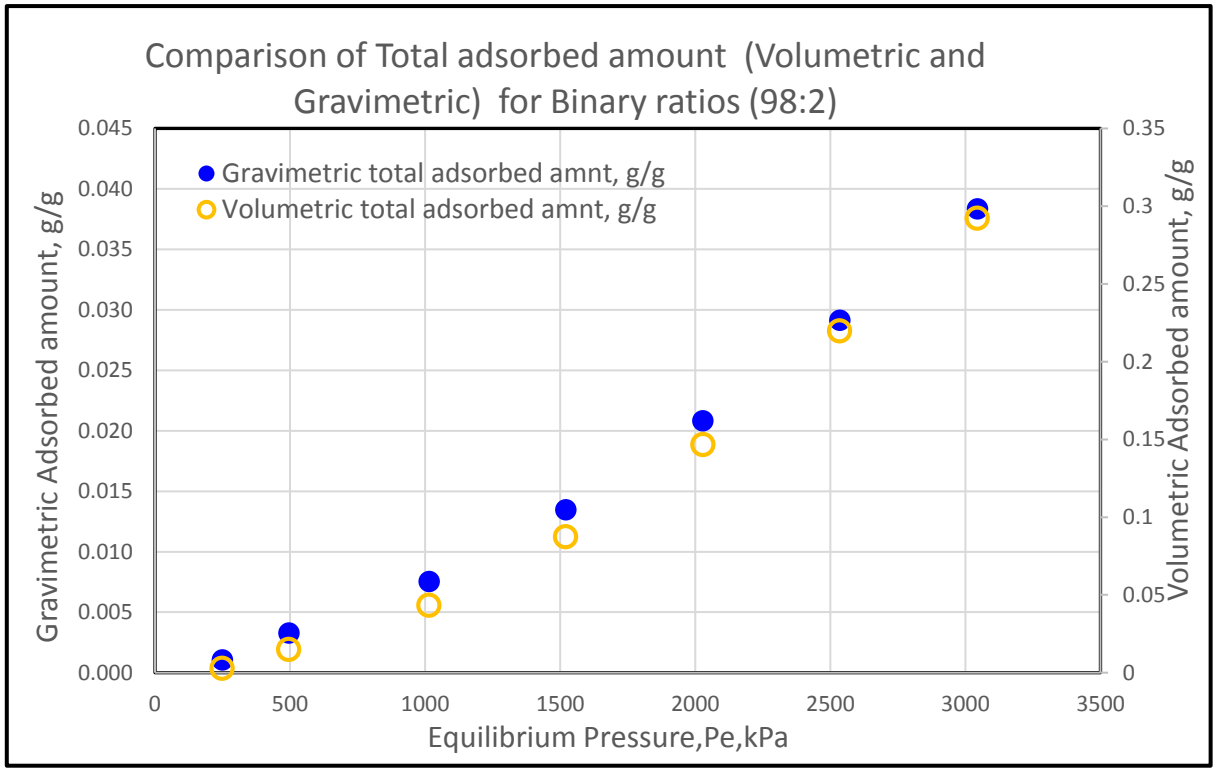

Figure 3-9 Comparison of adsorbed amounts (Gravimetric and Volumetric methods)

However, the plot Figure 3-10 added adsorbed volumes of CH_4 and CO_2 measured and the trend with changing pressure ranging from 500-3000 kPa.

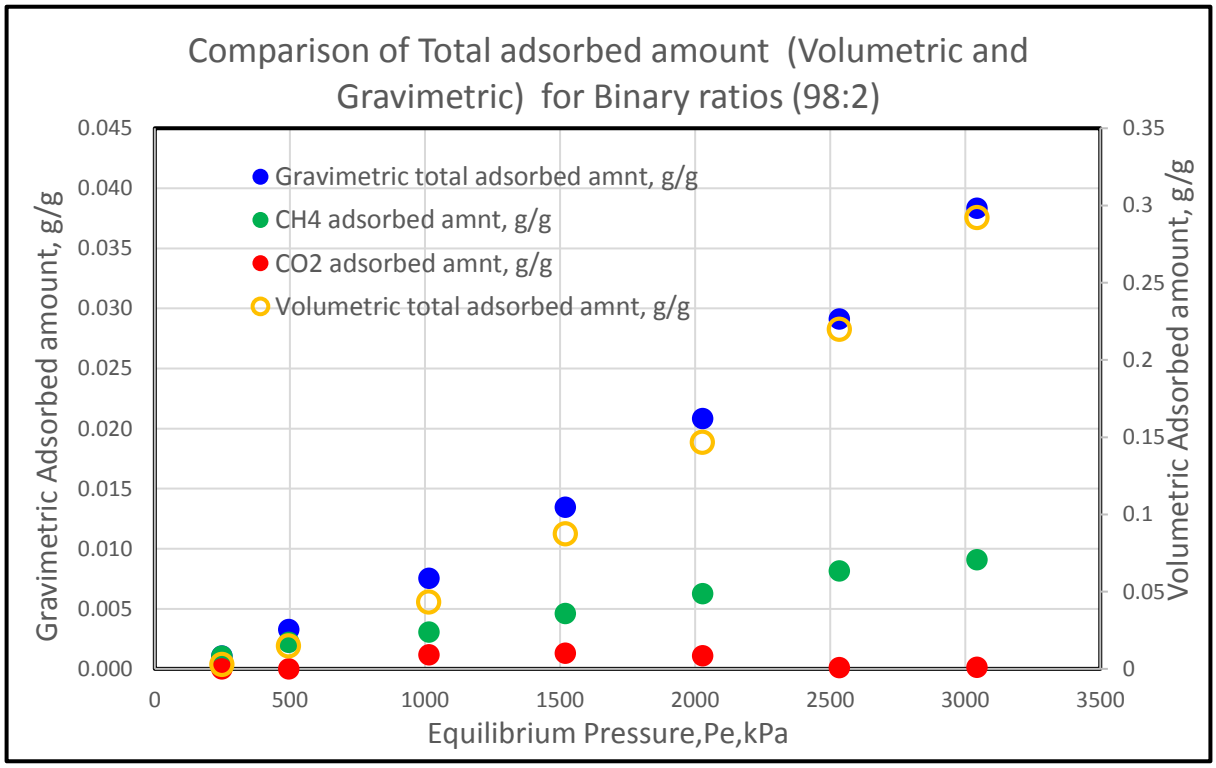

Figure 3-10 Comparison of Total adsorbed amounts (Volumetric and Gravimetric methods)l

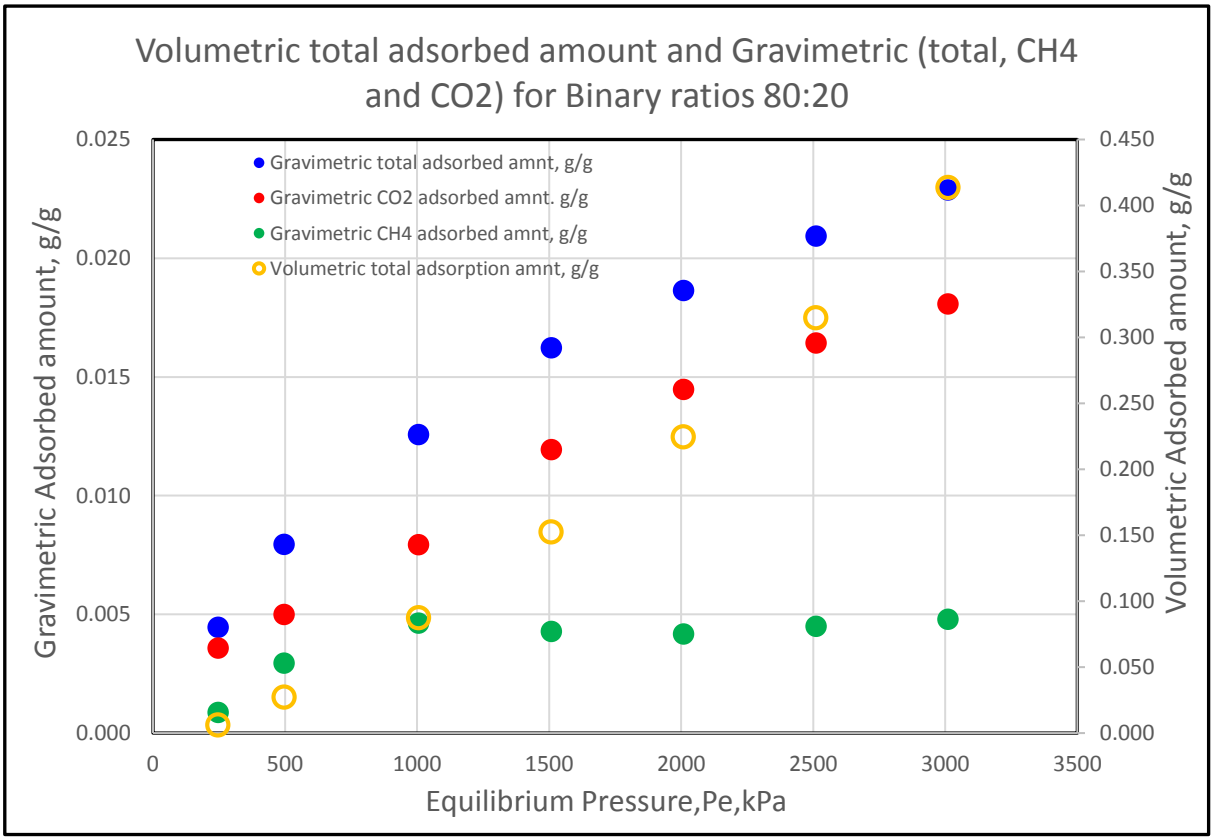

Figure 3-11 Binary Adsorption measurement from total and individual adsorbates (Gravimetric and Volumetric)

Figure 3-11 presents all the adsorbed amount data (total adsorbed amount from Gravimetric and Volumetric), (individual single component, CH4 and CO2 adsorbed amounts). There is an increasing trend between total adsorbed amounts from two methods and CO2 adsorbed amount vs. equilibrium pressure. But CH4 adsorbed amount showed more or less constant after 1000 kPa. However, total adsorbed amount from gravimetric method is equal to the sum of CH4 and CO2 adsorbed amount (the calculated adsorbed amount) for the entire testing period. At least mass balance can be assumed correct.

3.3.3 Binary gas adsorption calculation

Binary adsorption isotherm can be determined by either the constant volume method or the weight method.

The constant volume method gives the adsorption mole number (X) which includes the adsorption mole numbers of each gas (in this study, methane and carbon dioxide) using the EOS (Equation of State); Virial equation of state was used in Belsorp calculation of number of moles adsorbed for individual adsorbates.

$$Snx + Sny = X \qquad (3-1)$$

Where total adsorbed amount X, ml is known and,

Snx, Sny are number of moles adsorbed for adsorbates

'Y" (methane) and 'X' (carbonate dioxide).

X is the total number of moles adsorbed for two adsorbates. In the Belsorp calculation sheet, volumetric adsorbed amount is mentioned as ml [STP]/g (see the example excel sheet provided in Table 3-8).

On the other hands, the weighted method provides the adsorption weight (Y).

$$Snx.MWx + Sny.MWy = Y \qquad (3-2)$$

	Gravi Mas	g	mol	mol		g	g	g/g
V	Ads Mass	dW	dV_mol	Snx		Wx	Wx	Wx/g
ml	g			1		1	3	Gravi wt
			11			13		
7.29	0.00982	0.00982	9.50904E-05	0.000296632		0.01305477	0.0098214	0.00287
17.47	0.01827	0.00845	0.000132682	0.000226123		0.01977312	0.018274	0.00534
22.58	0.02943	0.01116	6.65843E-05	0.000360705		0.03414869	0.0294301	0.00860
32.17	0.03877	0.00934	0.00012502	0.000262332		0.04097535	0.0387724	0.01133
38.37	0.04606	0.00729	8.08474E-05	0.000214254		0.04820178	0.0460615	0.01346
51.68	0.05143	0.00537	0.000173592	9.25295E-05		0.05013375	0.0501338	0.01465
52.34	0.05623	0.00479	8.53261E-06	0.000166412		0.05745757	0.0562252	0.01643

Table 3-6 showing Adsorption measurement from Gravimetric and Constant Volumetric methods.

where MWx, MWy are mole weight of adsorbates *'y'* (methane) and '*x'* (carbonate dioxide). The weighted method gives weight of adsorbed amount per unit weight (g/g) (see example provided in Table 3-8)

3.4 Limitations of Belsorp BG

As mentioned earlier in the experimental set up and experimental procedure, the adsorption measurement was conducted using the weight measurement system (balance). As a critical part of experimental procedure, measuring dead volume and sample cell volume and changes of sample volume must be done accurately and repeatedly throughout the experiment.

From the experience of using two vastly different ratios of pure components (in this study, CH_4 and CO_2 ratios such as 80:20) an observation was made that CO_2 partial adsorbed amount could not be measured at pressure higher than 3000 kPa for binary ratio (80:20, 90:10, 94:6 etc.). The limitation of the Belsorp machine was confirmed by the Belsorp corp. It is essential to receive a higher CO_2 cylinder pressure as an incoming dosing pressure for CO_2 dose (which is very little compared to CH_4 dose due to significant ratio difference). It is also suggested to obtain a booster pump as an additional requirement to achieve the measurement at the higher pressure because CO_2 cylinder has maximum 4500 kPa as a starting point. CO_2 cylinder pressure depletes quickly throughout the test.

The pressure-volume relationship during the Binary adsorption measurement using CH_4:CO_2 (50:50) and CH_4:CO_2 (80:20) is elaborated and explained the issue more clearly using the excel spreadsheet provided below.

Two cases with different ratios of CH_4:CO_2, namely 50:50 & 80:20 are presented here. Basically, all the volumes (dead volume, sample cell vs1, vs2) are measured for both cases and the values are same; Vd =165ml, VS 1_C_B = 40.193 and VS2_B = 37.53 ml.

Table 3-7. The effect of different dosing

CH4:CO2 50:50

Example1		Total Pressure	Partial Press	Partial Press	Total Press
CH4	CO2	Pi	Pix	Piy	Pe
VS1_C_B	VS2_B	(KPa)	(KPa)	(KPa)	(KPa)
40.193	37.53	16000	8000	8000	5123.
			vs1+vs	vs1+vs	
ml	ml	vs1+vs2	2	2	
Vd		77.732	77.732	77.732	
165		ml	ml	ml	
ml					

Dosing `CH4`gas to Vs1

Necessary Pressure	15471.7	KPa

Dosing `CO2`gas to Vs2

achievable Pressure	16565.6	KPa

CH4:CO2 80:20

Example2		Total Pressure	Partial Press	Partial Press	Total Press
CH4	CO2	Pi	Pix	Piy	Pe
VS1_C_B	VS2_B	(KPa)	(KPa)	(KPa)	(KPa)
40.193	37.53	10000	8000	2000	3202.3
			vs1+vs	vs1+vs	
ml	ml	vs1+vs2	2	2	
Vd		77.732	77.732	77.732	
165		ml	ml	ml	
ml					

Dosing `CH4`gas to Vs1

Necessary Pressure	15471.7	KPa

Dosing `CO2`gas to Vs2

achievable Pressure	4141.4	KPa

The difference is dosing ratio of CH_4:CO_2. Example 1 has 50:50 ratio for CH_4 and CO_2 whereas Example 2 ratio is 80:20 CH_4:CO_2. As a result, the partial pressure for two different ratios will be different as shown in the table below

For the Example 1, the initial pressure was set to 16000 kPa which is made up of partial pressures of 8000 kPa for CH_4 and CO_2 equally since the gas mixture is made up of 50:50 of CH_4 and CO_2 .The precise description of the phase of the fluid is not important. In fact, the mixed fluid will be a gas below supercritical conditions.

On the contrary, in the Example 2, initial pressure, Pi is 10000 kPa which is the sum of two partial pressures 8000 kPa and 2000 kPa for CH_4 and CO_2 (80:20)

CO_2 partial pressure is influenced by low dosing pressure 4141.4 kPa, as a result total achievable pressure for CO_2 20% case is only 3202.38 kPa. The only way to achieve the desired equilibrium~5120 kPa is to use booster pump to raise pressure for CO_2 dose to 8000 kPa.

These are some workaround solutions to improve the Belsorp BG performance.

Hooked up with booster pump to CO2 cylinder in order to achieve required dosing pressure

Using pre-mixed single cylinder with high pressure

Modify algorithm of the software that controls the operational procedure of Belsorp machine.

The first option can be easily implemented. But a cautious plan is needed to maintain CO_2 at required experimental temperature.

The second option was planned to implement to improve the Binary results, but the permission to modify to collect gas sample was not granted to pursue. The idea was dropped.

The third option means the whole algorithm needs to be re-written, that will be costly and time consuming option with a lot of tests to verify a new algorithm works.

For this study, neither option is considered, the data obtained from highest possible pressure (~425 psi) will be used and will be extrapolated to a desired pressure (~800 psi) if necessary.

3.5 Analysis of experimental data and workflow to determine Binary Adsorption Equilibria

In this section, using single isotherms in determining optimized parameters from selected theories or models (e.g. Langmuir, Toth models) are provided. Using the parameters from selected models, binary adsorption isotherms with different ratios of free gases (CH_4:CO_2) (e.g. 10:90, 20:80) are determined on the basis of Ideal Adsorption Solution Theory (IAS Model) [20, 21]. Subsequently, the resultant binary isotherm data (total adsorbed amount for the mixture) are compared with Belsorp measured data to validate whether the experimental data are acceptable so that model generated binary isotherms can be used in the numerical modelling to predict gas concentration profile for some years forward.

3.5.1 Analysis of Single Component Isotherm data and to determine Parameters from respective models used

In this section, examples of single component isotherms (CH_4, CO_2) are presented, discussed compared with data from ASAP data from coals from the same location.

All single component isotherms (N_2, CH_4 and CO_2) were measured using Belsorp BG Machine at 45ºC and maximum ~6500 kPa (~6.5 bar).

The following section presents single isotherms measured using the Belsorp BG machine and the comparison of them with data from ASAP test on Surat coal samples.

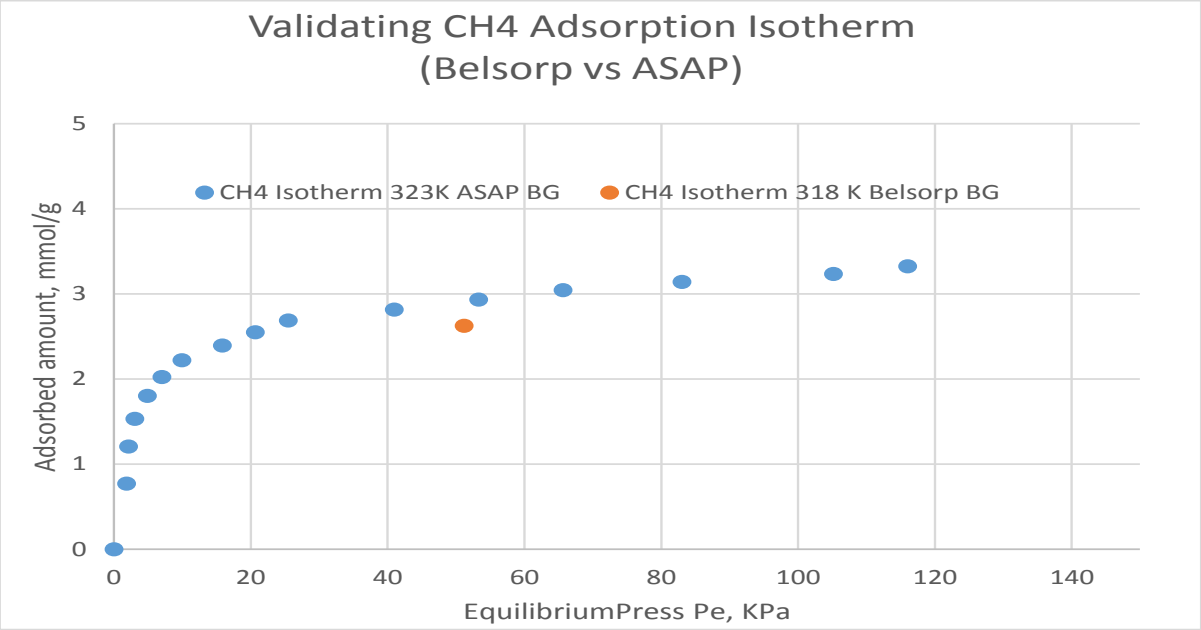

Figure 3-12 illustrates the comparison of two CH4 isotherms at 45°C

Similarly, CO_2 single isotherm measured by Belsorp machine and the comparison of the measured data against data from available ASAP coal samples from the same location are presented to ensure the single isotherm data are compatible and reasonable to use for further analysis to determine binary adsorption data.

The lab measured data show similar trends with ASAP data for the low pressure ranging up to 800 kPa. The comparison had been made possible for the maximum pressure of 800 kPa since the literature data were measured at maximum pressure of 800 kPa.

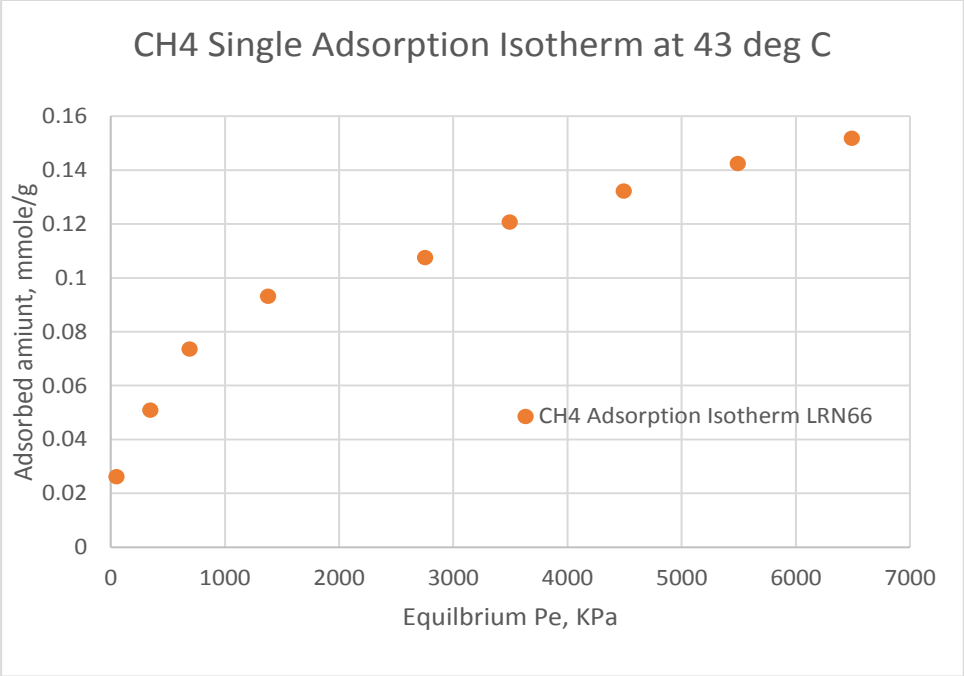

Figure 3-13 shows CH_4 Single Isotherm measured from coal sample at 316 K

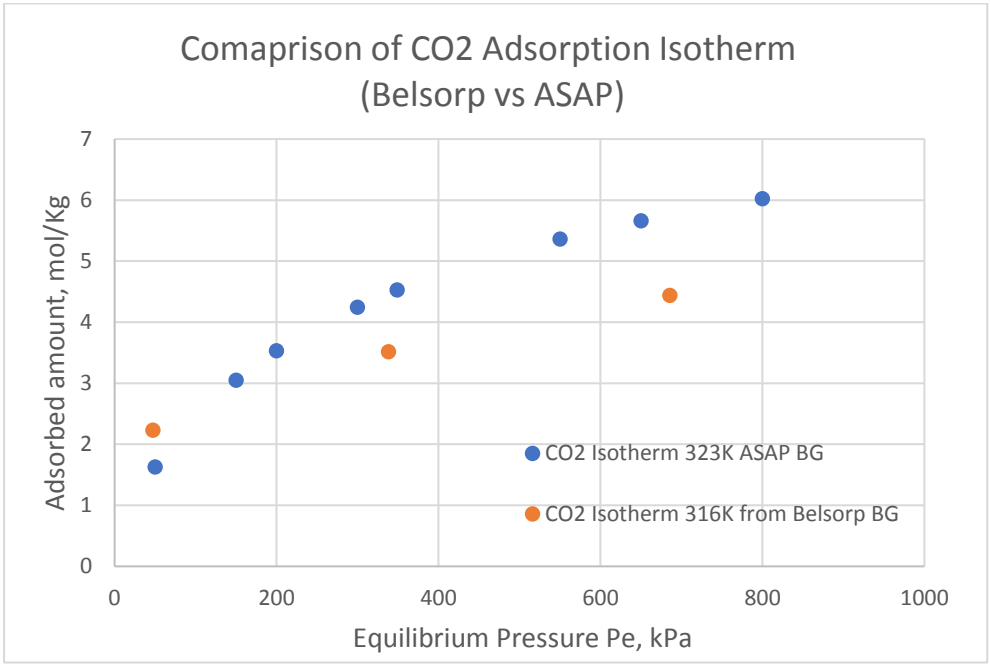

Figure 3-14 illustrates the comparison of two CO_2 isotherms

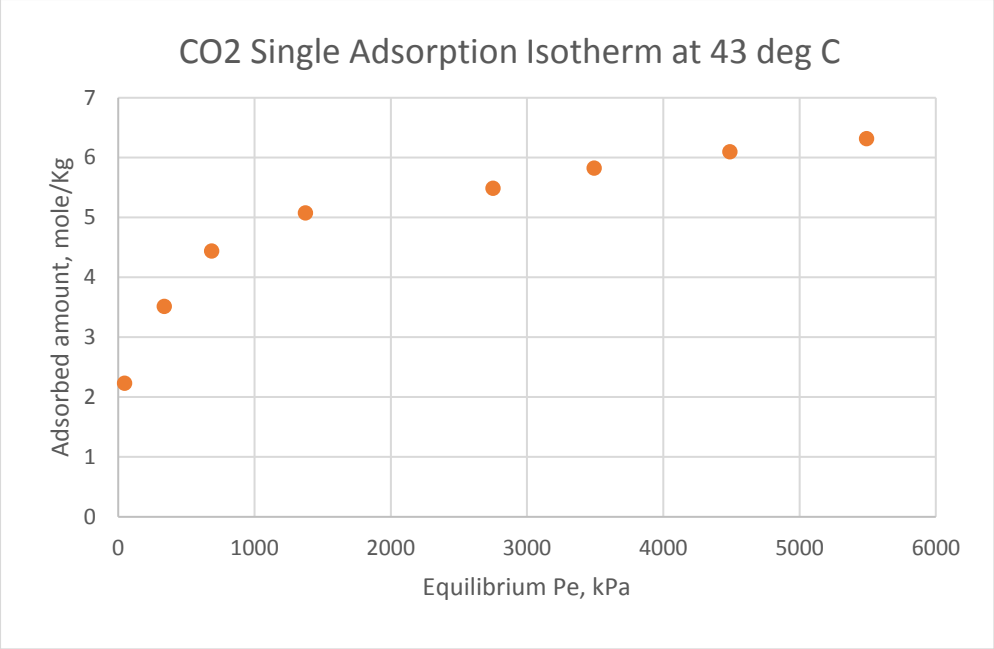

Figure 3-15 shows CO2 Single Isotherm measured from coal sample at 316 K

Next step in analysing single isotherms involves fitting experimental data with selected models (Langmuir, Toth, Sips etc.) to determine parameters that can be used in the model (IAS, Ideal Adsorption model) to predict spreading pressure, partial pressure and adsorbed amount of mixture for given binary ratios and under some pressure and temperature conditions.

Fitting experimental data from Belsorp is presented here in order to show the workflow to achieve binary adsorption equilibria from single component isotherms. In the Appendix A, all of the isotherms (ASAP 2020) and the resultant fit data will be presented for the sake of completeness.

The couple of examples of fitting Belsorp Isotherm data (CH_4,CO_2) with Sips, Langmuir and Dual Langmuir models are presented in the following plots (Table 3 7, Figure 3 16 and Figure 3 17).

The resultant optimal parameters for respective models are provided in Table 3-8

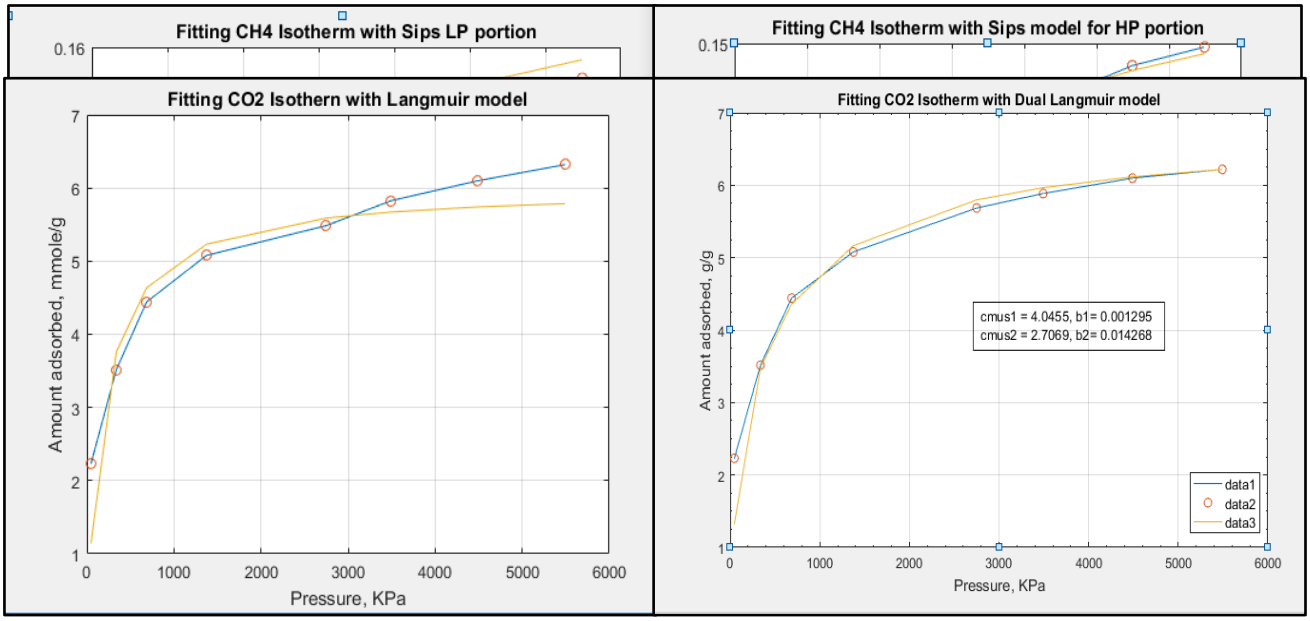

Figure 3-16 Measured CH_4 Isotherm was matched using Sips model for LP and HP portion of the tests

Figure 3-17 Measured CO_2 Isotherm was matched using Langmuir model and Dual Langmuir Model

In Figure 3-16, the plots for CH_4 Isotherm fit with Sips model as two portions. The first plot shows the match attempted to obtain a better fit at LP (lower pressure range) whereas the second plot delivers a better match at higher pressure range (HP). The prediction will be trailed out with both equations to cover uncertainties of the experimental measurements.

The resultant binary data from prediction using these parameters will be assessing in relation to the final gas concentration production prediction from the simulation model (the detail of simulation results will be discussed in section 5 “Numerical simulation with case studies”).

Table 3-7 Optimized parameters from the Fitting Model data vs. Experimental Data

Single Component	Model	Fitted Parameter Values (T = 293K)		
		Cμs (mmole/g)	b (kPa^{-1})	t
CH_4	Sips	4.88	0.016	n = 1.4
CH_4	Toth	4.78	0.01156	t = 0.9
CO_2	Langmuir	3.98	0.0442	

The parameters obtained from the matched are used to predict Binary Adsorption Equilibria with selected theoretical model (IAS Model as an example).

In this section, only a couple of examples with Sips and Langmuir models with the parameters obtained from the fitting with experimental data is presented. More results fitted from models with respective parameters and the resultant Binary Isotherm predicted from chosen model will be presented in the result and discussion section in detail.

3.5.2 IAS model data and Belsorp data comparison and issues

As part of quality control on Belsorp measured binary adsorption isotherm data, total adsorbed amount generated from the experiments for different binary component ratios (CH_4:CO_2, 20:80, 15:85, 10:90, 4:96) were plotted for similar pressure ranges.

It is convinced to observe the total adsorbed amount for different Binary ratios have consistently increasing trends with increasing pressures.

However, the adsorbed amounts for individual adsorbates (CH4 and CO2) (Wx, Wy in Belsorp work sheet) do not show a regular trend, the trend shows more irregular nature.

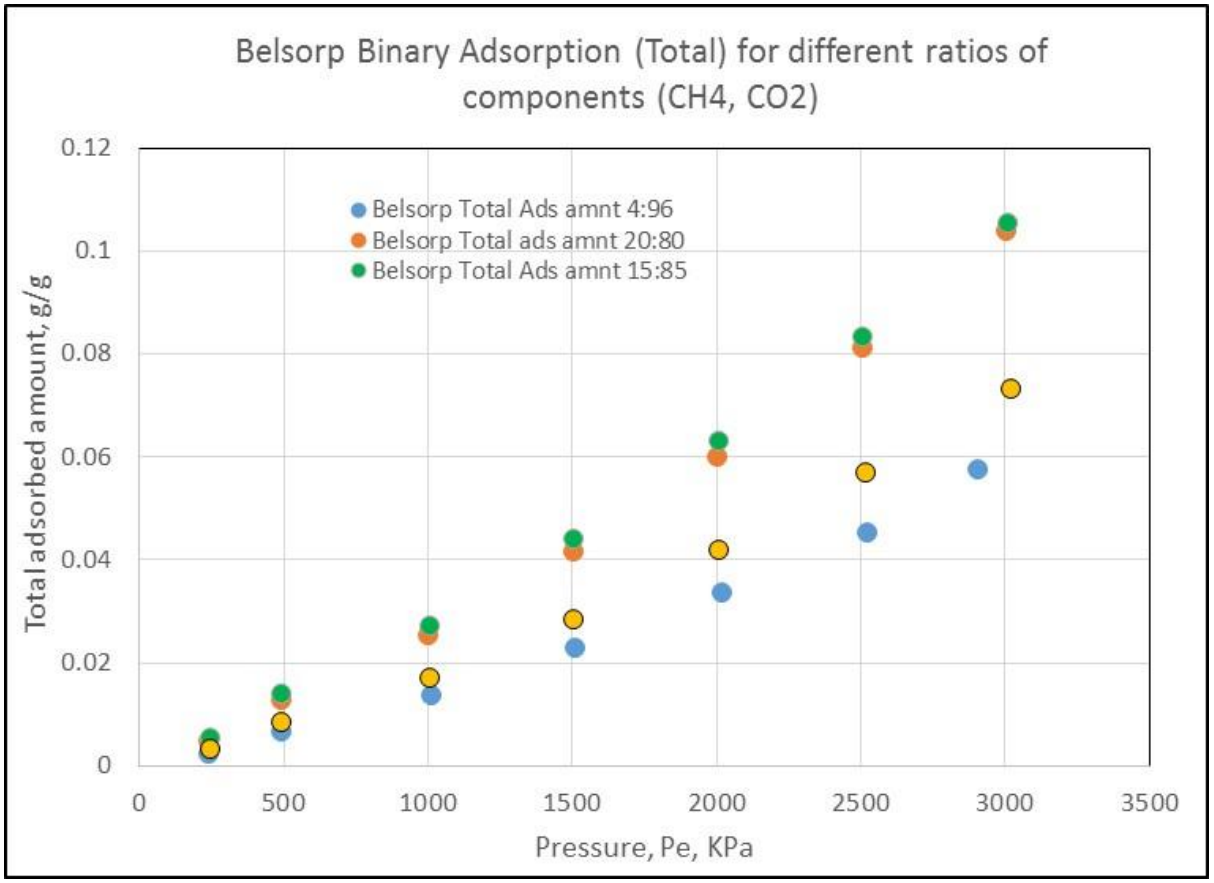

Figure 3-18 Comparison of Belsorp measured total adsorbed amount for different ratios of components (CH4 and CO2)

Applying IAS theory model with parameters from single isotherms, CH_4:CO_2 (94:6) ratio Binary Adsorption data (adsorbed phase mole fraction and concentration for mixed adsorbate) were calculated. To ensure the model generated data for Binary Adsorption Equilibria is realistic, the data from Literature were used to verify these set of data (shown in the Figure 3-18).

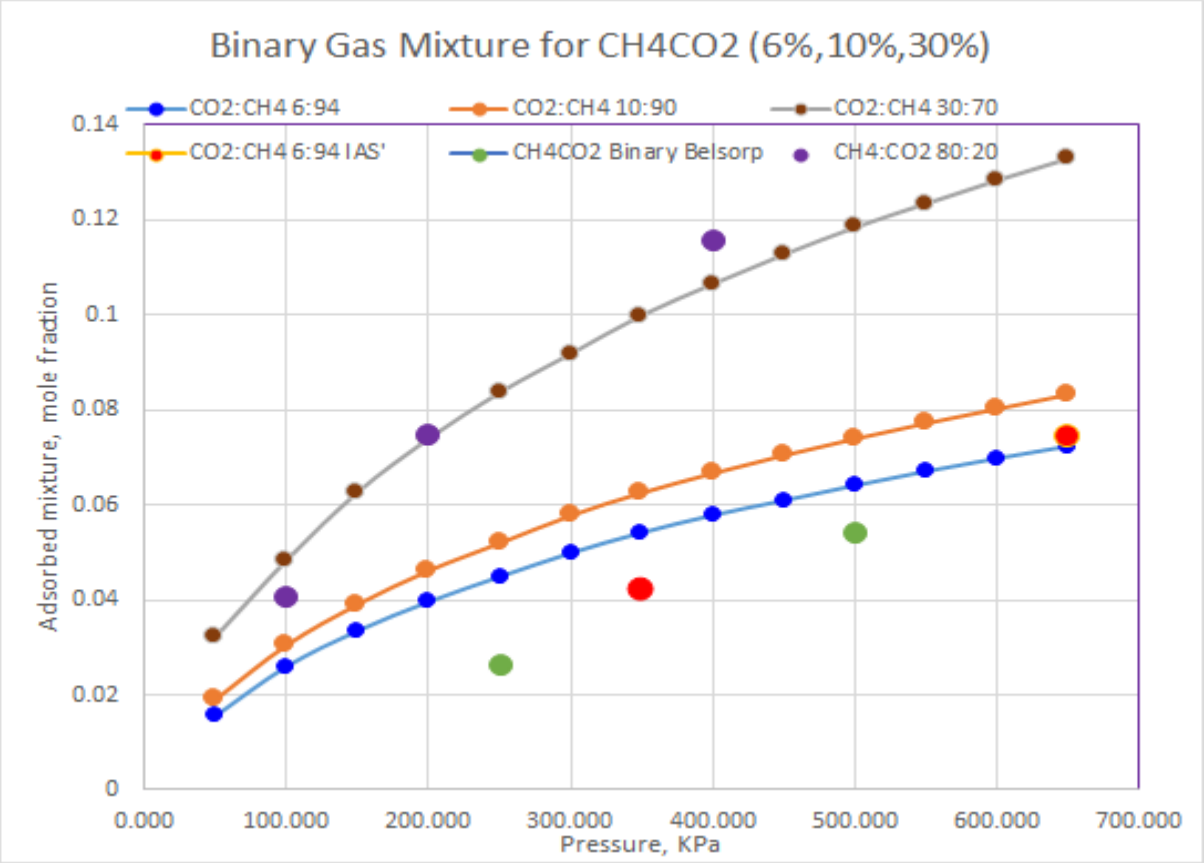

Figure 3-19 Comparison of Binary Adsorption Isotherms generated from IAS model, Belsorp measured data and Literature Binary Isotherm curve [22, 23]

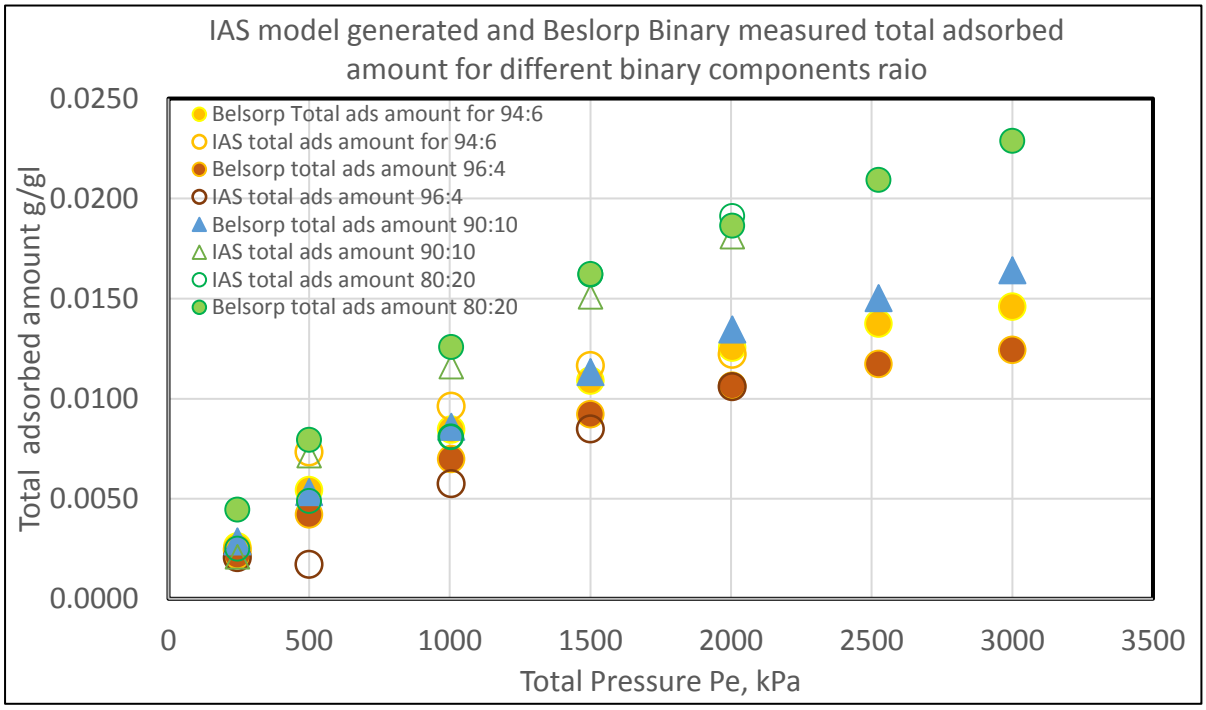

Figure 3-20 IAS model data vs Belsorp Measured data (total adsorbed amount, CH_4 and CO_2 adsorbed amount for 10:90 ratio case)

Table 3-8 Parameters obtained from IAS model using Single isotherm matched parameters for binary adsorption isotherms

Master Table for all calculations from IAS model for different ratios at different pressure using Sips, Toth and Langmuir models

	CH4:CO2	94:6			96:4			90:10			85:15			80:20		
Isotherm Model		Sips	Toth	Langmuir	Sips	Toth	Langmuir	Sips	Toth	Langmuir	Sips	Toth	Langmuir	Sips	Toth	Langmuir
PT =101																
Spreading P		0.055759	0.019353	0.038899	0.046452	0.0149	0.029138	0.071578	0.039798	0.060278	0.093887	0.054814	0.085481	0.071578	0.039798	0.11057
po1 KPa		224.5674	649.9492	450.0042	176.7094	442.8991	328.6078	340.4249	1123.4	708.3029	523.8109	1816.9	1063.8	340.4249	1123.4	1458.5
po2		10.4984	7.0961	7.6804	8.919	5.1721	5.731	13.7794	0.011	11.587	18.1198	1.59	1.65	13.7794	0.011	2.14
x1 mole frac		0.4228	0.1461	0.211	0.5487	0.2189	0.2951	0.267	0.0809	0.1283	0.1639	0.0473	0.0807	0.267	0.0809	0.0554
x2		0.5772	0.854	0.789	0.4513	0.7811	0.7049	0.733	0.9192	0.8717	0.8361	0.9528	0.9193	0.733	0.9192	0.9446
cmuT mmole/g		0.044807	0.02325	0.039181	0.036647	0.017608	0.029287	0.062081	0.034041	0.058887	0.08472	0.04639	0.08364	0.062081	0.034041	0.10766
cmu1		0.0189	0.0034	0.0083	0.0201	0.0039	0.0086	0.0166	0.0028	0.0076	0.0139	0.0022	0.0067	0.0166	0.0028	0.006
cmu2		0.0259	0.0138	0.0206	0.0165	0.0138	0.0206	0.0455	0.0313	0.0513	0.0708	0.0442	0.0766	0.0455	0.0313	0.1017

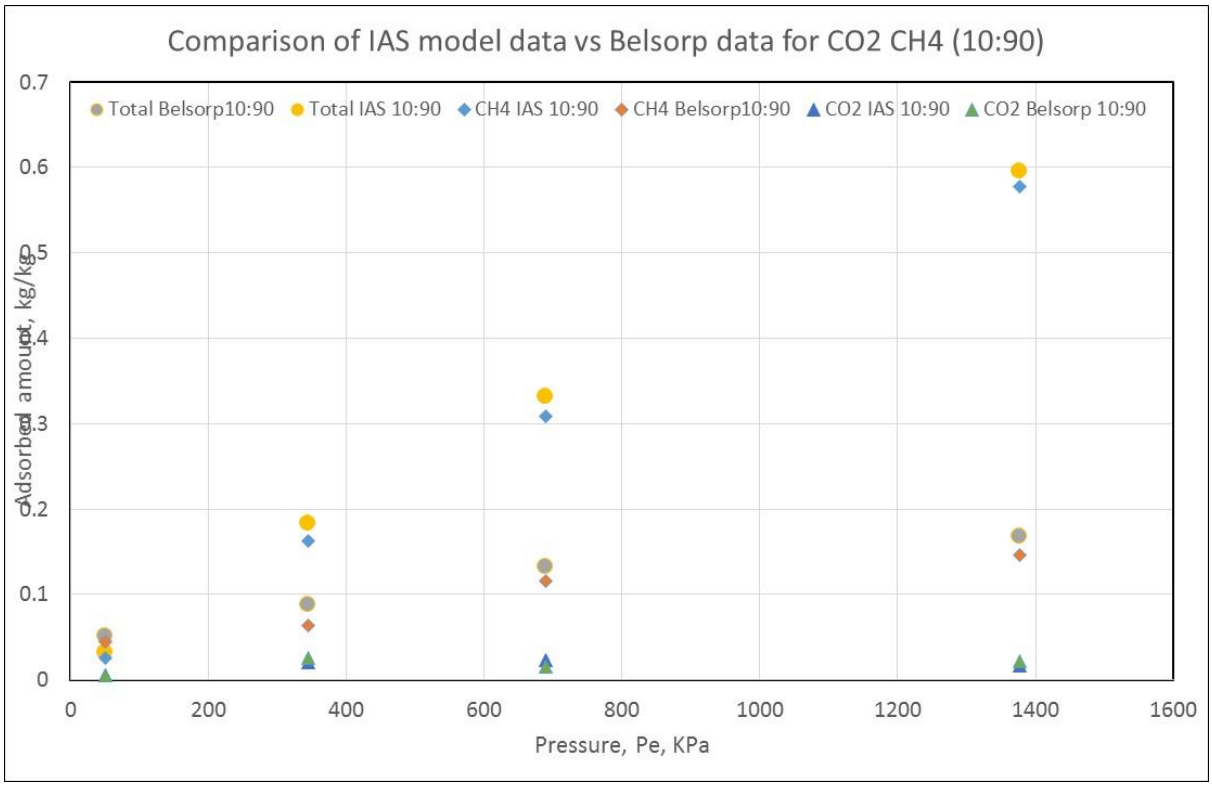

Figure 3-21 IAS model data vs Belsorp Measured data (total adsorbed amount, CH_4 and CO_2 adsorbed amount for 10:90 ratio case)

3.6 Conclusions

High Pressure binary adsorption unit (Belsorp BG) from BELL Japan Company was utilized to measure single and binary isotherms for coal powdered samples from Lauren field. The machine has provided excellent single component isotherms for methane and carbon dioxide gases. However, there is a limitation in the Belsorp machine to measure binary sorption isotherm with one component being very low ratio (i.e. CH_4:CO_2, 98:2). There are some suggested solutions that can be used in future projects and brief discussion was made on this matter.

From reliable and repeatable single component isotherms with IAS theory was employed to generate desired binary adsorption isotherms. Detail methodology is presented with example data from this project. Among three models utilized to generate binary isotherms, Toth model is the most agreed binary isotherms fitted to the experimental results. It is worth noted here that only binary ratio (CH_4:CO_2 80:20; 85:15, 90:10) were used due to the inaccuracy of the results for the Binary isotherms with binary ratios (CH_4:CO_2, 94:6 to 98:2).

Detailed results from three models in combination with IAS are provided in a tabular form for all binary ratios for CH_4:CO_2. Nevertheless, only the binary isotherm data will be used in simulation for predicting gas concentration (CH_4 and CO_2) profiles for future use in this particular field.

Chapter 4. SORPTION KINETICS IN COALS

This chapter explains gas transport modelling works on unipore and bi-disperse diffusion models (theoretical details of which are referenced to previous researchers' extensive work [55–58]*). This chapter covers the application of these models to experimental data from coals from Australia (Surat Basin) and shows that the bi-dispersed model is better than a unipore model, probably due to effects of coal heterogeneity.*

The model was regressed to determine gas diffusion coefficients for a respective porous model by matching parameters against some experimental data on coal samples. The adequacy of bi-disperse model in coal is re-enforced with superior matching of laboratory data. Some details of experimental data (pore size distribution, isotherms etc.) are presented and discussed to provide more insight on the relationship between porosity models and coal heterogeneity.

4.0 APPLICATION OF DIFFERENT MODELS TO INVESTIGATE EXPERIMENTAL DATA

Before utilizing experimental data in the numerical models to determine diffusion coefficients, some additional information on gas transport mechanism and its relationship with coal heterogeneity from previous research works are provided to discuss the importance of selecting an adequate model for coal seam gas transport mechanism [55–58].

Recent studies suggest that lower-rank coal (sub-bituminous and bituminous) usually exhibits a non-uniform pore structure with significant fractions of the total pore volume being larger than 30 nm and smaller than 1.2 nm [24].

Significant gas storage, through the mechanism of physical adsorption, occurs mainly in the coal matrix, which acts as a source for gas production [25] . The diffusion transport within the pores of the coal matrix follows the Fick's law of potential gradient dependent transport flux, wherein the gas molecules diffuse though the variety of pores [55]. In several historical investigations, the coal matrix is often assumed to consist of a uniform pore size and structure and that a single stage diffusion model is sufficient to describe the gas transport. Such presumptions often limit the accurate deduction of gas transport within the matrix. There have been several studies that have identified that the pore structure in a coal least homogeneous. At the lowest level of heterogeneity, a coal is considered to consist of micro and mesopore structures, where the micro pore structure are the gas storage location while the meso-pores are the larger channel which provides the access path to the micro-pore storage sites [26]

In this study, the focus is on two models of gas diffusion inside the coal, i.e. unidisperse gas transport model and bidisperse gas transport model, both of which have been commonly

explored and compared the transport prediction of the model with the experimental observations.

In a unidisperse, or also referred as unipore, gas transport model, the coal is assumed to consist of single type of pores in the entire matrix, which for convenience is referred to as micro fractures. The gas stored in coal desorbs out of the coal matrix and diffuses out though these micro fractures Once out of the matrix, the gas is then transported through the large channels present between the coal matrixes, referred to as cleats.

The primary assumption in the unipore model is that the micro fractures are considered to be homogeneous and hence a single diffusivity value is sufficient to describe the gas transport in the entire matrix.

In contrast, the bidisperse model assumes that coal matrix consists of two types of pores, i.e. micro pores and mesopores. The model, thus requires at least 2 diffusivity values to independently describe the gas transport within the micro and mesoporous structures.

There have been various reports on describing the transport within the coal matrix in three of even more types of pore hierarchies [26-29] however, such models often end up being computationally too expensive to be commonly utilised for any reasonable gas transport predictions. Besides, the multi-pore model requires an additional model parameter, i.e. the pore size distribution of each pore type, which is not only difficult to obtain but also varies significantly from site to site and even within different locations on the same sites.

Gas transport through the matrix is assumed to be concentration driven and is modelled using Fick's Law whereas the laminar flow through the cleat is pressure driven and can be modelled with Darcy's Law. But the purpose is to emphasize the two different driving forces (pressure and concentration difference). The shorthand "Darcy law" short-hand reference should be understood by readers to mean the equivalent of viscous flow

However, the coal matrix diffusion has little effect upon long term gas production from coal seams whereas gas transport through the coal seam fractures is considered to be a greater control upon the long-term gas production [27-29] . Therefore, it is worthwhile to investigate the adsorption rate data from experiments using different type and rank of coals from different locations against different types of models, namely; unipore and bidisperse models.

In the present investigation, the research work focused on modelling methane transport within the coal matrix based on the two models of coal matrix structures described above. To that end, some key assumptions made for the modelling are listed as below.

1. The transport process takes place under isothermal condition.
2. The transport inside the matrix takes place only by diffusion and hence the matrix is assumed to be free of any faults or large cracks.
3. There is no counter diffusion of any other species inside the pores.
4. In this study, the coal is assumed to be filled with only one gas, i.e. CH4.
5. Coal is composed of coal matrix. It contains pores various sizes micropores mesopores and macropores ranging from >50nm to <2nm.

The description of the pore structures within the coal matrix based on unidisperse and bidisperse model is shown below.

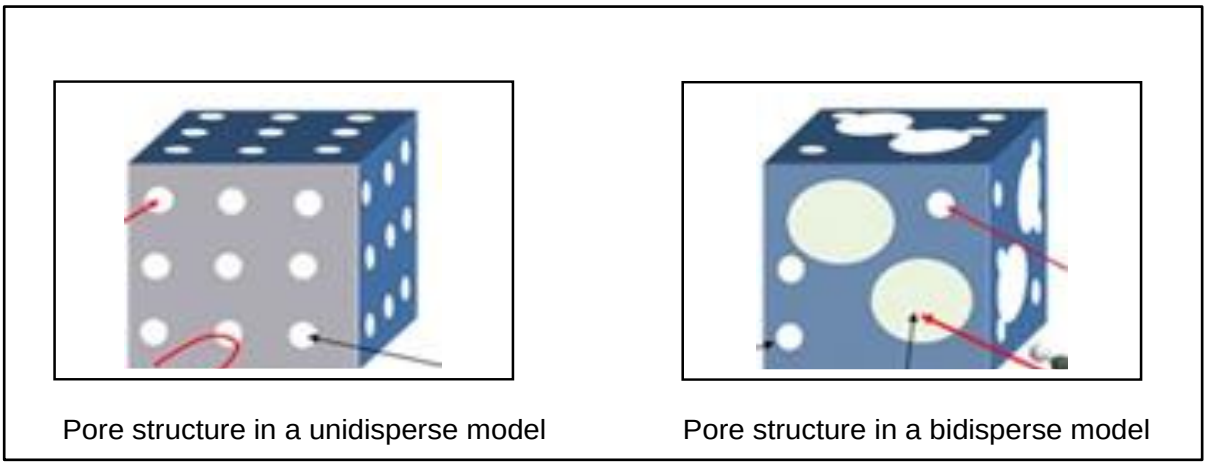

Figure 4-1 Pore structure in a unidisperse model and bidisperse model

To physically verify the proposed coal models, we have conducted some experiments to measure the uptake rate of methane gas inside the coal matrix. To that respect, a few coal samples were obtained from two different sites in Australia. The samples were carefully prepared for the experimental analysis as described below.

Sample preparation and experimental procedure to obtain diffusion and sorption data is described in this section to make this information more relevant with the presentation and discussion on the results generated from the corresponding tests.

4.1.1 Coal sample preparation

Few coal samples of coal piece “A” were randomly selected from an appraisal or exploration well in the coal seam of interest in a gas field. The gas transport within the coal sample was studied by subjecting the coal sample to a known concentration of methane gas.

However, prior to the experiment, the coal sample was hand-crushed and grounded to obtain fine particles. The particles were wet sieved to obtain an average size of roughly 80 microns. The upper limit of the samples size was 88 microns while the lower size was 75 microns. The aforementioned particle size was selected to ensure the absence of any large cracks within the particles which may cause result in some pressure dependent convection transport. On such a small particle size, a bulk convection transport is virtually ruled out. The sample was then air dried and degassed in a vacuum chamber at 80^{o}C and stored in desiccator until further use.

4.1.2 Method of measuring gas transport in small coal particles

The methane gas transport within the coal particle was studied by measuring the time resolved gas uptake form a batch system.

Prior to the actual test, the dead volume of the sample cell is determined using helium gas. Then, in a typical test, a fixed mass of sample particles was placed in a glass cell and degassed overnight at 80 ^{0}C to remove any atmospheric moisture which may have been adsorbed on the coal during sample loading. The degassed sample cell was transferred to the adsorption port where the sample was initially evacuated and then dosed with helium gas.

The sample was then evacuated and dosed with fixed amount of methane. The change in the cell pressure was recorded by the pressure transducer which was then used to calculate the amount of methane lost from the gas phase in the cell. The accuracy of pressure transducers was 0.01- 0.001 psig. In a closed system, the amount of methane lost from the cell gas phase is equal to the methane adsorbed inside the coal. That may be why there is some irregular trend in the Binary experimental data. The experimental data is validated with some data from literature to ensure the experimental error is acceptable. This is explained in the text

The instrument schematic is as shown in the Figure 4-1.

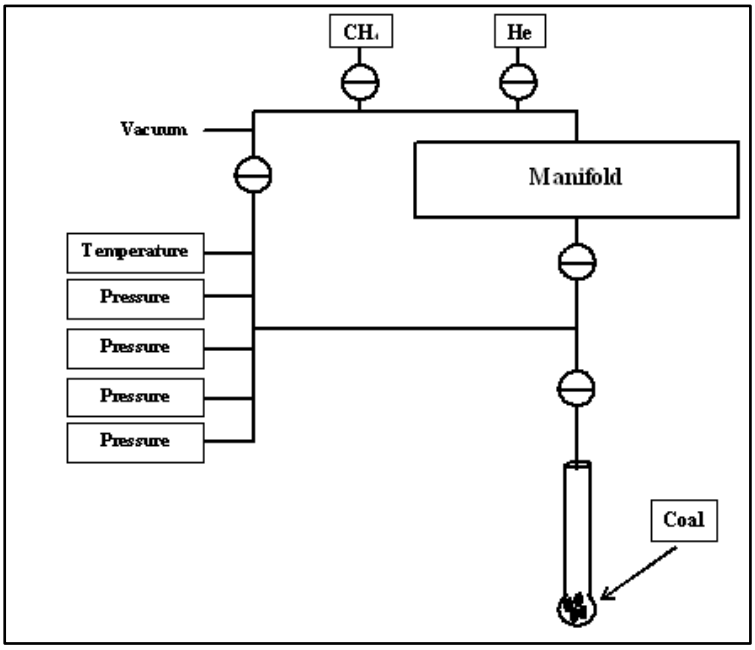

Figure 4-2 Experimental instrumental schematic for Adsorption kinetic measurement

The adsorption amount was calculated as from equation below

$$P_t = P_{init} + \frac{MZRT}{Ve}(C_{init} - C_t) \qquad (4-1)$$

Where P_t is the pressure in the cell measured by the transducer at time t; P_{init} is the initial cell pressure at time zero; M is the mass of the sample in the cell; R is the gas constant; T is temperature in the cell; Z is the gas compressibility factor; V_e is the dead volume of the cell; and C_{init} is the specific moles adsorbed.

The diffusion experiments were carried out at 3 temperatures (30, 50 and 70 ^{0}C) and numerous pre-determined experimental initial pressure steps from 26 to 100 kPa.

4.2 Describing gas movement in coal matrix

In this section, detail of unidisperse and bidisperse models will be presented and discussed.

Unipore and bidisperse models are employed to test the model results against experimental adsorption data and the optimized diffusion coefficients from two models are compared.

4.2.1 Unipore Model for gas transport in coal seams

In the unipore model, it is assumed that the coal particle consists of a single type of pores with uniform size. The coal particle is assumed to be spherical particles of 80 micron in size to match the experimental particles, as illustrated in figure 4.2.

The governing diffusivity equation in material (unipore) is developed using a mass balance on a radial element (spherical porous material) volume and Fick's diffusivity law. This can be expressed as an equation 4.2. The formulation and derivation of formula, model assumptions can be found from many previous research works

$$\frac{dC_p}{dt} = \frac{D_{eff}}{r^2}\frac{d}{dr}\left[r^2\frac{dC_p}{dr}\right] \qquad (4-2)$$

where , D_{eff} = the effective diffusivity in the coal particle

The above equation is coupled with the mass balance of methane in the cell to obtain the uptake profile in the coal particle.

The methane mass balance in the cell is given as

$$V_b\frac{dC_b}{dt} = \frac{3m_p}{\rho_p R_p}\varepsilon_p D_{eff}\left[\frac{dC_p}{dr}\right]_{r=R_p} \qquad (4-3)$$

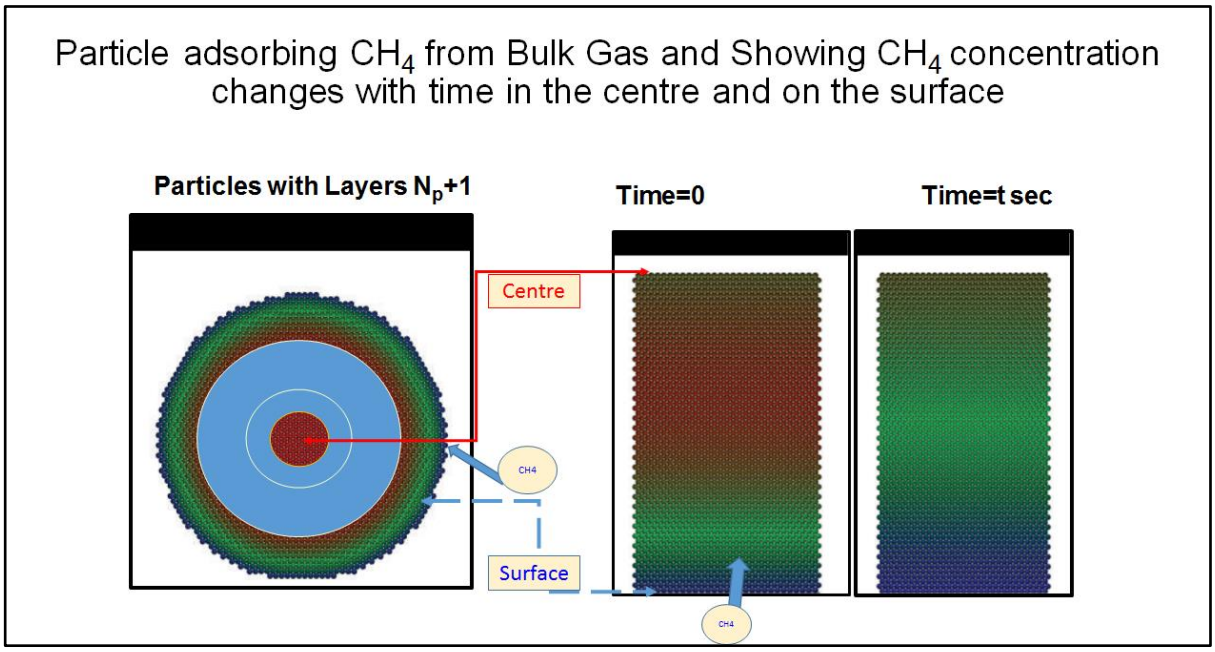

Figure 4-3 The microporous coal particle with R radius is subdivided into Np section [30]

The figure above illustrates the microporous coal particle with methane gas concentrations at Time=0 sec and Time=t sec. The colour scale represents the gas concentration from initial (Time=0 sec) and end of experiment (Time=t sec) at the centre of the particle and also at the surface of the particle. Detail gas concentration changes at initial condition, inner (centre)

and outer (surface) boundary can be formulated. The formulation is presented and explained as follows:

The above described partial differential equation with respect to time and particle radium is solved by discretising into spatial domain. The spatial discretization will require special boundary condition at the surface and the centre of the coal particle, given as follows:

Inner boundary condition; A symmetry boundary condition is assumed at the centre of the spherical porous material.

$$\text{Where } \frac{dC}{dt} = 0 \; at \; r = 0$$

Outer boundary condition: At the surface or outermost layer of the spherical porous coal particle, bulk concentration of the gas; $C_{bulk;}$ can be expressed as:

$C(R_p, t) = C_{bulk}$ (from the experimental data; $C_{bulk;}$ is 15.386 mole/ m^3)

Finally we also have the initial condition of the experiment, i.e.

Initial condition; Time = 0 sec

$$C(r, 0) = C_{init}$$

Where C_{init} is the initial gas concentration in the centre (innermost part) of the spherical porous matrix (from experimental data; ($C_{init;}$ 10.7174 mole/m^3) and C(r, 0) is concentration inside the particle at any position r and at Time = 0 sec.

Four powdered coal samples were tested in the lab to acquire sorption and Kinetic Diffusion data. In the following section, some of the data will be presented and discussed the relevance and adequacy of both models.

4.2.2 BG 2 Sample experimental data vs. Unipore model data

The gas concentration changes in the unipore model data for the centre, outermost layer the remaining layers and outside (surrounding area) are presented in Figure 4-4 and 4-5.

Figure 4-4 contains two plots showing CH4 concentration changes with time in the centre of the particle (on the left) and surface of the particle (on the right).

From the plot on the left, the uptake of methane in the centre of the particle is slow compared with the plot on the right, the methane uptake on the surface of the coal particle is instantaneous. It takes approximately 400 sec for the methane to reach the centre of the particle whereas almost the equilibrium has reached on the surface approximately after 500 sec. The surface of the particle at the ~ 500 sec is almost saturated. It is fully saturated on the surface after 1000 sec, more adsorbed methane will advance towards the centre of the particle.

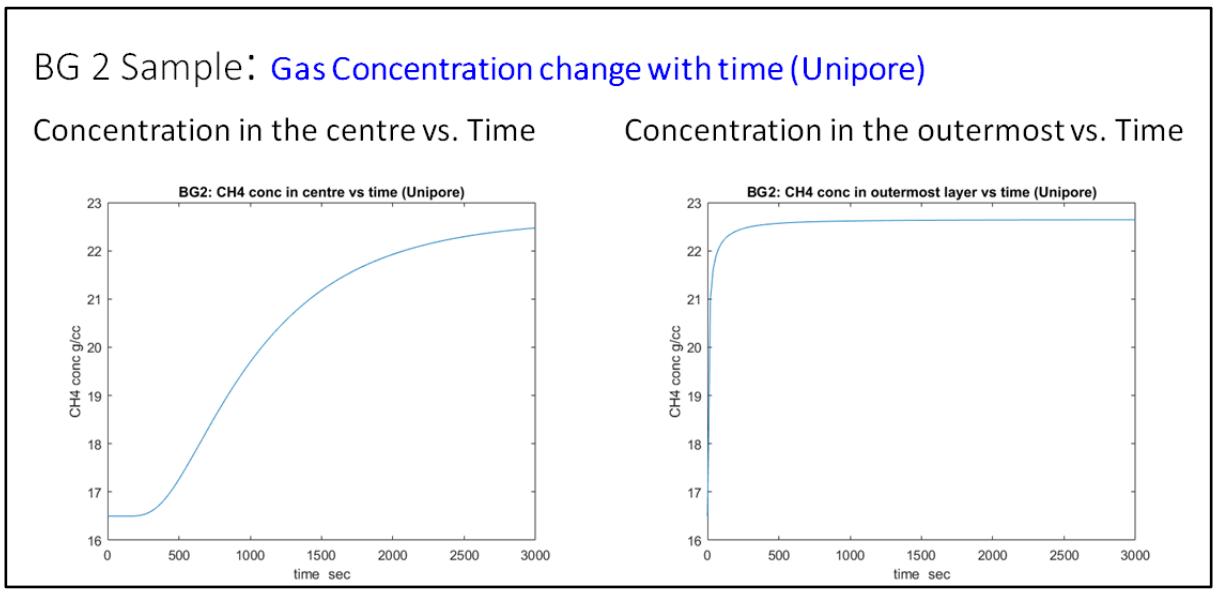

Figure 4-4 Concentrations in the centre and the outermost layer of the porous material (Unipore)

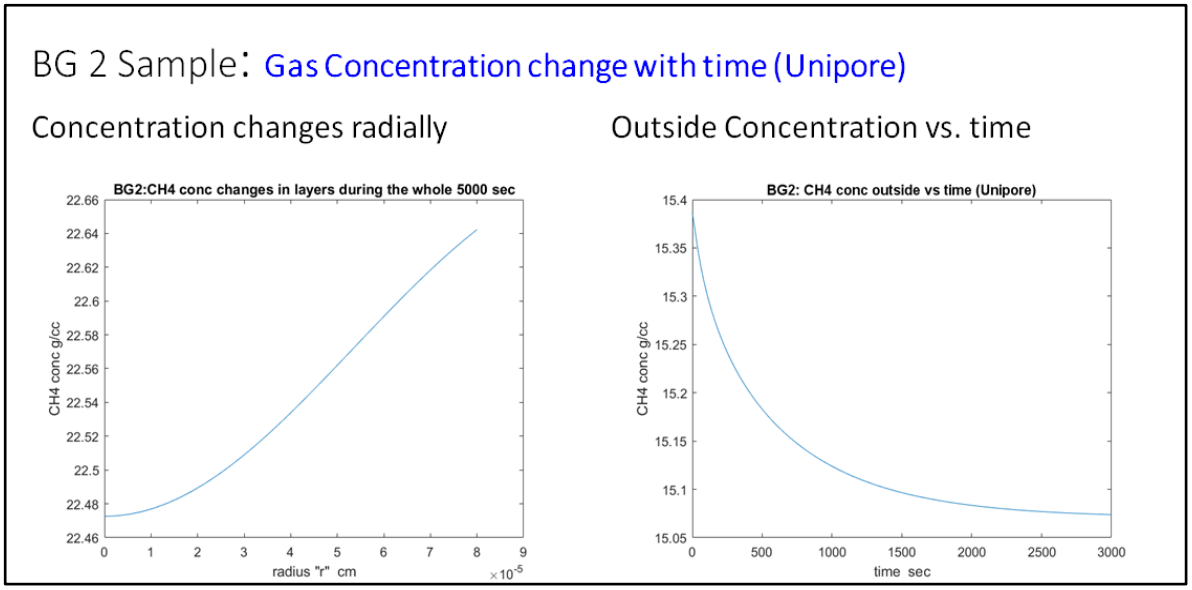

Figure 4-5 Concentration changes radially and outside (Unipore model)

Above Figure 4-5 has two plots; on the left, the plot illustrates methane concentration changes radially for the entire 5000sec, experiment time (i.e., methane change at r=1, 2, 3, 4 etc.

On the right of figure 4-5, it clearly shows that methane concentration outside environment gradually decreasing with time. The sharp change of methane concentration is observed until 1000sec and the change becomes slow and almost stable at the end of experiment (Time = 5000sec). It is about the time equilibrium has reached in this particular experiment.

BG2 sample unipore model data and experimental data matched plots were presented in figure 4-6.

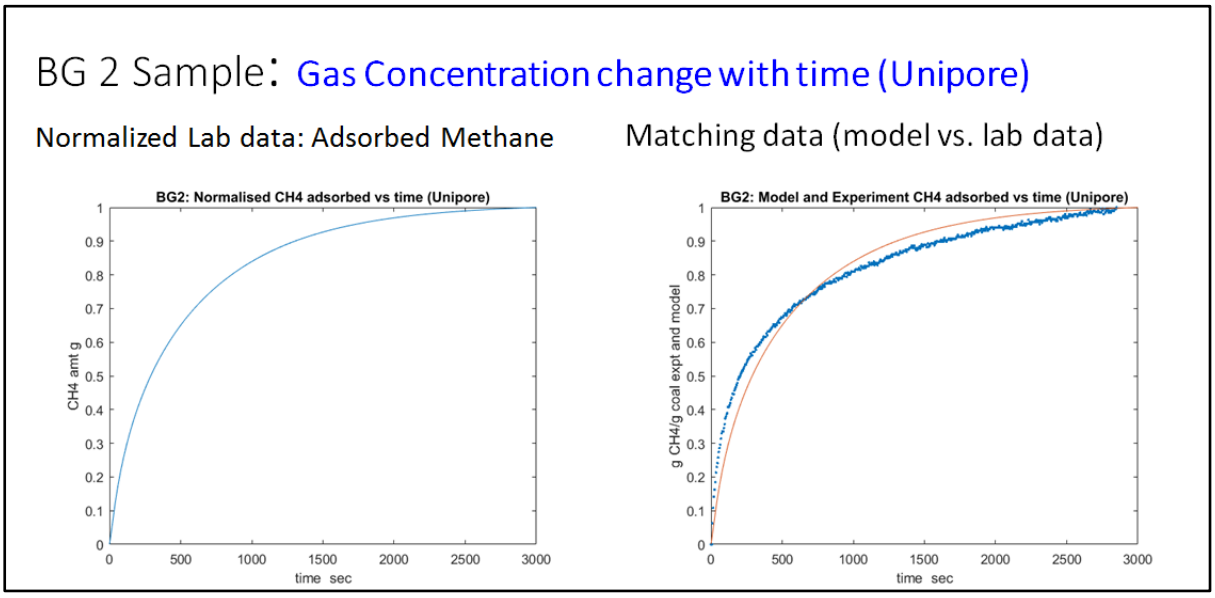

Figure 4-6 Normalized Lab data (Unipore) and fitted to the model data

Figure 4-6 attempts to demonstrate that unipore model data was not perfectly matched to the experimental data. On the left, the plot shows normalized experimental data vs. experimental time in sec. On the right of the Figure 4-6, it is clear that the model data (red line) was not fitted completely to the experimental data. Approximately first 500 sec, the experimental data is higher i.e. the experimental methane uptake in the initial period is much higher than the one from the model. At later period of the experiment, model methane uptake data was found to be much faster than the experimental methane uptake. The reason is that in the unipore model, the assumption was applied that all the pores are uniform and of equal size. On the contrary, the experimental data suggests that some of the pores are very large which allows very fast transport whereas few pores are smaller through which the transport is relatively slow, hence it took longer time to saturate.

4.2.3 Bidisperse Model for gas transport in coal seams

Based on the unipore model fitting we have found that there was significant discrepancy in the initial stage and later stage of the methane uptake within the coal samples. This suggest that the actual coal sample may consist of 2 types of pore structure which dictate the fast filling at the beginning and slow diffusion in the small pore. Coal structures have been well known to have a wide range of pore sizes which controls the overall transport behaviour. In a bidisperse model, the pure carbon part of the coal is assumed to consist of tiny micro particles which are agglomerated together due to the large overburden pressure in to larger particles. The pure carbon based microparticles would have a much smaller pore and hence high storage capacity of methane. Typically, the pore opening inside the microparticles would be the gap between the graphitic layers in the carbon. In contrast the spacing between such small carbon microparticles constitutes towards the macro or mesopores. These pores are essentially feeder channels which supply the gas to the outside of the microsphere which then diffuse inside the microparticles.

Brief development of the bidisperse model will be described with the schematic diagram shown in Figure 4-7.

A spherical macroporous particle which consists of many small spherical microporous particles of equal size [31, 32] The radius of microspheres is much smaller than that of the macrosphere.

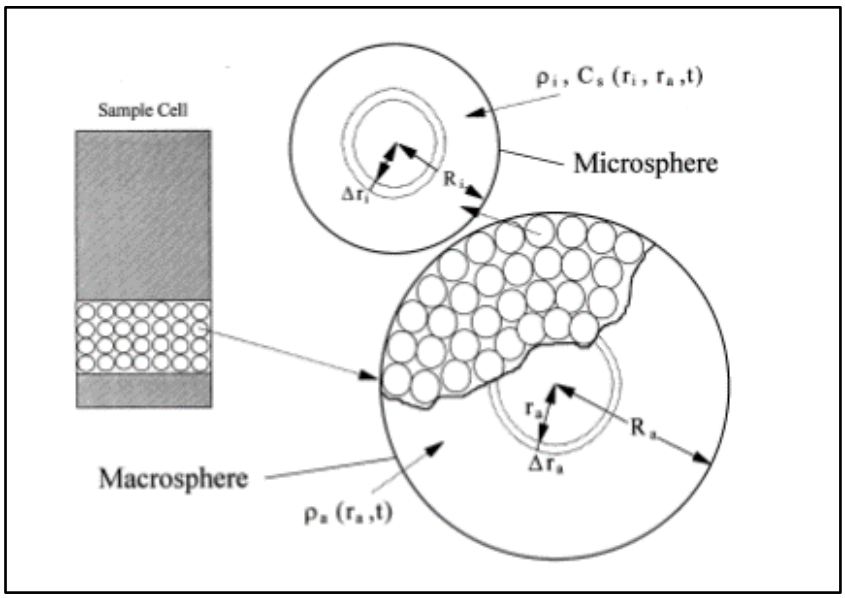

Figure 4-7 Schematic Diagram of a sorbent particle for a Bidisperse model [33]

The bidisperse conceptual model is developed as a single macrosphere particle which consists of many small spherical microporous particles of uniform size shown in Figure 4.7

The particle is initially at equilibrium with surrounding fluid (gas with concentration, C_{bulk}). At time (Time) =0, a change in the concentration of the gas external of the particle is made. Then, the gas diffuses into the macropores, adsorbs on the macropore walls, and also diffuses into the micropores and is sorbed the micropores [33]. A macrospherical coal particle with a radius R, is subdivided into many elemental spherical layers with smaller radius; r_1, r_2, r_3, r_{30}.

The methane gas transport within the elemental section of macro sphere is given as follows:

$$\varepsilon_p \frac{dC_p}{dt} = \frac{1}{r^2}\frac{d}{dr}\left[r^2 D_p \varepsilon_p \frac{dC_p}{dr}\right] - S_\mu D_\mu \left[\frac{dC_\mu}{dr_\mu}\right]_{r_\mu = R_\mu} * \frac{No\ of\ micro\ particle}{vol\ of\ pellet} \qquad (4-4)$$

On further simplification

$$S_\mu * \frac{No: of\ micro\ particle}{volume\ of\ pellet} = S_\mu * \frac{Total\ volume\ of\ micro\ particle}{volume\ of\ 1\ micro\ particle} * \frac{1}{volume\ of\ pellet} = \varepsilon_\mu \frac{S_\mu}{V_\mu}$$

Thus (4-4) simplifies to

$$\varepsilon_p \frac{dC_p}{dt} = \frac{D_p \varepsilon_p}{r^2}\frac{d}{dr}\left[r^2 \frac{dC_p}{dr}\right] - \frac{S_\mu}{V_\mu}\varepsilon_\mu D_\mu \left[\frac{dC_\mu}{dr_\mu}\right]_{r_\mu = R_\mu} \qquad (4-5)$$

With Initial and Boundary Conditions,

At the centre of the particle, a symmetry condition is applied, thus

At

$$r = 0, \frac{dC_p}{dr} = 0 \qquad (IC1)$$

since we have the ratio $\frac{1}{r}\frac{dC_p}{dr}$ in equation$BC1$, applying L'Hospital's rule to $IC1$

$$\lim_{\Delta r \to 0} \frac{1}{r}\frac{dC_p}{dr} = \frac{d^2C_p}{dr^2} \qquad (BC1)$$

At the surface of the particle, we have separated the isotherms for individual phases to represent the concentration on the particle surface with respect to the bulk concentration and the concentration on the surface of microparticles with respected to the localized particle concentration.

At

$$r = R_p, C_p = C_b \qquad (BC2)$$

$$r_\mu = R_\mu, C_\mu = \frac{q_{max} K_L C_p}{1 + K_L\, C_p} \qquad (BC3)$$

The mass balance in the microparticle phase is given as

$$\frac{dC_\mu}{dt} = \frac{D_\mu}{r_\mu^2}\frac{d}{dr_\mu}\left[r_\mu^2 \frac{dC_\mu}{dr_\mu}\right] \qquad (4-6)$$

Equation (4-6) is subjected to the following initial and boundary conditions

$$r_\mu = 0, \frac{dC_\mu}{dr_\mu} = 0 \qquad (IC2)$$

$$r_\mu = R_\mu, C_\mu = \frac{q_{max} b_L C_p}{1 + b_L\, C_p} \qquad (BC4)$$

The average concentration in the microparticle at any position r within the particle is given as

$$\overline{C_\mu} = \frac{3}{R_\mu^3}\int_0^{R_\mu} r_\mu^2 C_\mu dr_\mu \qquad (4-7)$$

Since we have used a finite volume vessel of liquid adsorbate, the overall methane balance in the experimental cell is given as

$$V_b \frac{dC_b}{dt} = \frac{3m_p}{\rho_p R_p}\varepsilon_p D_p \left[\frac{dC_p}{dr}\right]_{r=R_p} \qquad (4-8)$$

The initial concentration in the macroporous material will be C_m.

At time (Time)=t sec, outermost layer or surface will adsorb some bulk gas, as a consequence, the concentration of the outer most layer starts increasing. The diffusion/adsorption process will advance radially towards the centre of the particle.

As the model specifies, there are 2 types of diffusivities, D_m for micropores and D_{mo} for macropores in the bidisperse formula. Both parameters are fine-tuned to experimental data to obtain a good match.

4.2.4 BG 2 Sample experimental data vs. Bipore model data

This section presents similar results but for Bidisperse pore model. It is obvious to see the gas concentration change vs. time in the micropore and macropore are significantly different.

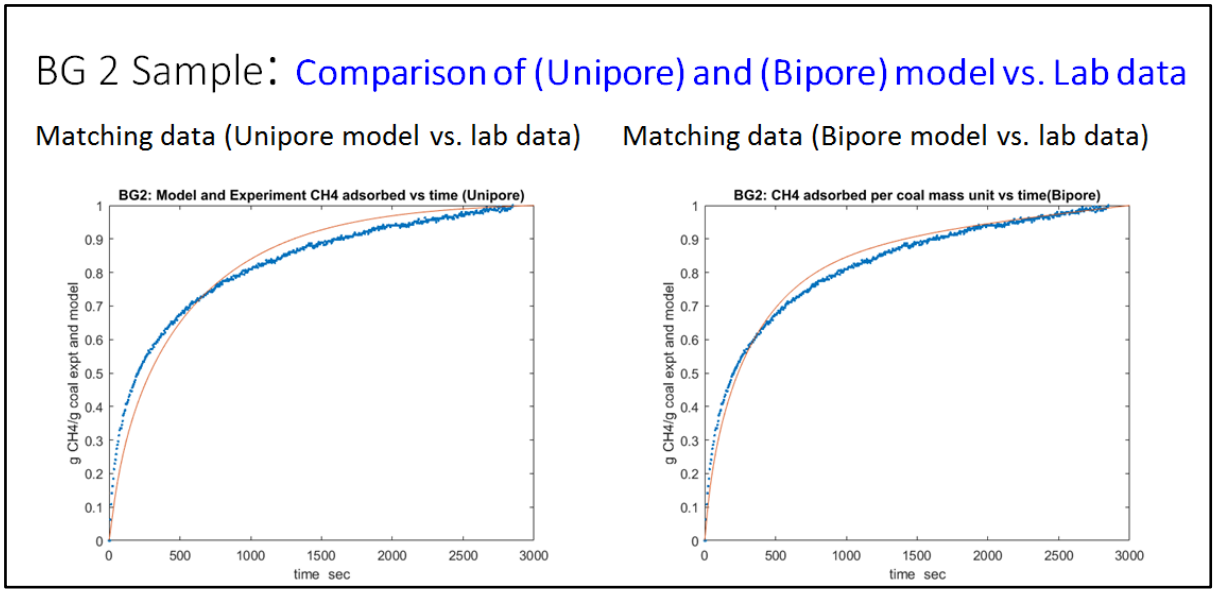

Figure 4-8 Comparison of the fitting of experimental data with Unipore and Bidisperse models

As seen from the Figure 4-8 above, the bidisperse model provides a much better representation of methane transport within the coal samples. The diffusivity of methane in both the pores are given in the table below.

Sample	Macropore Diffusivity	Micropore Diffusivity
BG 2 Unipore Model	--	$9.90 \times 10^{-13}\ m^2/s$
BG 2 Bidisperse Model	$7.99 \times 10^{-14}\ m^2/s$	$1.99 \times 10^{-12}\ m^2/s$

The concentration profile of methane inside the innermost section of the macro and micro coal particle of 0.08 mm radius is shown in Figure 4.9. It is noticed that the micro particles are saturated within a short time span of 1500 sec. This is due to the virtue of small grain size of the microsphere. Despite having a higher diffusional resistance, the micro-particle provides a lesser distance to traverse. Contrarily, the inner most section of the macro particle remains only partially saturated even after an experimental time of 3000 sec.

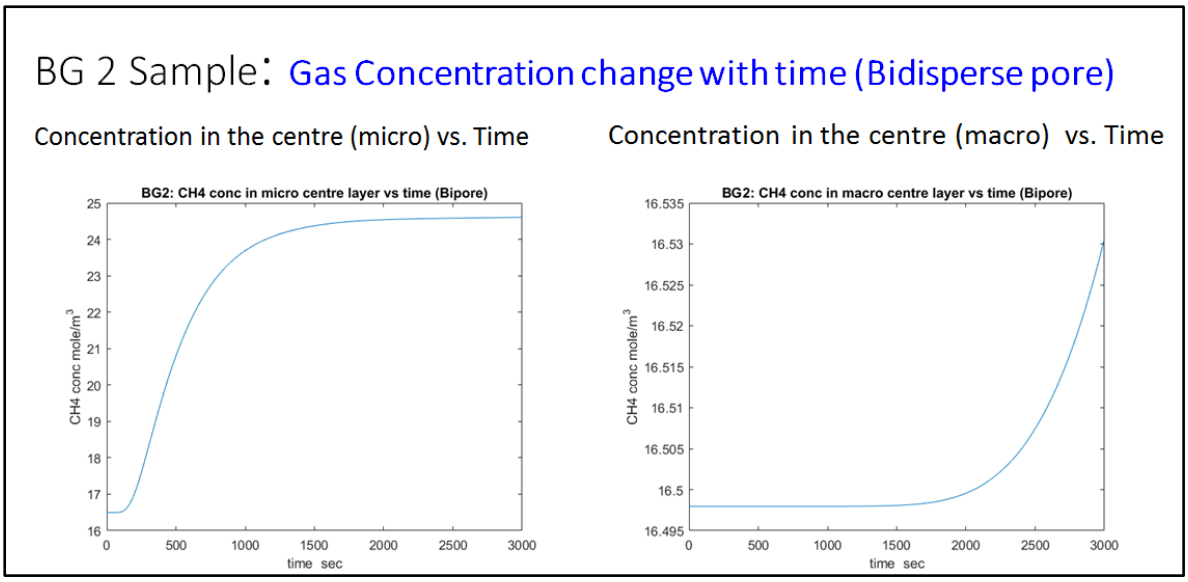

Figure 4-9 the methane concentration profile in the centre (micro & macropore) of the particle

The methane concentration profile on the surface of the macro and micro particle shows a predictively early saturation, with micro particle showing almost instantaneous saturation. The macro particle shows a delay in saturation.

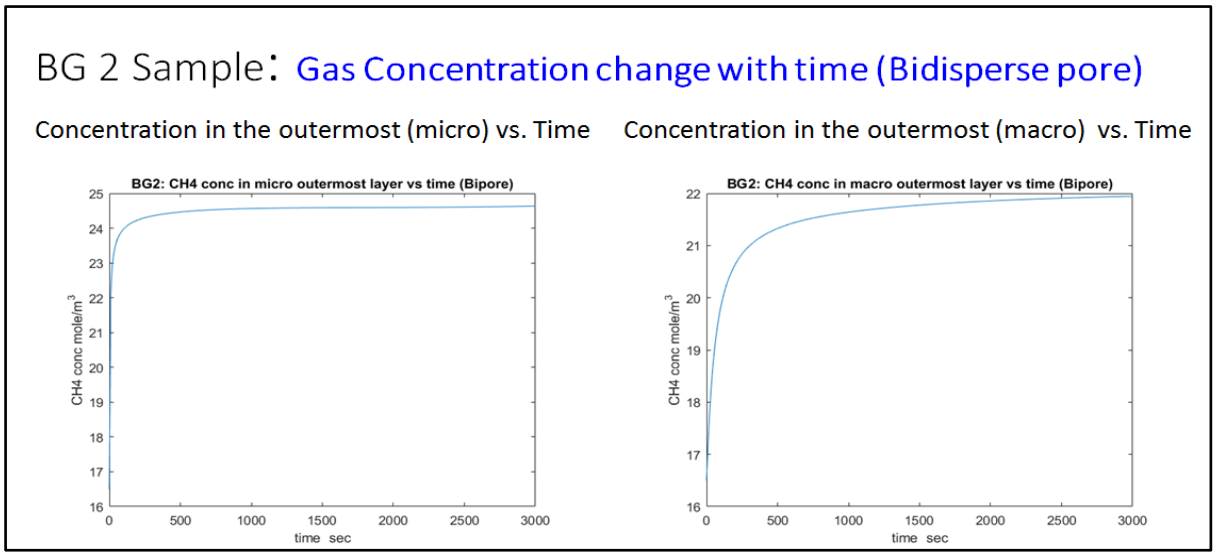

Figure 4-10 Concentration Change in the outermost for micropore and macropore (Bidisperse model)

The radially concentration change in micro pores is relatively faster than the one in macro pore in this BG2 sample. Figure 4-11

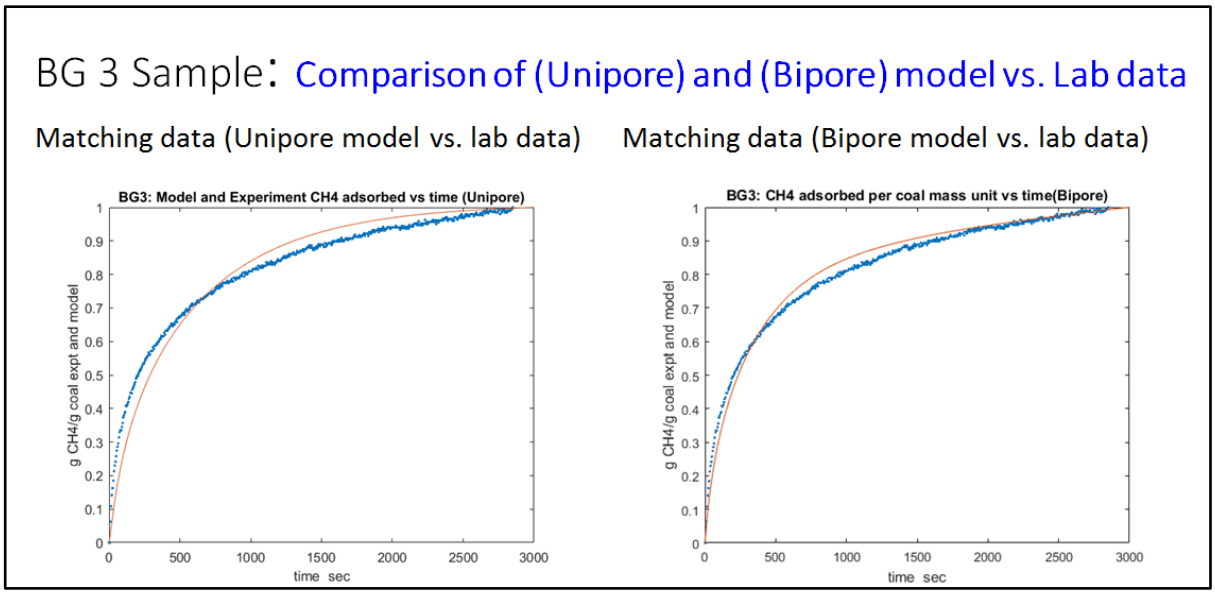

Figure 4-11 Concentration change radially in micro and macropores (Bidisperse model)

4.2.5 BG 3 Sample experimental data vs. Bidisperse model data

Similar to BG2 sample, the concentration change vs. time for three different subdivisions of the spherical porous material will be presented.

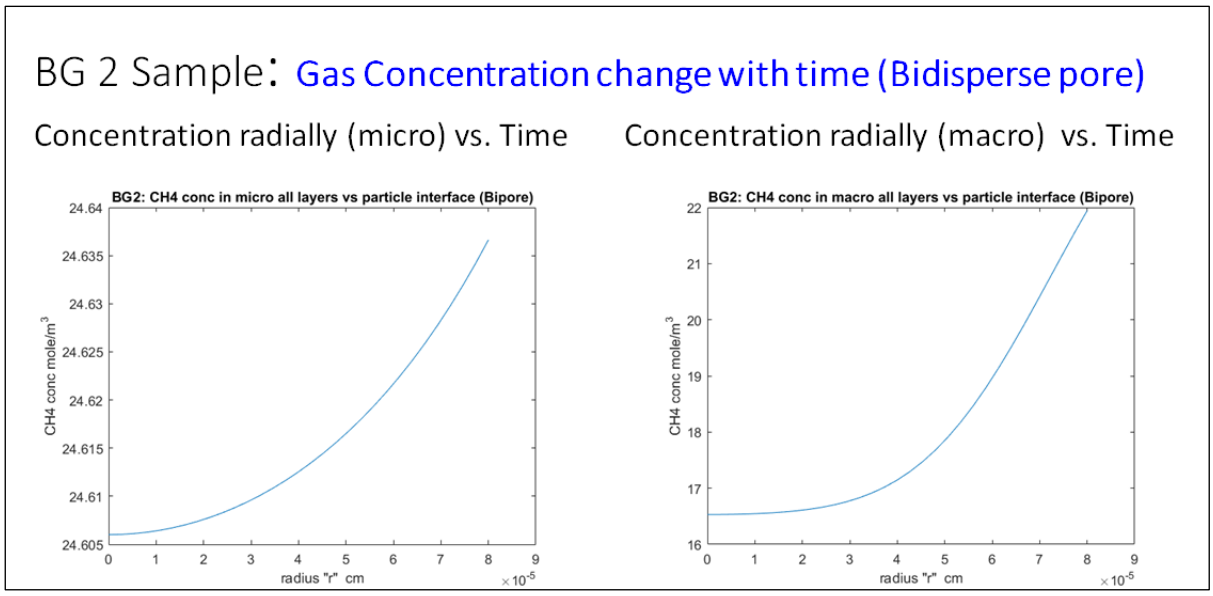

Figure 4-12 Comparison of Unipore Bidisperse model data vs. Experimental data

Comparison of methane adsorbed amount changes in the unipore and Bidisperse model indicates that bidisperse model is superior to unipore model in matching experimental data. Unipore model data initially is much lesser than the experimental data whilst bidisperse model data show a fairly good match to the experimental data for the first 500sec. This may well be interpreted as the sample consists of two types of pores rather than one single pore (which is assumed in unipore). Again, after 2000sec till the end of experiment (5000sec), bidisperse model provides almost perfect match compared to unipore model.

The diffusivity of methane in both the pores are given in the table below.

Sample	Macropore Diffusivity	Micropore Diffusivity
BG 3 Unipore Model	--	$1.80 \times 10^{-12}\ m^2/s$
BG 3 Bidisperse Model	$1.10 \times 10^{-12}\ m^2/s$	$1.14 \times 10^{-11}\ m^2/s$

Overall bidisperse model provides better match to both BG2 and BG3 experimental data. It is true and depends upon the heterogeneity of the coal

The concentration profile of methane inside the innermost section of the macro and micro coal particle of 0.08 mm radius is shown in Figure 4.13. It is noticed that the methane uptake in micro particles during 3000 sec is much greater than the one in macroporous particles for the same experiment time. From the left plot, microporous materials in the centre of the particle is ~ 32 mole/m3 compared to the methane uptake in macroporous material which is less than 1.98 moles/m3. It shows that less concentration methane occupied in macropores whereas methane concentration in micropores is very high.

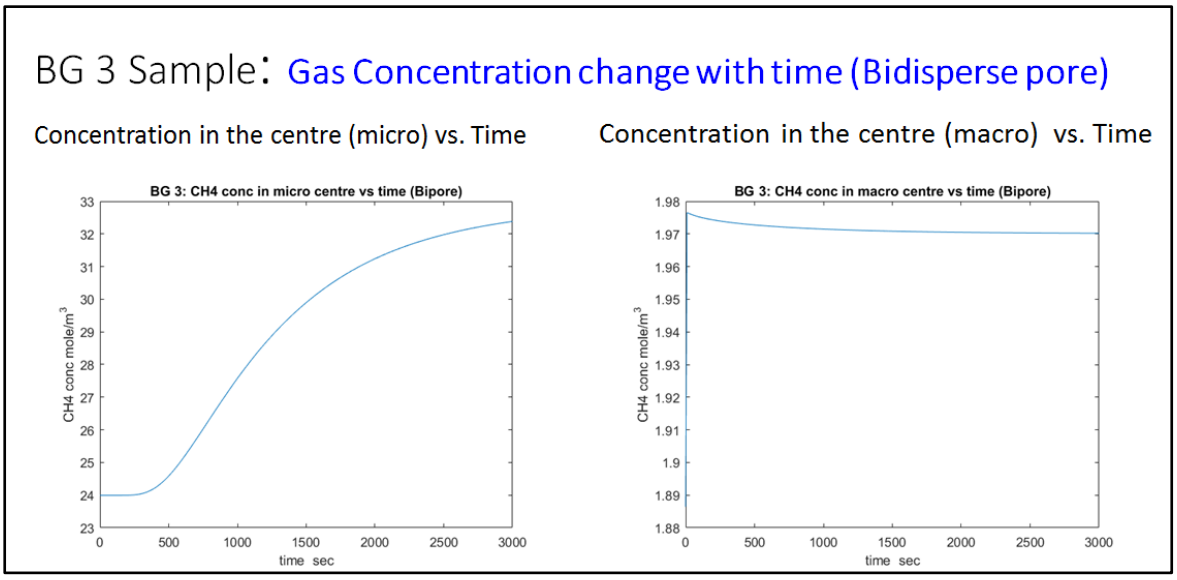

Figure 4-13 Concentration Change in the centre for micropore and macropore (Bidisperse model)

This is due to the virtue of small grain size of the micro-sphere. Despite a greater diffusional resistance, the micro-particle provides a lesser distance to traverse. Contrarily, the inner most section of the macro particle remains only partially saturated even after an experimental time of 3000 sec. As for the methane uptake in the surfaces (outermost) of micro-particle and macro-particle, it is very similar profile except methane concentration in macro-particle shows slight decrease in methane intake after it reaches the peak instantaneously. However, the methane uptake or concentration in macro-particle is much less than the one in micro-particle which is still in agreement with what has been observed in the centre (i.e. only partially saturated in macro-particle, micro-particle has lesser distance to travel despite greater diffusion resistance) [59].

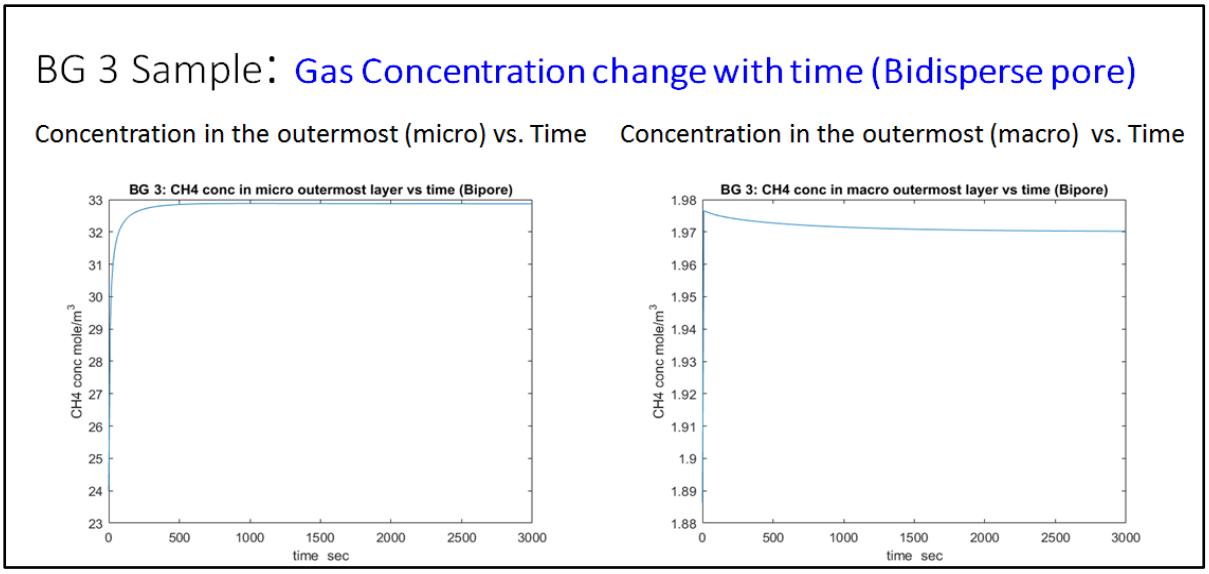

Figure 4-14 Concentration Change in the outermost for micropore and macropore (Bidisperse model)

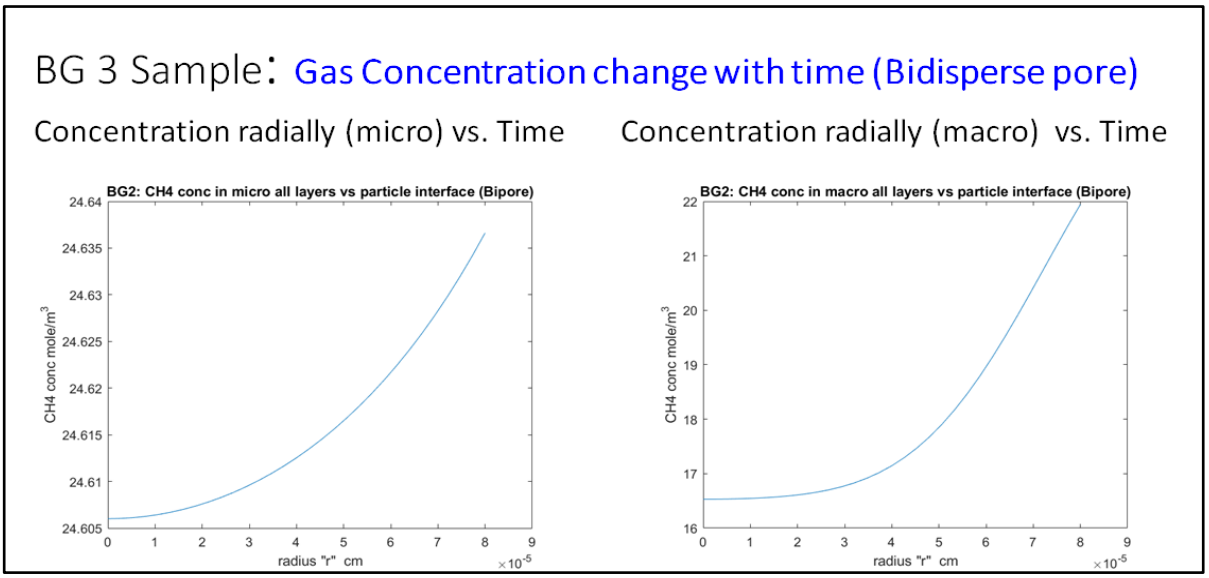

Figure 4-15 Concentration change radially in micro and macropores (Bidisperse model)

Methane uptakes radially in micro-particle and macro-particle seem to be slightly different in shape of the trend, but the magnitude or methane uptake appears to be similar (24 moles/m3 and 22 moles/m3 for micro and macro-particles).

4.2.6 Santos 1082 Sample experimental data vs. Bidisperse model data

The Bidisperse model results will be represented in a similar fashion and compare the unipore and Bidisperse model results in the end.

In this case, Santos 1082 both unipore and Bidisperse model data do not fit experimental data from the start to time 2000 sec. However, after 2000 sec, unipore model data fit much better than Bidisperse model data. This may indicate that this particular sample is more like unipore structure.

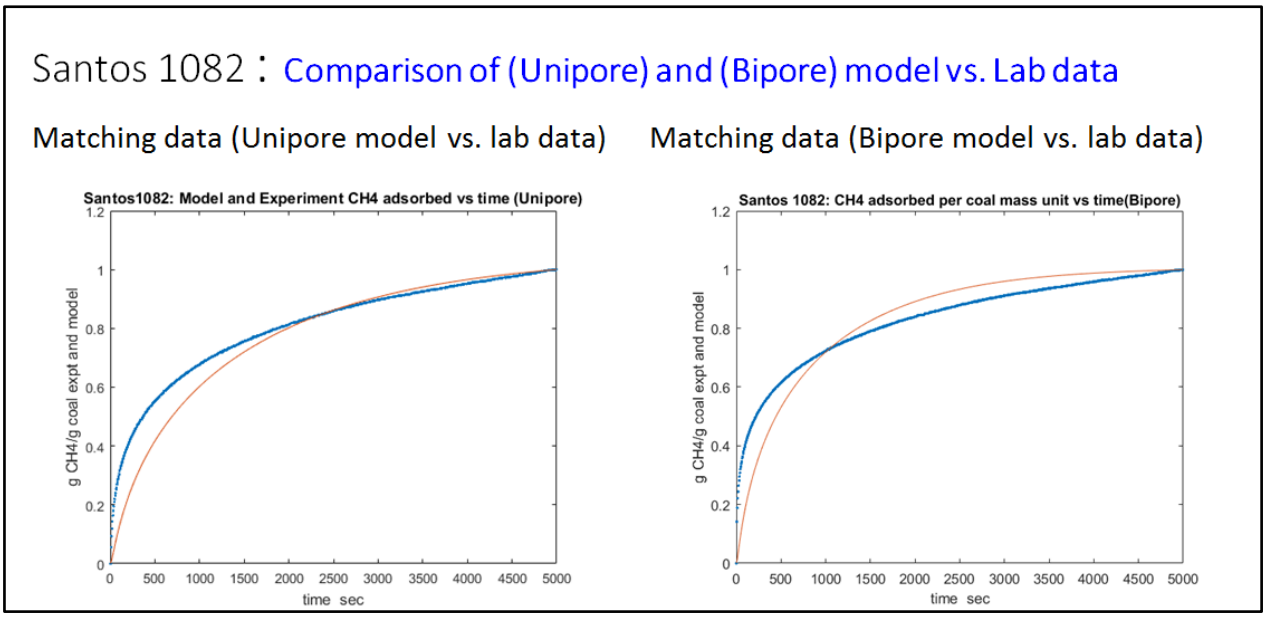

Figure 4-16 Comparison of Unipore Bidisperse model data vs. Experimental data

The diffusivity of methane in both the pores are given in the table below.

Sample	Macropore Diffusivity	Micropore Diffusivity
Santos 1082 Unipore Model	--	$3.50 \times 10^{-13}\ m^2/s$
Santos 1082 Bidisperse Model	$1.90 \times 10^{-11}\ m^2/s$	$2.15 \times 10^{-12}\ m^2/s$

Bidisperse model predicts higher methane uptake after 1000 sec, perhaps it may be incorrect to have bidisperse model to match this sample data.

It is evident from the pore size distribution data from all samples (Santos and BG (QGC) samples) which indicate Santos samples are dominant of more microporous materials compared to BG samples (Figure 4-17). In particular QGC-3 (BG3) show larger fraction of pore volume consists of macropore size, very small amount of micropore size.

Due to the different pore size range and wide distribution, suitable model should be selected to match experimental data so that representative diffusivity coefficients can be determined from the adequate model [59].

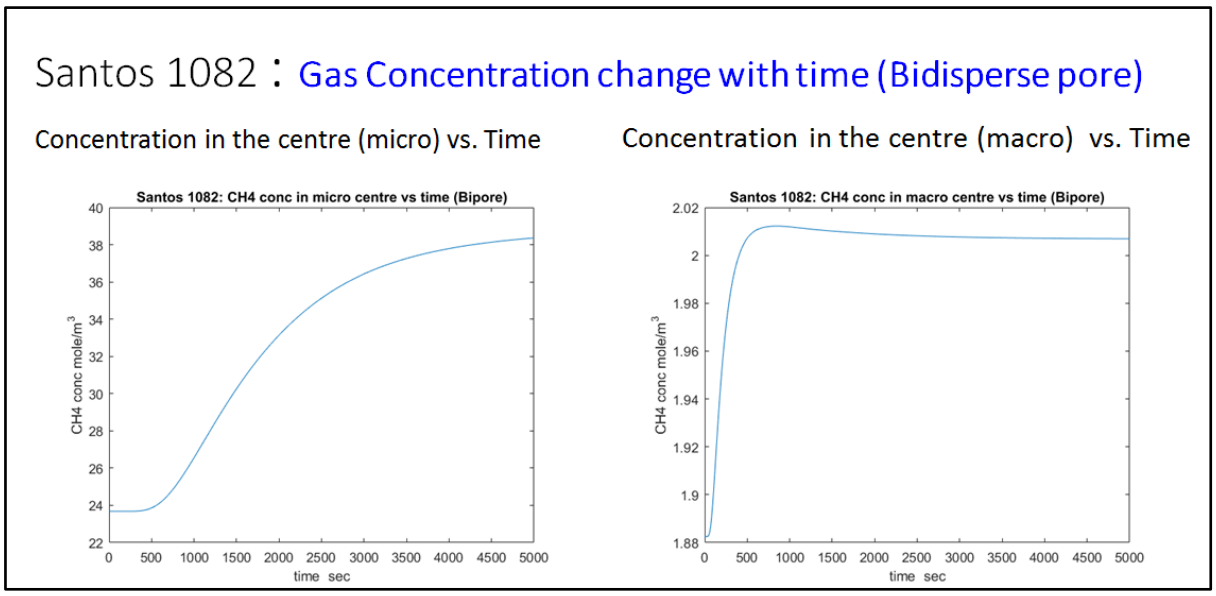

Figure 4-17 Pore size distribution from all samples (QGC (BG), Santos)

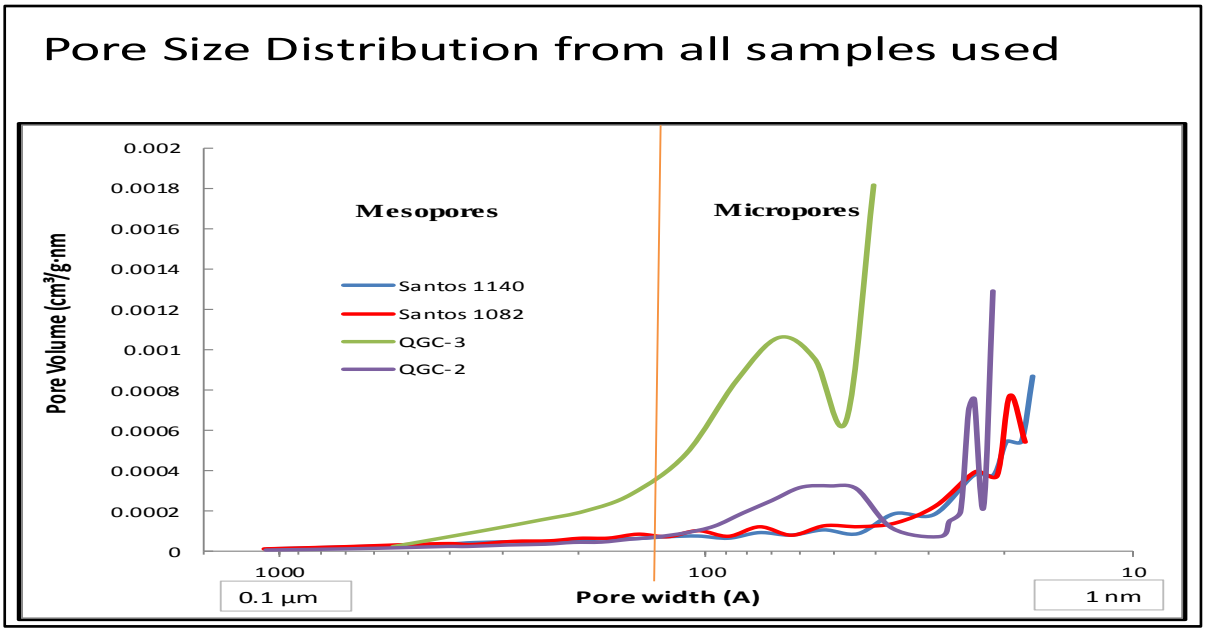

Figure 4-18 Concentration Change in the centre for micropore and macropore (Bidisperse model)

In this example, Figure 4-18 shows more uptake methane (concentration) is observed in the centre of micro-particle than the methane uptake in the centre of macro-particle. In addition, the centre of macro-particle is faster filled up with methane gas compared to the one in the centre of micro-particle which is more steadily increasing slope until it reached equilibrium.

The methane uptake in the outermost layer or surface of micro and macropores shows very similar trend, except the methane concentration in macropores is much lesser thane the one in the micropore at the end of the test (5000sec) (i.e.2 moles/m^3 vs. 38 moles/m^3) (Figure 4-19).

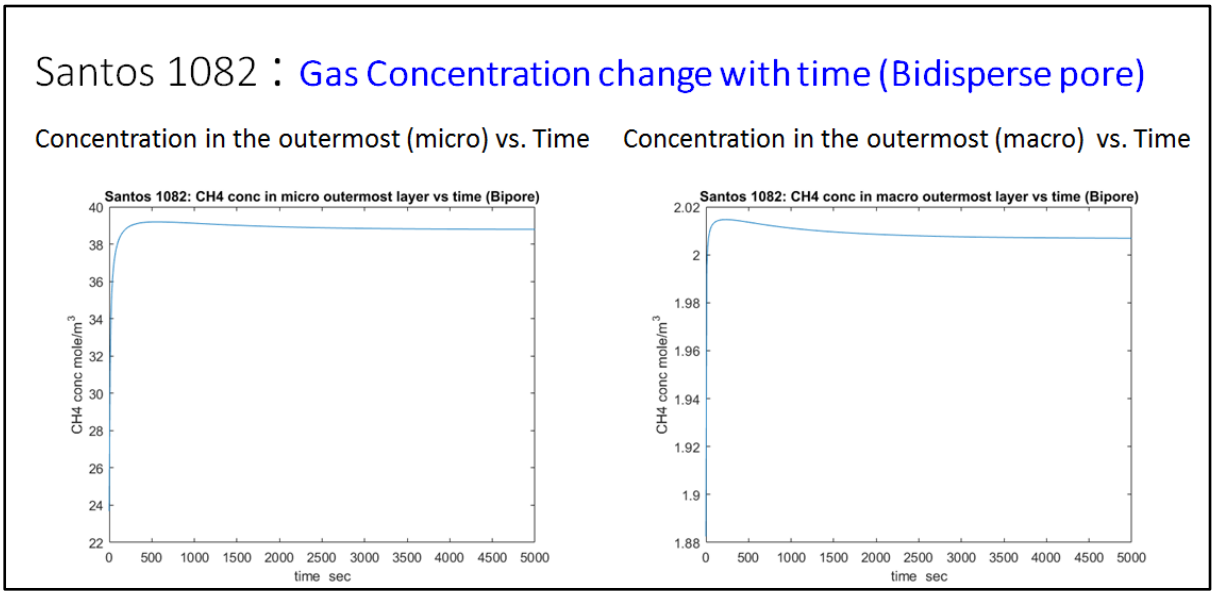

Figure 4-19 Concentration Change in the outermost for micropore and macropore (Bidisperse model)

Diffusivity coefficients for all cases (Unipore and Bidisperse models) for four coal samples are presented in a tabular form (Table 4-1). The numbers are quite consistent among BG two samples which support the improvement in Bidisperse model for those samples is achieved.

For Santos samples Unipore diffusivity coefficients are much smaller (shows slower diffusion in micropores) compared to BG samples. It is interesting to see BG3 macropore Diffusivity coefficient (7.99e-14) is much smaller than the other samples' macro diffusivity coefficient numbers. This number relates to the larger pores (meso or macro pores) in BG3 and the larger pores require for methane to traverse longer. This needs further works to understand the hypothesis.

Table 4-1 Diffusivity Coefficients for Unipore and Bidisperse models for coal samples

Sample Number	Unipore Diffusivity Coefficient (D, m2/s)	Bidisperse (micro) Diffusivity Coefficient (D_m, m2/s)	Bidisperse (macro) Diffusivity Coefficient (D_mo, m2/s)
BG 2	1.80E-12	1.41E-11	1.20E-12
BG 3	9.50E-14	1.99E-12	7.99E-14
Santos 1082	3.50E-13	2.15E-12	1.90E-11
Santos 1004	6.20E-13	8.45E-12	1.10E-12

4.3 Conclusions and Recommendations

This study undertakes two types of modelling approach utilizing experimental data to match and applied single component isotherms and parameters from the models employed.

However, the unipore models did not deliver satisfactory results if the coal consists of both micro and macro-particles. Bi-disperse model on the other hand showed superior match to the lab data from the samples with bidisperse pores.

The results from both unipore and bidisperse models were presented with some explanations to support the modelling ideas for different pore-particle coals.

As many researchers have conducted similar works on coal with slightly different results in the past. The experimental results may bias to local coal properties which also means that the findings in this study may be relevant to coals in Surat basin.

More research works may be required to come up with more conclusive solution, but this work will assist me to conduct better numerical simulation study which hopefully provides more accurate gas production prediction.

Chapter 5. INTEGRATING BINARY ADSORPTION DATA INTO DYNAMIC MODELLING TO PREDICT GAS CONCENTRATION PROFILES

This chapter incorporates the laboratory results and the model-generated binary isotherms with different binary component ratios and how they were integrated into a reservoir simulation model so as to enable predicting of future gas concentrations profiles of a particular Australian coal seam reservoir from.

This chapter addresses the weak point of dynamic simulations in determining gas concentration profiles. Prediction gas concentration profiles with better accuracy was achieved by introducing accurate diffusivity coefficients with binary isotherms (adsorbed phase amounts of individual adsorbates at corresponding partial pressure) with relevant ratios of two single components (CH_4 and CO_2). The analysis also demonstrated the improvement generated by using diffusivity coefficients and relevant Binary isotherms as opposed to estimated days of desorption for a particular coal to model gas production rate profiles (eventually concentration profiles) from a particular coal seam.

Using the derived diffusion coefficients, reservoir simulation models predicted gas concentration profiles for pre-selected wells for future.

Some sensitivity runs (single well prediction without using historic data) were made to ensure the overall model is capable of predicting gas concentration profiles with relevant input values. Finally, the cases of variable component ratios, and of usage of desorption days vs. diffusion coefficients were presented for comparison purpose. The chapter concluded with a statement on limitations and uncertainties of the current study. Other recent ongoing approaches in the same fields were briefly discussed and some recommendations for improvement in the same application to any coals were provided.

5.0 BASE COAL SEAM MODEL

Coal seam model is constructed in a Builder module (part of CMG, Computer modelling Group). Geological model (Static model) was constructed using corresponding contour maps and depth maps (from seismic data). The well log data (gamma ray, density and sonic logs) were used to construct porosity, coal density maps were utilized to correlate inter well properties (porosity, perm, saturation and pressure data). Later the built-in application was used to populate the whole model and generate a representative porosity, permeability, saturation and pressure maps. There are some core porosity and permeability data which were used to build a porosity permeability relationship equation. For coal adsorption data, many isotherms measured data were used to determine initial gas contents, maximum gas content at the reservoir conditions. There is no inversion to help populate these properties. The simulator (GEM, Compositional simulator) takes care of compositional change when simulation advances. The compositional changes were modelled using readily available EOS Model (Equation of State) such as Peng Robinson correlation [60]. Similarly relative permeability curves were generated using built in correlations such as Corey equation, Kozeny Carman relation [61]. But the end points (initial water saturation, critical gas saturation and connate water saturation) were obtained from lab data from core samples or/and log data.

The Methodology to build a dynamic simulation model for a coal seam gas reservoir required following:

A static model in order to describe the geological settings with basic reservoir properties distributions. This includes depth map, thickness map and structure map which are products of geophysical, geological and log interpretation data: In this study, the area of interest covered all Walloon coal seams and the underlain and overlain formations such as Springbok Sandstone, Tangalooma sandstone so that fluid movement within and outside coal seams and aquifers were accounted for. The impact of coal seam fluid production on the formations below and above Walloon coal measures could be modelled accurately.

Suites of Input data for a model, general input properties such as porosity, permeability, fracture spacing, orientation and rock-fluid interaction properties such as relative permeability, capillary pressure were included in the model and assigned to all active cells.

Specific information for modelling coal seams such as adsorption isotherms data, initial gas contents, Langmuir adsorption constant and pressure constant to model initial gas adsorption content [62]. In addition, some special parameters such as diffusivity coefficients or desorption times are required as input in the model to mimic the diffusion and desorption process. The physical conditions (initial reservoir pressure, critical adsorption pressure and reservoir temperature) to initiate the model are necessary.

Well specifications (locations, perforation intervals) and some historic data such as gas production rate, CH_4 and CO_2 mole % from collected well head samples and some pressure data to calibrate permeability values in the model.

In order to model binary component sorption process, special input data such as binary isotherms with specific ratios of single components (in this case CH_4 and CO_2) are required as input data.

PVT properties (such as gas specific gravity, viscosity, formation volume factor etc.) were determined using the *P*eng Robinson, Equation of State model to provide fluid properties and input data to model thermodynamic behaviour.

5.1 Base Model Construction

A coal seam reservoir model is constructed using a normal workflow which is: first the construction of a static model followed by populating basic rock properties. The static model generally considers the structural elements such as fault, net to gross, dipping and pinch out etc. In this model, the initialization is implemented using contacts, pressure and saturation information collected from some wells. The model has properties such as saturation and permeability were populated using available well data.

It is a common practice to counter check these values at the well locations against known values from logs and well testing data (the available data acquired from exploration and appraisal wells can be pressure data *(Repeated Formation Tester, RFT)*, porosity and saturation logs data.

This process will be conducted before actual simulation run is carried out because it is essential to make sure all the static properties are populated properly. In this study, log derived porosity, saturation from wells have been checked to be compatible in the model. Similarly pressure data from DST (Drill Stem Test) were used to check the model input and verify the input are representative.

Then, history matching process are carried out where historic production data are available. As briefly explained earlier, history match process is a kind of assurance of input data in the model are representative. For example, layer 1-5 must have pressure higher than 6-7 because measured pressures (RFT/DST) indicate this trend. Similarly, few static properties (porosity, permeability, pressure and Kh and Skin etc.)

Throughout the CSG field production life, the production of CH_4 and CO_2 (in moles) or the gas and water may change. The model accounts for the compositional changes in the reservoir due simulation period using Peng-Robinson EOS model

Roughly, the grid cell size in the model is 125 meters, however, not every cell is125 meters because some grid shape needs to change the size slightly (for example around the wellbore, along a big fault with high throw etc.). Similarly, the thickness may vary slightly when there is a shale lenses or pinch out in the area (see figure 5.1 as an example).

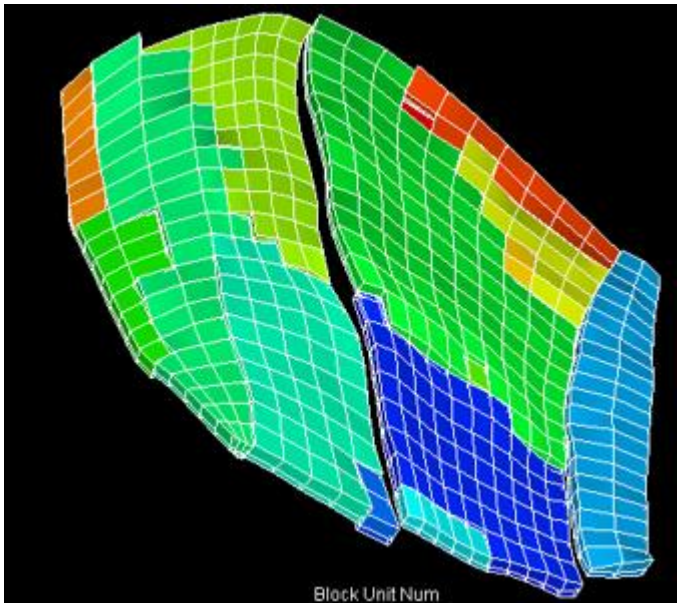

Figure 5-1 Example of grid size (average 125mx125m) variation across the field

The model is composed of three layers which represent three major coal seams measure (Upper Juandah, Lower Juandah and Taroom) in the area of interest.

5.2 General input data and the sources

The model is constructed with Static model data and Dynamic reservoir data. The general input data for a simulation model are:

5.2.1 Porosity

Porosity is measured on coals (small piece or plug) using Hg (Mercury) injection method or He (Helium) porosimeter. Two methods should provide similar results except mercury method destroy the sample after the measurement. In a coal seam reservoir, definition of dual porosity (matrix and fracture or cleat) is applied, different porosity values assigned to matrix and cleats using core data.

Porosity input in the model is obtained from porosity measurements of coal samples. Porosity from the interpretation of porosity logs are used to QC core data only. It is also a common practice to validate core porosity with log porosity and note if there is a significant discrepancy so that uncertainty of the input data can be accounted for.

5.2.2 Permeability

Similarly, permeability values are also assigned to matrix and fracture cells in the model to simulate fluid movement due to pressure changes in the reservoir. Normally, the relationship between porosity vs. permeability must be established before the properties were populated. In this model, the permeability porosity relationship was established from core data, the input permeability comes from these relationships. The limited amount of permeability value can be obtained from other sources, such as well tests (DST or MDT) are used to QC permeability input to the model. The input values of permeability are provided in the table 5.1

5.2.3 Water Saturation

Water saturation of a coal seam can tell a lot about the reservoir flow history (how the fluids had been accumulated and moved) including degree of water saturation change and wettability. Saturation can be measured from a core plug using Dean Stark method or can be determined from the saturation log (Reservoir Saturation log or Water flow log). It is a normal practice to use movable and immobile saturations. Model saturation value needs to be calibrated against log measured known saturation of any particular reservoir.

In this study, water saturation data from core samples (limited) and from logs were used to assign initial water saturation for the cells in the model.

5.2.4 Reservoir pressure

It is not unusual, there are many resources to obtain reservoir pressure. But it is very critical to acquire and use representative pressure in the model. Since the pressures are recorded from different tools (DST or Mini DST and RFT), the pressure data were corrected to the datum depth before using them in the model.

5.2.5 Reservoir temperature

As a common practice, the model is built under an isothermal condition using reservoir temperature. The reservoir temperature from logs is used as input for the model.

5.2.6 Rock compressibility and density

Coal samples were used to measure the compressibility at various pressure up to original reservoir pressure. Density of coals was determined from measured coal mass and volume of dried coal sample.

5.2.7 Dimension of grid cells, thickness

The model keeps the thickness approximately 1.2 -2 m average and the average sizes of the grids are created ~ 125 m.

Details of the input data for the reservoir and coal properties used in the model are provided in Table 5-1 Details of simulation model input data

Table 5-1 Details of simulation model input data

Base Case Model Input Data			
Reservoir size and dimension			
dimension	30 X 32 X 3		
grid size	125 m		
Thick_avg	1.2 - 2m		
numbers of active c	2880		
number of layers	3		
RockProperties			
Porosity	*%*		
Fracture	1 to 2		
Matrix	0.1		
Permeability	*mD*		
Fracture I,J,K	180, 90, 30		
Matrix I,J,K	0.1,0.1,0.01		
Coal Properties			
Density	1539.7	kg/m3	
Compressibility	3E-05	kPa-1	
Diffusion coefficient			
CH4	1E-11	cm2/s	(Reference BG 3 sample)
CO2	2E-11	cm2/s	(ASAP Kinetic data matched)
Desorption time			
CH4	10000	days	
CH4	500	days	
Irreducible Sw			
Relative permeability table 1 & 2 (see Appendix at the end of Chap 5)			
Table 1 Relative permeability measured in the lab with curvature			
Table 2 Rock curve which is straight line curve for fracture			

Coal Special Properties		
	CH4	CO2
Sorption Parameters	0.3729	0.7625
Langmuir adsorption constant, VL m3/t	321	372
Maximum adsorption mass, PL, 1/kPa	0.0009	0.0021
(BG samples Belsorp Isotherm, kP	1062	474
Initial gas content, m3/ton	136	142.8
Composition for all cells		
Fracture		
CH4	0.01	fraction
CO2	0	
Matrix		
CH4	0.96	
CO2	0.04	
Initial Reservoir Pressure		
Fracture	4431	kPa
Matrix	4431	kPa
Initial Water satura	%	
Fracture	0.85	
Matrix	0.15	

5.2.8 Z factor from EOS (PR) vs. Belsorp Z

The powdered coal samples used for adsorption measurements were collected from different locations (Lauren and Berwyndale south) situated in the Surat Basin. Total adsorbed amounts of a particular gas mixture were measured at every pressure intervals during the Binary adsorption measurement.

In Table 5-3 Binary Adsorbed amount component CH4 input 96% ca, the table provides Z values vs. pressures that are calculated from experimental data of Binary adsorption measurement.

In the Table 5-2, the Z factor distribution in the simulation model calculated from PR EOS is shown as a map. The variation of Z values across the field in relation to initial reservoir pressure is shown. As part of QC to ensure the model input Z value is similar to the Z value obtained from the experiment.

In the Figure 5-2 The initial Z value = *0.95975 – 0.95830* in the simulation model is found to be reasonably close to Belsorp Binary measured Z 0.*96032* at 6075 kPa in the table of Figure 5-3.

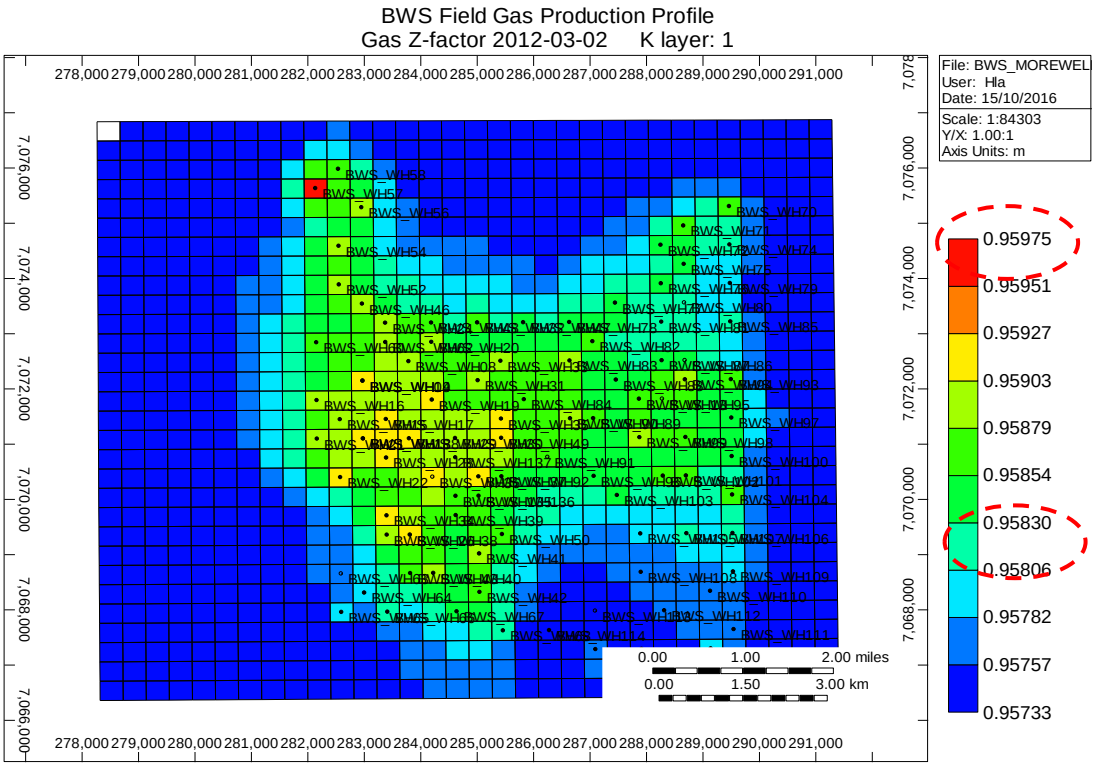

Figure 5-2 Z factor map from simulation model at P_{int}

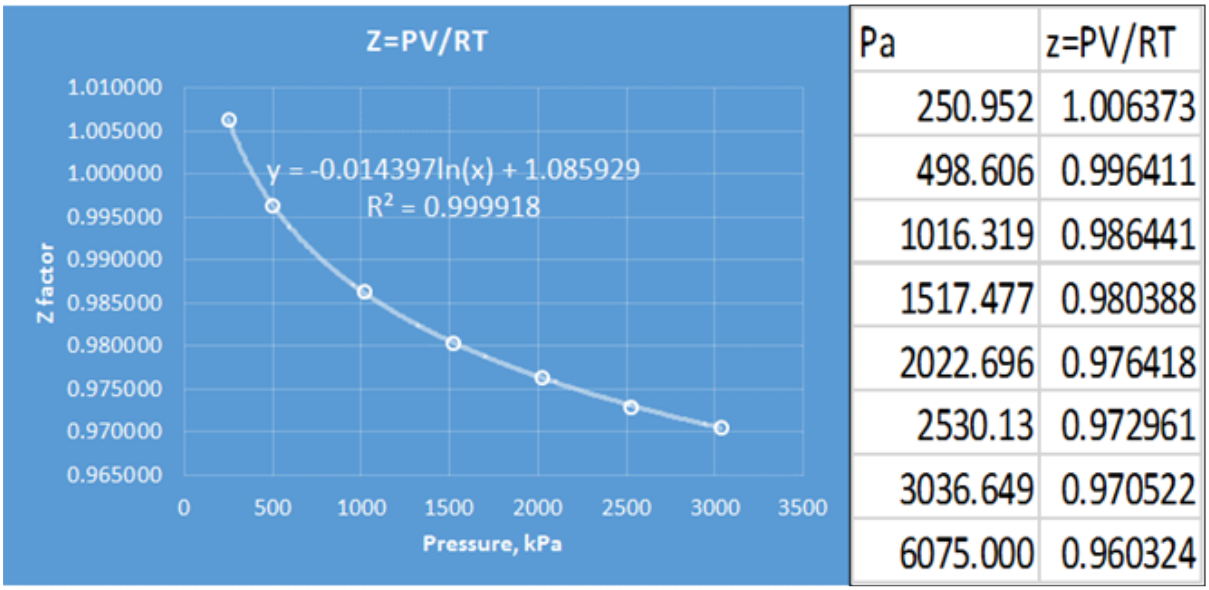

Pa	z=PV/RT
250.952	1.006373
498.606	0.996411
1016.319	0.986441
1517.477	0.980388
2022.696	0.976418
2530.13	0.972961
3036.649	0.970522
6075.000	0.960324

Figure 5-3 Z factor calculated from Belsorp data; using density to calculate mass, pressure

5.3 Specific input parameter to model binary sorption process

In this section, specific input data related to diffusion process and binary desorption equilibrium are presented and discussed in detail about the importance of equilibrium for two gas components to coexist. This particular information are required to model binary sorption process in the model.

As part of input data, single component isotherms (CH_4 and CO_2) were determined from input data such as Langmuir volume constant and pressure constant (V_L, P_L). Then, the ratios of two single components (CH_4 and CO_2) were provided to model a reservoir with a particular binary ratio (CH_4 98% and CO_2 2%) to model a mixture with appropriate PVT properties calculated using pre-selected EOS model.

In the Chapter 3, details of how total mixture adsorbed amount and single component adsorbed amounts were obtained from experimentally measured single isotherms in conjunction with the usage of IAS model.

The resultant total adsorbed amount with corresponding pressure and adsorbed amounts for individual components with partial pressures were utilized to model gas concentration production profiles for a particular binary ratio (e.g. 98:2, 96:4 and 80:20) so that accurate gas concentration production profile can be predicted.

In other words, it is really critical to use relevant adsorbed amount for a particular ratio (e.g. 96:4; CH_4:CO_2) if the field data shows 4% CO_2 as the initial gas concentration. Relevant adsorbed amount data with partial pressure is required to include as an initial starting point. It is similar to initial water saturation in a relative permeability curve for the simulator to assign correct water saturation during initialization process (the example of the tabular input data is provided in Table 5-2)

5.3.1 Initialization of both components at same equilibrium pressure with initial gas content

It is critical to make sure that the model is initialized "at correct equilibrium condition for both components" so that the both gases can be modelled to coexist at the same conditions (at same reservoir pressure). Both single isotherms with initial gas contents for CH_4; 219.07 SCF/ton and 512.0 SCF/ton for CO_2 at the equilibrium pressure (i.e. 3641.9 kPa in this case, please see the table 5-2) will be included. In this case, the equilibrium condition prevails as saturated and it reflects initial performance of the wells and the field (i.e. single-phase flow, water production only at day one). The initial reservoir pressure used in the model for both matrix and fracture is 4431 kPa. The gas will desorb from coals and diffuse into cleats when the reservoir pressure declines below the critical desorption pressure.

Enter initial gas content, Builder will compute equil. ...			
Initial gas content	SCF/ton	219.07	512.001
Equil. pressure at initial gas content	kPa	3641.91	3641.9

Table 5-2 showing correct initiialization pressure used for both component isotherms

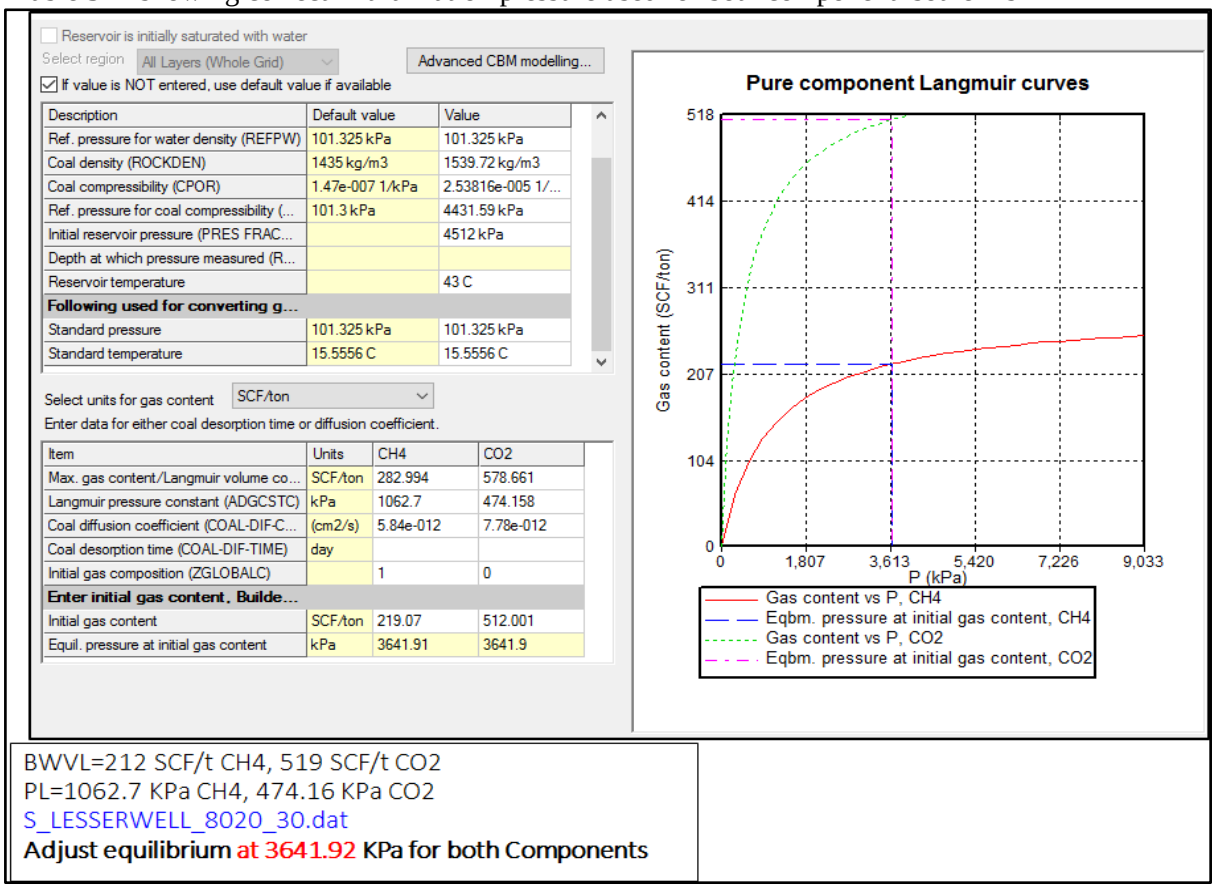

Input pressure and temperature for the reservoir are obtained from DST (Drill Stem Test) conducted in collective coal seams and in some cases, the pressure for a particular coal seam is obtained using Mini DST or RFT (Reservoir Formation testing tool) test data. The initial condition of a reservoir can be either under-saturated or saturated depending on the current reservoir pressure in relation to the original reservoir pressure.

In this base case simulation run, Binary ratio of 96:4; CH_4:CO_2 is used because most of producers are producing with CH_4 96% concentration.

The picture in Figure 5-4 illustrates the initial adsorption map (in this case methane adsorption from day one, 1st July 2003, on the left and after 5 years simulation 1st July 2008).

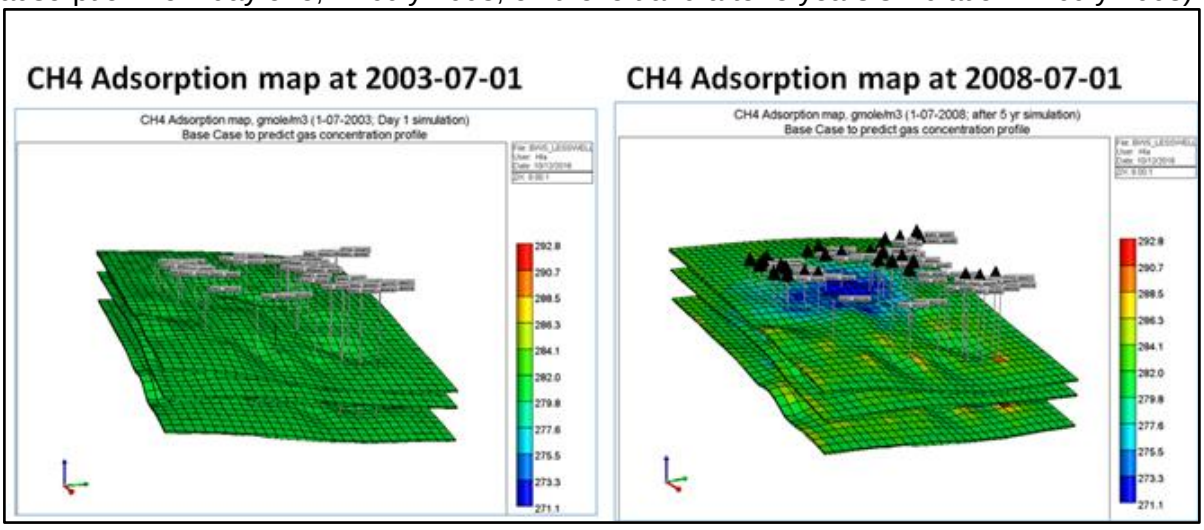

Figure 5-4 CH_4 Adsroption change during 5 years simulation run

It is essential to validate model generated data so that future prediction data will be carried out with confidence. The mole % of the gases (CH_4 and CO_2) regularly collected from a well head are shown in the plot of Figure 5-5. The gas samples were collected on a regular basis (every 3 or 4 months) from pre-selected wells.

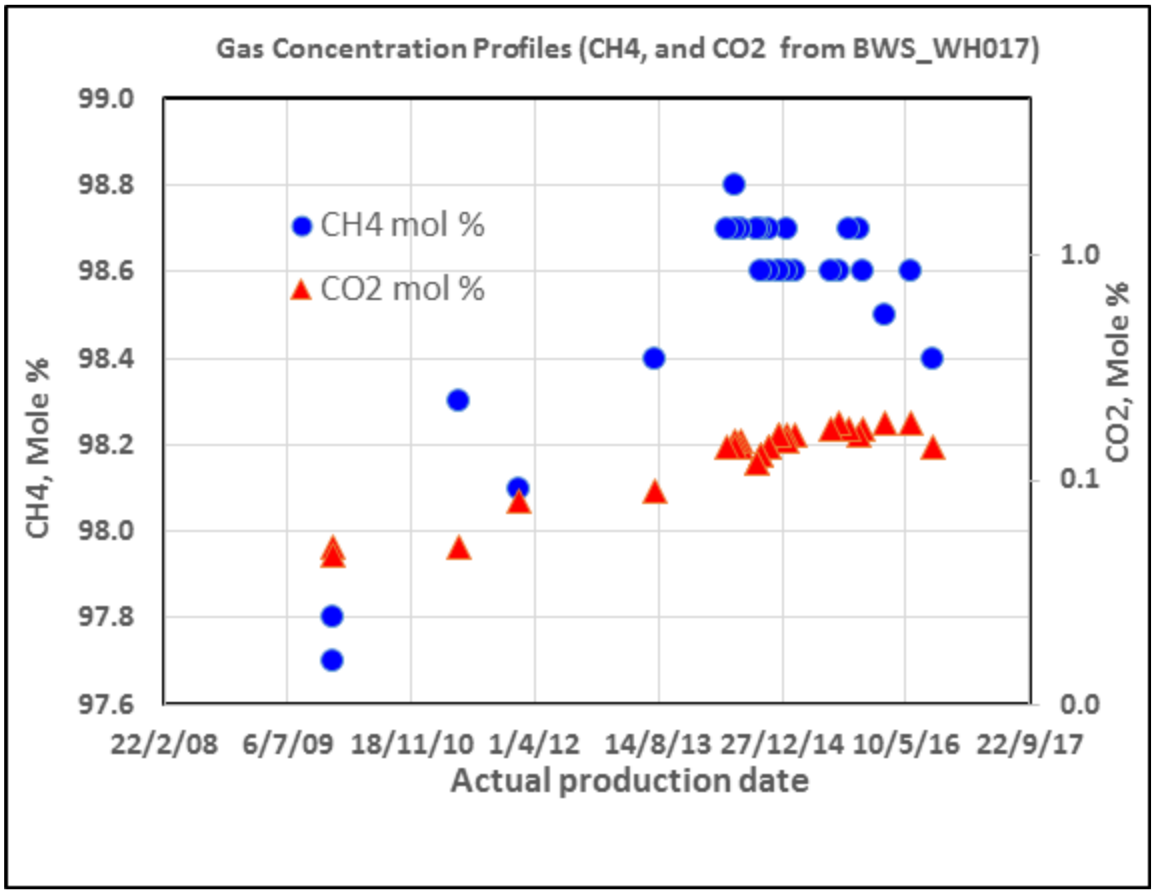

Figure 5-5 Actual CH_4, CO_2 mole %trend from BWS_WH017 well

For this study, the wells which provided sustainable production flow with increasing CO_2 mole % were selected. One example of these wells, BWS_WH017 with CH_4, and CO_2 mole % trend with time is illustrated in Figure 5-5.

These data will be used to compare the model predicted gas concentration profiles to provide a means of validating the outcome.

However, it is worthwhile to mention that the gas sample quantity collected in the field were recorded in mole % whereas the model generated CH_4 and CO_2 trends and quantify in gmole/m3. There are few steps to get model gmole/m3 to mole % to match these two gas concentration profiles from selected wells with some historic data.

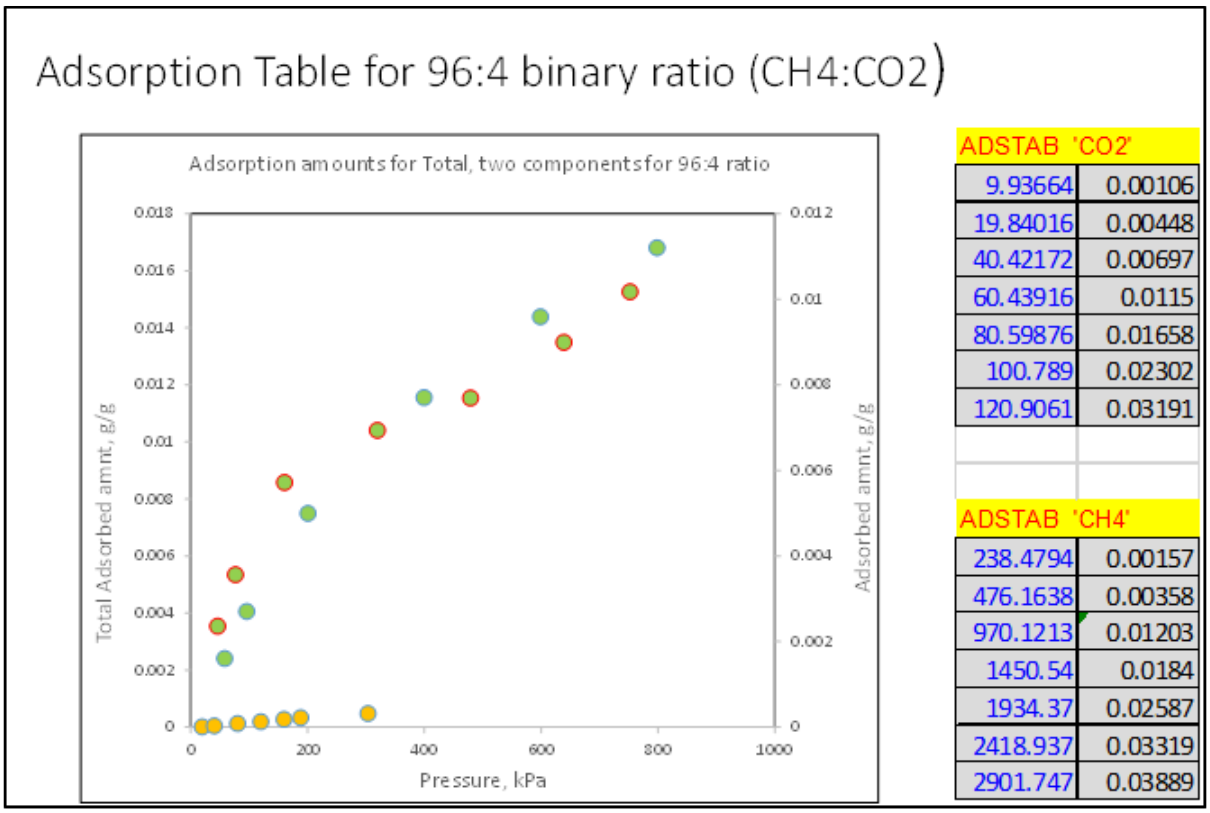

ADSTAB 'CO2'	
9.93664	0.00106
19.84016	0.00448
40.42172	0.00697
60.43916	0.0115
80.59876	0.01658
100.789	0.02302
120.9061	0.03191

ADSTAB 'CH4'	
238.4794	0.00157
476.1638	0.00358
970.1213	0.01203
1450.54	0.0184
1934.37	0.02587
2418.937	0.03319
2901.747	0.03889

Figure 5-6 Binary adsorbed amount input for CH4:CO2 80:20 ratio run

5.3.2 Adsorption amount of CH4 and CO2 input

This input data is entered as a tabular format with GEM Keyword (ADSTAB, adsorbed amount of particular component provided vs. pressure in a tabular form). The example of adsorbed CH_4 in the mixture with feed composition of 96% CH_4 (see Table 5-3). Basically, adsorbed amounts of CH_4, CO_2 in the binary mixture (CH_4:CO_2, 96:4) are required to include with partial pressure of individual components.

The methodology includes

1. Confirm IAS model generated total adsorbed amount for that particular mixture against total adsorbed amounts for a particular mixture from experiments by matching
2. Once both total adsorbed amount is confirmed, the individual adsorbed amounts (CH_4 and CO_2) at partial pressure can be calculated using IAS model [21]
3. Once the adsorbed amounts of CH_4 and CO_2 are obtained with confidence, the tabular format with keyword (shown in Figure 5-6) is included in the model.

Table 5-3 Binary Adsorbed amount component CH4 input 96% case

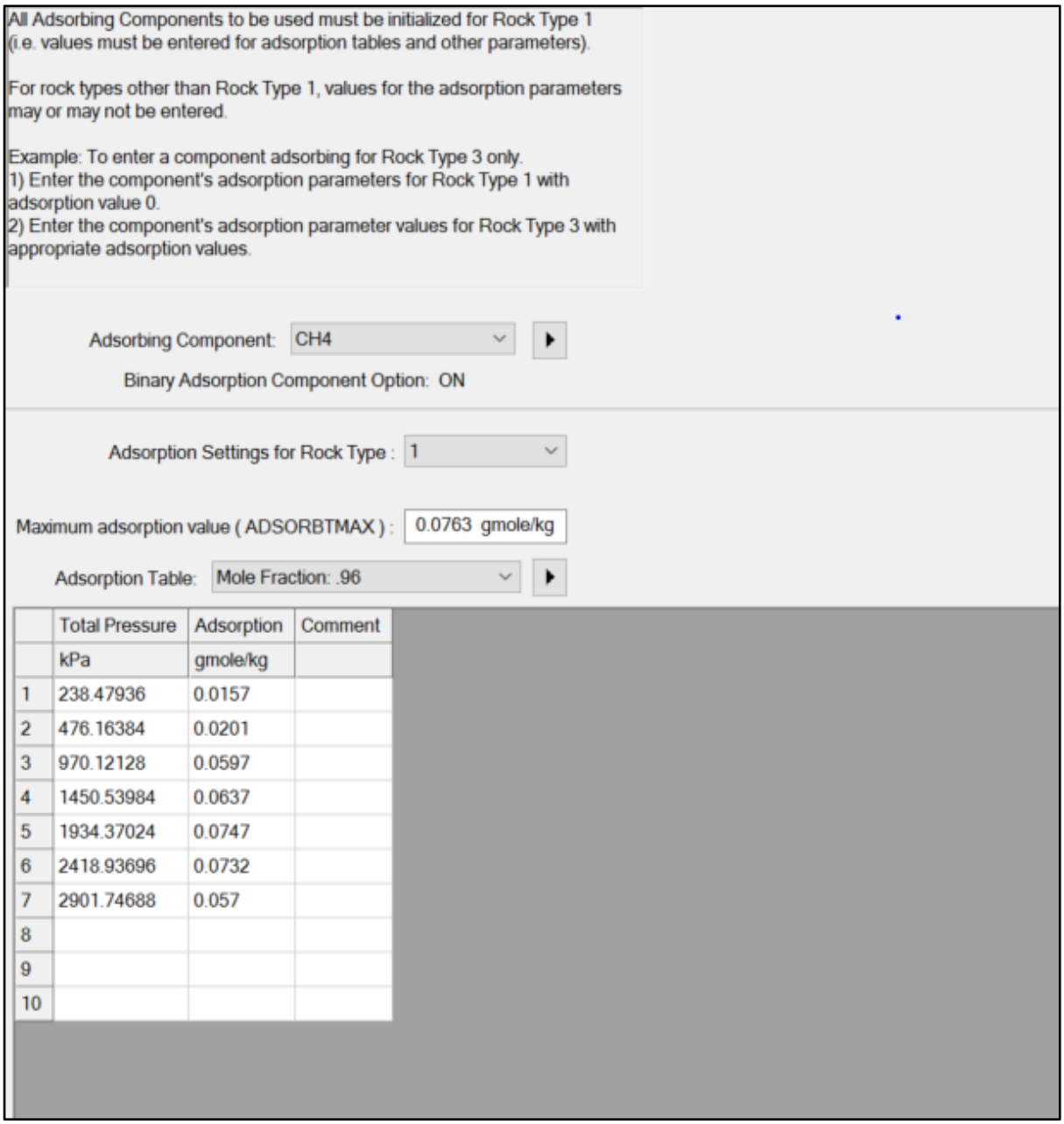

	Total Pressure	Adsorption	Comment
	kPa	gmole/kg	
1	238.47936	0.0157	
2	476.16384	0.0201	
3	970.12128	0.0597	
4	1450.53984	0.0637	
5	1934.37024	0.0747	
6	2418.93696	0.0732	
7	2901.74688	0.057	
8			
9			
10			

5.4 Data set from Base run with history match

After the model is initialized with complete input data, the base case was run with 16 wells with known gas production history so that the model can be validated against it. Basically, well gas production rate was history matched by varying some parameters such as “kh” (perm*thickness), relative permeability curve for gas breakthrough and well connectivity and saturation around the wellbore. But most of the cases, only end points and relative perm curvature were needed to achieve a good match. It is important to mention that all selected wells are producing without pump assistance, also called “free flow wells”, in the complete dewatering state, so the gas rates are considered a single-phase flow with only small amount of water associated.

This base run was conducted up to the end of 2013 where the last known CH_4 and CO_2 mole % were available which were used to check against the model generated gas

concentrations. However, the model provides only rates of CH_4 and CO_2 in gmole/d which later converted to mole % to compare against gas concentration from CH_4 and CO_2.

5.4.1 Simulation results from Base case model

The Base case run is conducted with gas rate as a control model to history match using gas production history from selected wells (~ 16 wells). As results of history matches, gas concentrations of CH_4, CO_2 from the model and CO_2 calculated from field samples form BWS-WH033 and 107 were plotted in Figure 5-7 and Figure 5-8

The concentration of CH_4 profile is plotted together to show the change of CH_4 trend with time since other heavier components such as Ethane, Butane will be released from the coal at later production life of the wells.

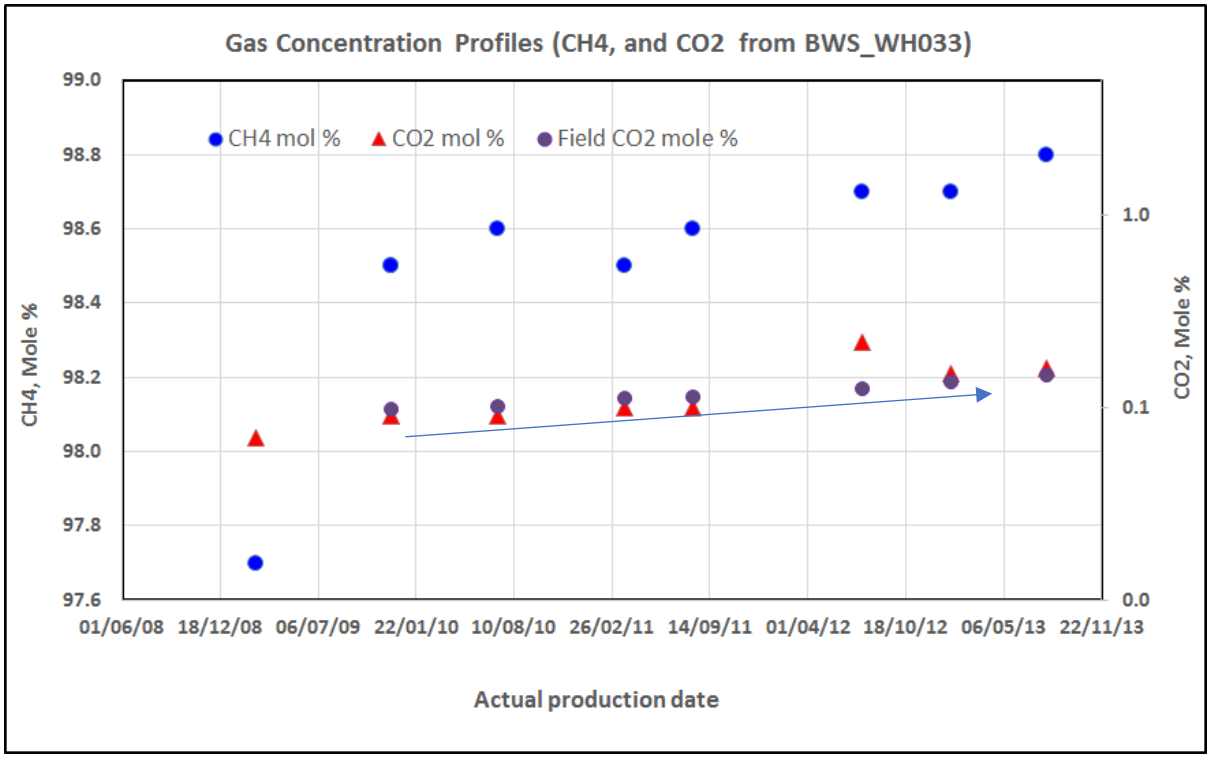

Figure 5-7 Comparison of field CO_2 concentration vs. modelled CO_2 concentration profiles for BWS_WH033

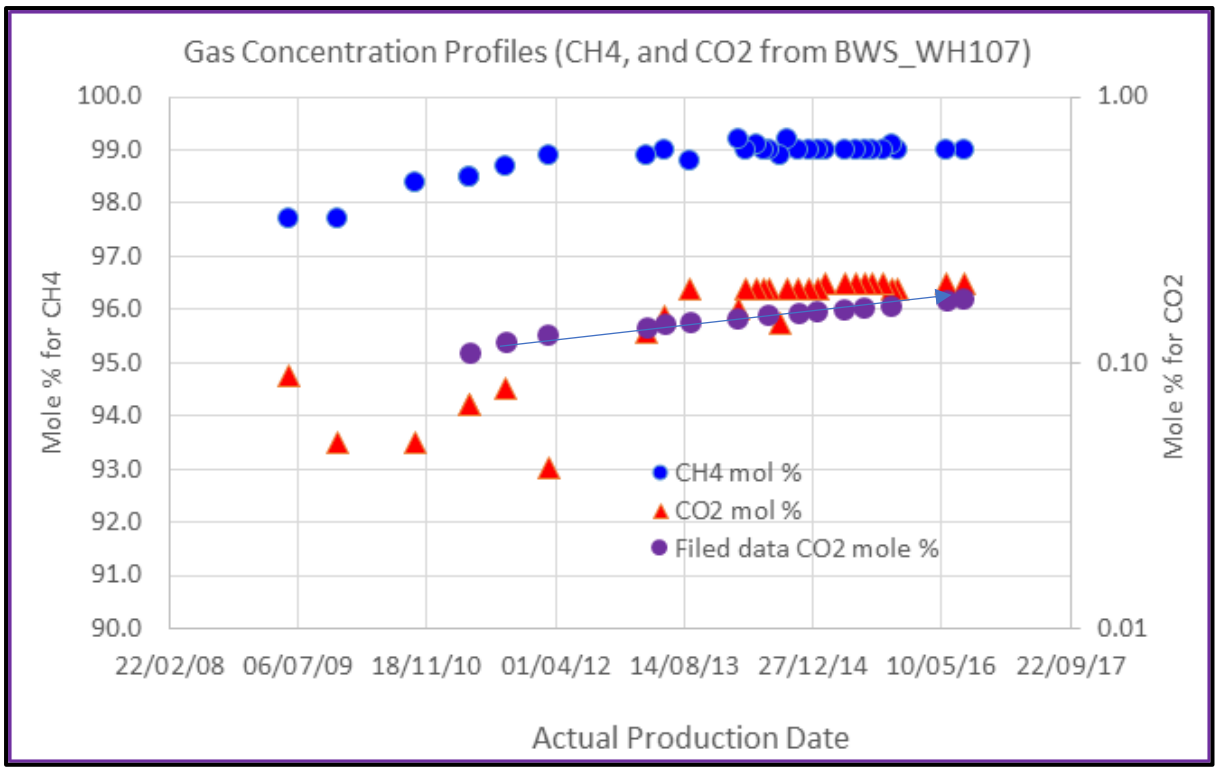

Figure 5-8 BWS_WH107 CO_2 concentration profiles showing continued increasing trend with time

During history matching process, some wells were identified as producers under BHP controlled mode. This means that the well is not under full potential of its deliverability. However, the gas concentration will not be different since it is based on the amount of gas flow and associated CH_4 and CO_2. Consequently, prediction of gas concentration production profile should not be affected.

In total less than 5 wells in BWS are selected as good candidates for the history match. Among them, BWS_WH107 and BSW_WH033 results are presented in in Figure 5-7 and Figure 5-8

The results from these two wells show the CO_2 gas concentration in BWS_WH107 is steadily increasing with time and CO_2 mole % trend in BWS_WH033 found to be stable with little change over a period of later time production (Jul-2012 to Jul-2015).

Another important point to highlight here is that there are some minor gas (N_2) detected from the analysis of samples collected from the selected wells. So, the balance of CH_4 and CO_2 will not add up to exact 100%. Nonetheless, these minor gases contribute very little to the change of profiles since they are more or less constant throughout the well production history.

5.4.2 Prediction of gas concentration results from Base case model

As mentioned at the beginning of this section, the simulation work is done using a Commercial simulation package (CMG, Computer modelling group). Also in the data input section, the cleat or fracture properties such as fracture spacing, fracture width, length etc. are provided. The flow in the cleat or fracture is modelled using Darcy's law and from only

Matrix to Fracture flow is allowed since dual porosity model is selected to model the matrix to fracture flow. In addition, CMG allows to adjust the transmissibility between matrix and fracture which is a parameter to be used for history matching. There are two dual porosity models [63,64] which accounts for the grid dimensions (x, y and z directions) to model flow and transport mechanism in coals (both in cleats and matrix) [reference: CMG simulation modelling manual]. After the model is validated with known gas production rate with a satisfactory history match, the prediction run is conducted. Below the example well BWS_WH048 and the preliminary match, and prediction run results are presented.

History matching process uses known observed data (such as methane and carbon dioxide %) to validate the model so that future production profiles of gas concentrations can be forecasted. It is a normal process used in every simulation works (used a known historic data to validate the model, so the confidence in the prediction results can be improved)

For the prediction run, the simulation model generates only gas production rate. Therefore, the prediction of gas concentration profiles (CH_4 and CO_2) was recalculated in mole % and the plot is presented in Figure 5-12

Preliminary data from BWS-48 is presented in Figure 5-12to show the history match of CO_2 from the model against CO_2 calculated from collected field gas sample (in Mole %).

The CO_2 data from field sample shows much less than the model for the period (2009 – 2013) which are the only available data since the sampling from this well was stopped. From the model CO_2 mole % shows increasing trend but not significant.

Figure 5-9 History matched results for BWS_48 with binary ratios CH_4:CO_2 ; 80:20.

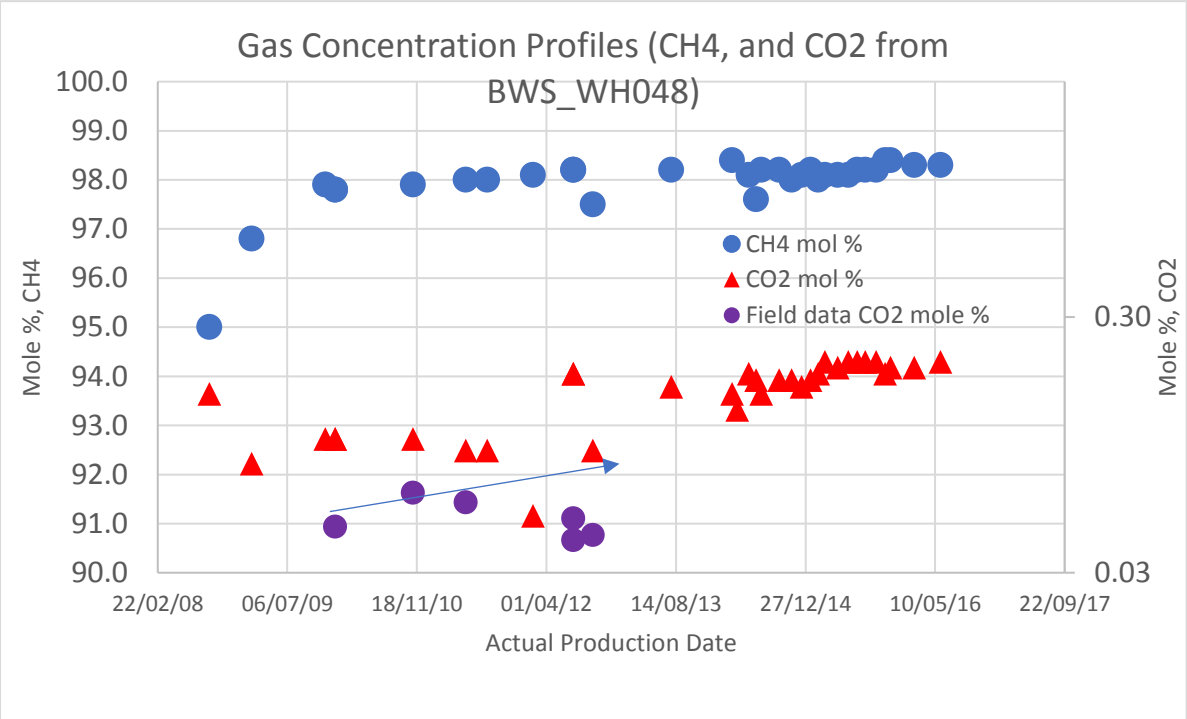

After preliminary history matched data, the model continued with prediction for BWS_WH048 and the production trend of CH_4 and CO_2 rates with gas production rate are plotted.

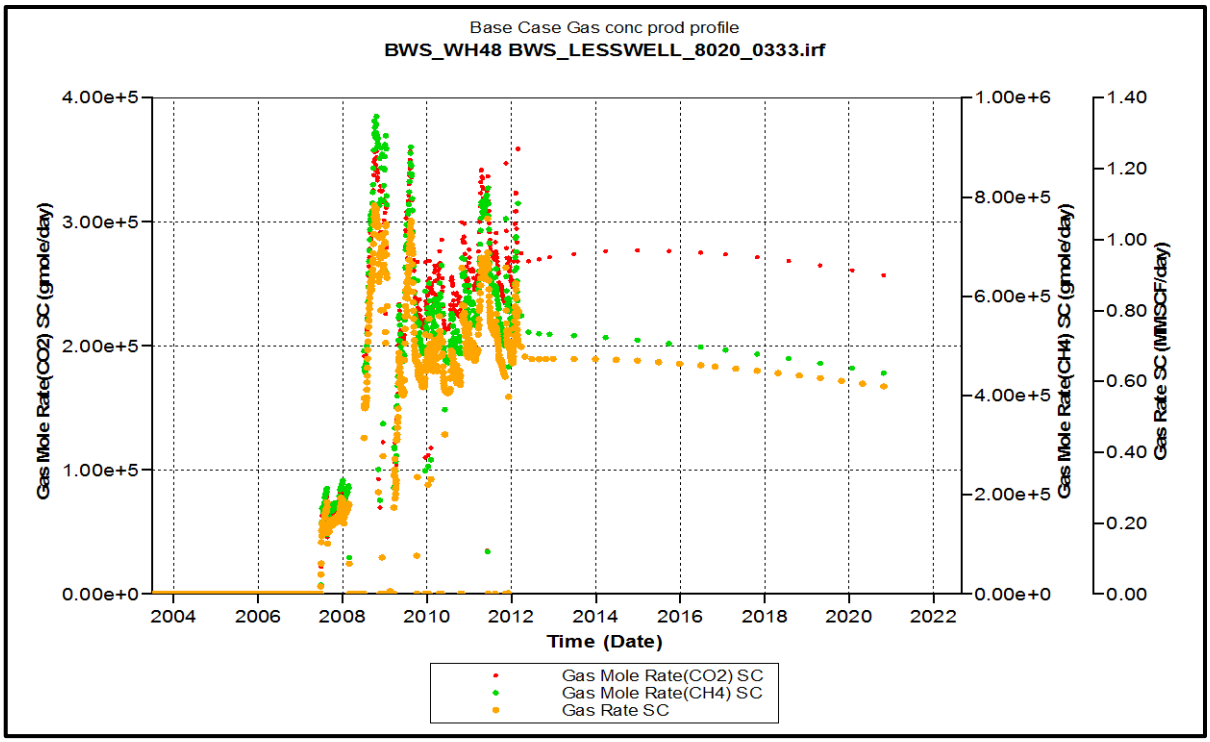

Figure 5-10 Prediction of BWS_WH048with CH4 CO2 gas production rate

Figure 5-11 CH4 and CO2 gas mole rate (gmole/day) and total gas production rate MMSCF/D for BWS_WH048

Using these prediction data, CH_4 and CO_2 gmole/day rates are converted to mole % to show the trend of CO_2 in a prediction CH_4 and CO_2 concentration profiles BWS_WH048 with binary ratios 80:20

The plot from this result is presented in Figure 5-12

BWS_WH048 seems to show reasonable CO_2 prediction instead of gmole/day (which is default unit from CMG). The attempt was made to show gas concentration using exported data set from simulation run to excel format. The conversion from gmole/day for CH_4 and CO_2 from the model to mole % is a simple calculation which will be provided in the Appendix B.

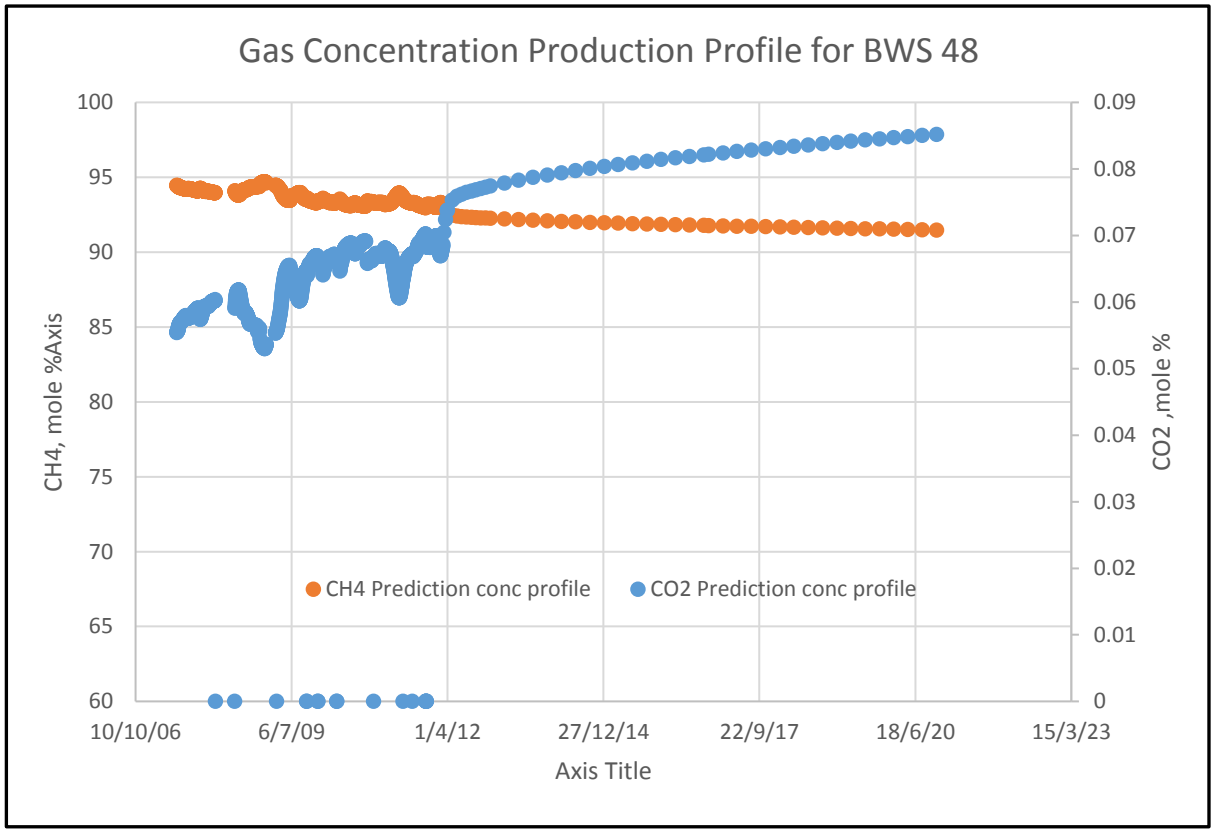

Figure 5-12 CH4 and CO2 concentration profiles in mole % for BWS_WH048 (96:4 case).

Comparison of CH4 CO2 concentration trends (mole%) vs. gmole/day

BWS-48

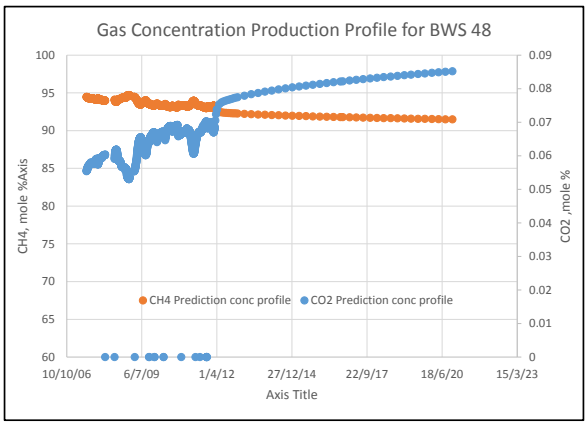

BWS-48

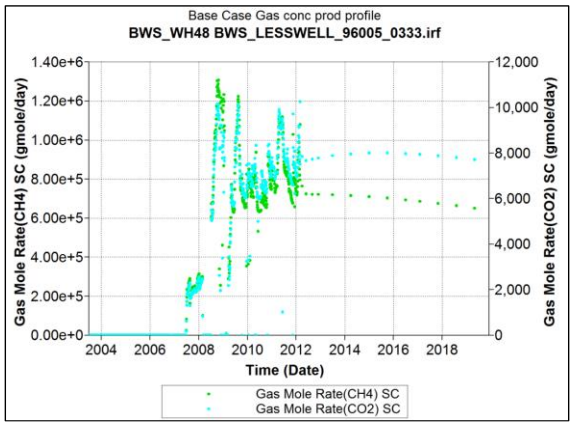

The plots shown in the figures below compare the CO_2 CH_4 trends prediction for 10 years after history match.

The prediction for CH_4 and CO_2 from the model for BWS_WH054, BWS_WH064, BWS_WH067, BWS_WH076, BWS_WH100 and BWS_WH108 are presented to show the prediction profile trends.

BWS_WH054 shows a continuous increase of both CH_4 and CO_2 trends.

Both BWS_WH064 and BWS_WH067 show continuous trends of decreasing both CH_4 and CO_2.

BWS_WH100 and BWS_WH108 shows faster CH_4 decreasing compared to CO_2.

These wells with similar kind of profile trends can be related to their locations and reservoir properties. In fact, the wells with similar trends located in the same vicinity which shows coal properties control on the gas concentration trends.

Binary adsorbed phase amount compared for two cases (96:4)

Binary adsorbed phase amount compared for two cases (96:4)

BWS-100

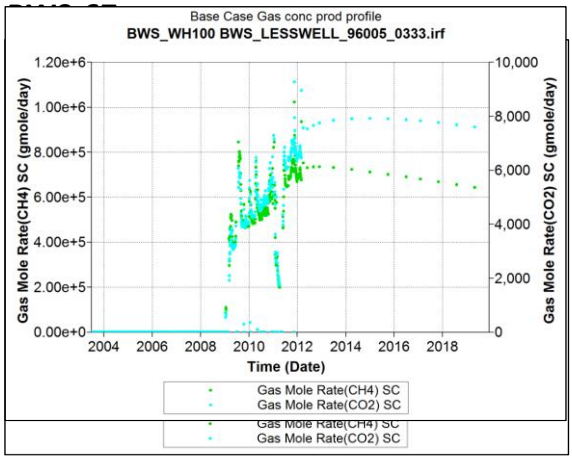

BWS-108

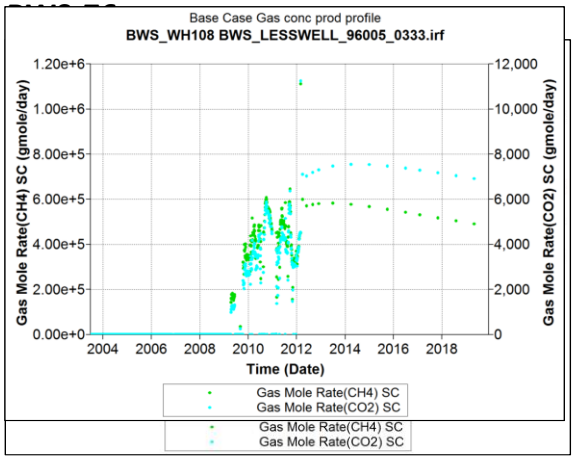

Binary adsorbed phase amount compared for two cases (96:4)

BWS-54

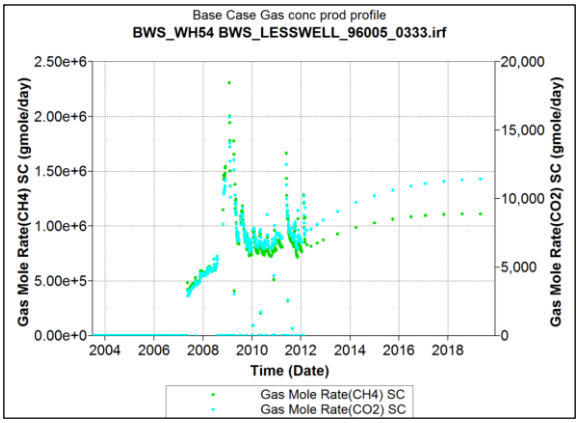

BWS-64

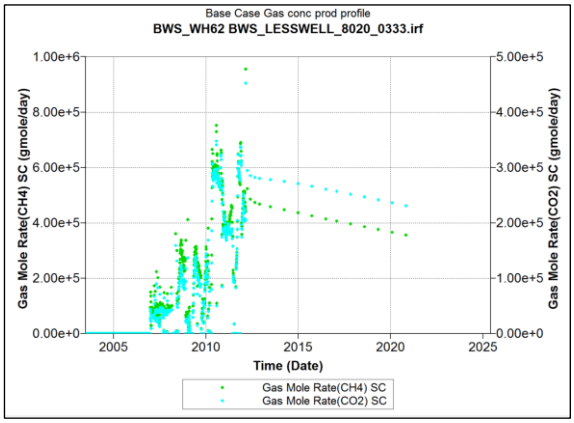

As a main objective of this study, the gas concentration profiles for CH_4 and CO_2 for wells with historic data and wells without production data were predicted after the model is calibrated or history matched using known production data.

5.5 Sensitivity runs with some influenced parameters on simulation results

For the base case run, the properties such as binary ratio for individual components (96:4), adsorbed amounts for total mixture, adsorbed amounts for single component (CH_4 and CO_2), diffusion coefficients and desorption time (days) were included.

It is essential to prove that these parameters and the variation of them will significantly impact on the outcome (CH_4, CO_2 production rate profiles as model output which are indirectly linked to prediction of future gas concentrations) of a particular model.

This section will cover the sensitivity runs of these governing parameters and the comparison of the relevant cases to confirm the importance of these parameters and usage in the simulation tasks.

A simple simulation model with 2-3 wells is applied to test these parameters to save run times and avoid complicating things with some reservoir heterogeneity affecting the results rather than input parameters earlier described.

Well BWS_08 is located in more refined grids formed with refined local grids to show the grid size has not significant impact on the resultant outcomes.

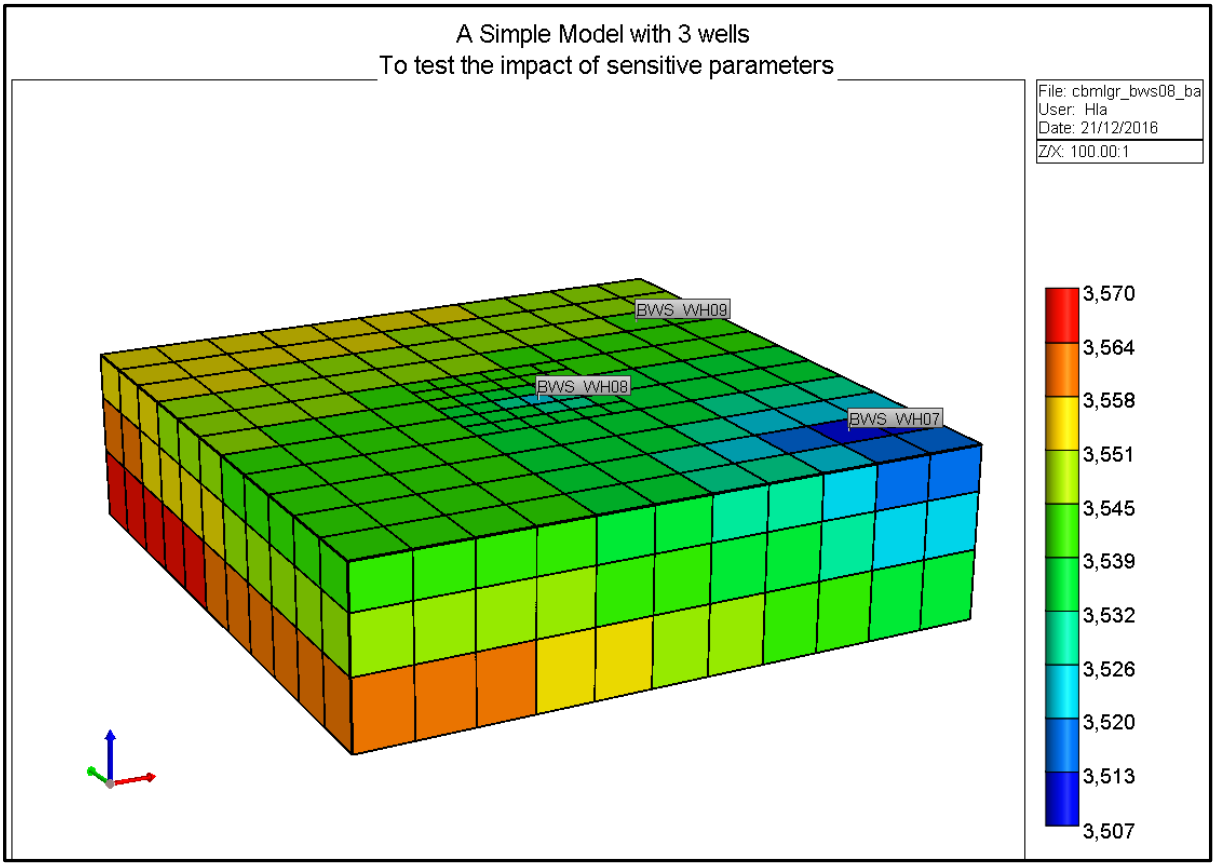

Figure 5-13 Simple simulation model with 3 wells sensitivity study

As a first comparison case, the two cases with different binary ratios (98:2 CH_4:CO_2) and (80:20 CH_4:CO_2). All other input data were kept constant to see the impact of using different binary ratio on the prediction of CO_2 production in long term.

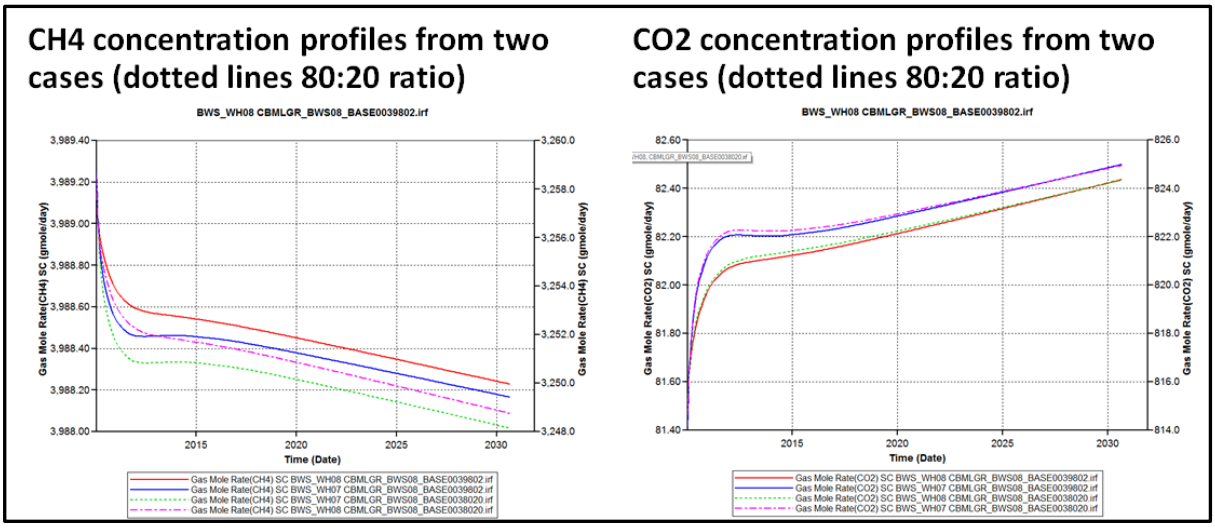

Figure 5-14 CH4 and CO2 concentration profiles without constraints for cases with different Binary ratios (96:4 and 80:20).

The plots shown in the Figure 5-13 are comparison of CH_4 and CO_2 production rates in gmole/d (the rates are compared in order to show the difference of results from using different binary ratio). It is not a direct comparison of gas concentration, but it will give some indicative comparison of both CH_4 and CO_2 production from two different cases (CH_4: CO_2; 98:2 and 80:20 binary ratio). It is not a significant difference but still somewhat measureable.

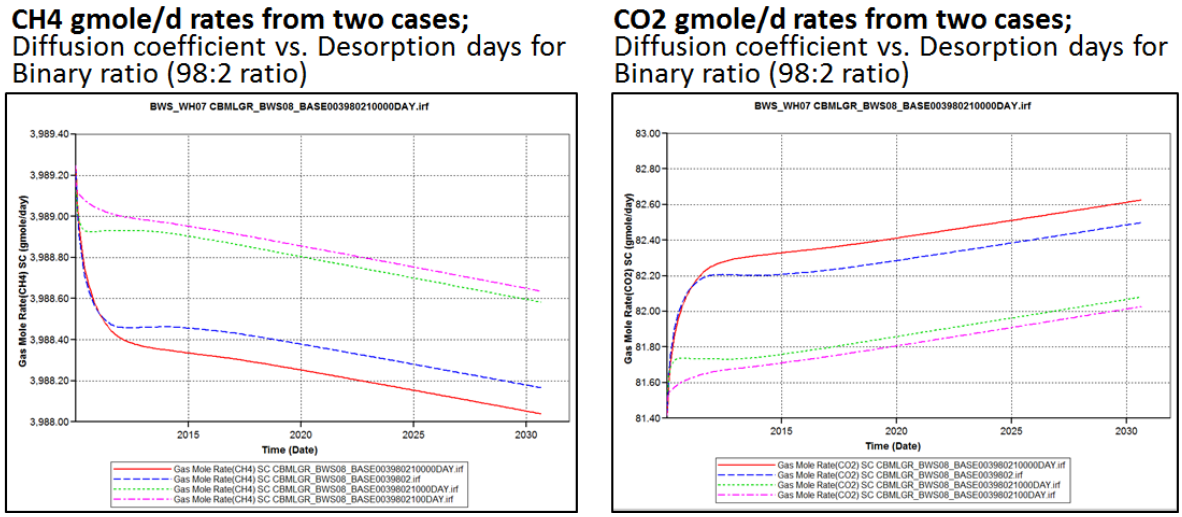

Figure 5-15 Comparison of cases using Diffusion coefficients and Desorption days

Figure 5-14illustrates the importance of using relevant coal diffusivity coefficients to model CO_2 and CH_4 gas concentration profiles more accurately. In the case of using “DAYS” desorption time (100, 1000 days; 10000 days; for CH_4 and CO_2) the resultant production profiles are compared with those from diffusivity coefficient. It is not a compelling case to put a mandate that Desorption days case will be less accurate, rather to show there is some difference in CO_2 prediction (especially if using concentration instead of rate).

In order to make more robust comparison cases for desorption date vs. diffusion coefficient input data the original base case was used with full field scale model. As expected, the results for both CH_4 and CO_2 from desorption time (100 days) and diffusion coefficients were

found significantly different. Both cases were used same gas control history match mode with all other input data kept same (Figure 5.15)

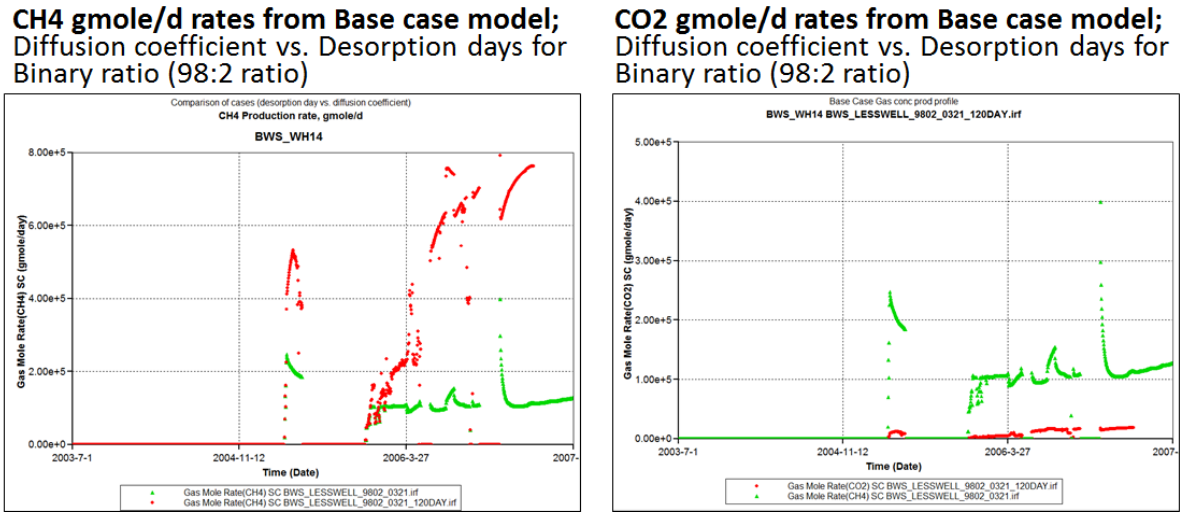

Figure 5-16 Comparison of cases using Diffusion coefficients and Desorption days

Similarly, three cases with different binary ratios (98:2, 96:4, 80:20, CH_4: CO_2) were run to compare the CO_2 production rate (directly relate to concentration). The results show that using different binary ratio as input provides significantly different CO_2 production profiles for three cases.

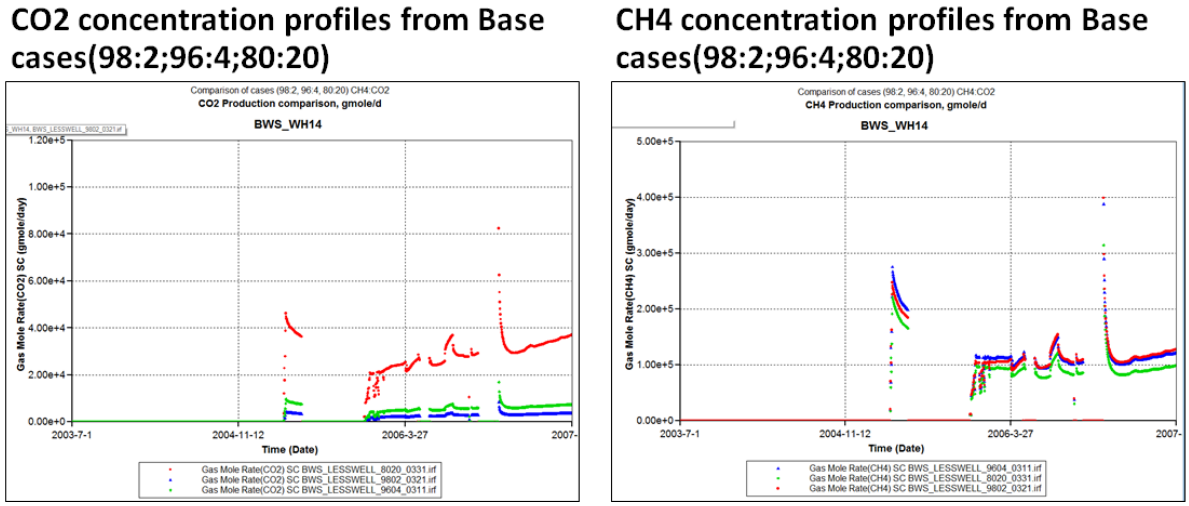

Figure 5-17 CH4 and CO2 concentration profiles cases with Binary ratios (98:2; 96:4 and 80:20).

In conclusion, the importance of using correct ratio of binary component as well as diffusion coefficient instead of using desorption time as random numbers (100 days, 1000 days etc.) could not be underestimated. In fact, it is very critical to use correct binary ratio, adsorbed amount in the input table with representative diffusion coefficient to achieve correct and accurate prediction of CO_2 production either rate or concentration.

5.6 Conclusions and Recommendations

The main objective of this research is to enable in predicting gas concentration profile (for CH_4 and CO_2) coal seams during the dynamically changing reservoir conditions (pressure and saturation changes) due to continuous production for many years.

To achieve this goal, two main input components are required as input in the simulation model. First, Binary Isotherms required to model the adsorbed amounts of binary components, as well as mixed adsorbate with changing pressure condition, is obtained from experimental works and the second input is obtained from historic production data from wells on line for several years. The uncertainty of adsorbed volume of binary components and mixture and the changes with pressure were validated by matching some known data from literature. The results of adsorbed volumes from experiments for binary components and mixture were found acceptable.

Certainly, there are more similar works done in the same field of study. However, most of the research works are concentrated on non-coal (synthetic materials) [16,17,13] .

During the workflow to obtain binary adsorption isotherms with different (CH_4:CO_2) gas ratio using pure gas isotherms in combination with models, there is no issue with getting accurate pure gas isotherms and relate to existing correlations or model to predict adsorption isotherms. However, the accuracy of binary adsorption Isotherm measurements with very low CO_2 is needed some improvement.

A new approach was introduced in predicting gas concentrations using CMG software. The methodology includes usage of diffusivity coefficient to model diffusion instead of using desorption time as input (which varies from 10 – 120 days).

Second input is the amount of adsorbed volume of two components vs. changing reservoir pressure. The input was included in the model as a look up table. The changes of adsorbed amount of mixture in the simulation model is calculated depending upon pressure variations.

Traditional approach in CMG uses pure component isotherms as input to model changing adsorbed volumes with pressure and rely on built in EOS model to calculate amount of adsorbed mixture volumes.

Different binary ratios (maximum 3 ratios) were used to compare the sensitive of binary ratio input data on the prediction of gas concentrations.

In this study, most of data and parameters used in the model are real data with latest available dates, therefore the study may not be absolutely updated with the well performance. Hence prediction of gas concentration profiles may be slightly different (in some cases CO_2 trends may be continue increasing trend, in others stable steady trend).

To prove the difference in modelling gas concentrations trend, diffusion coefficients from actual coal data from the same field were used whereas desorption days are just approximate numbers (normally used as history matching tools).

The base case model is assumed under-saturated or saturated situation with both CH4 and CO2 are in equilibrium to avoid one has preferred sorption option to the other.

For the existence of water in the fracture network as well as matrix, dual porosity and dual permeability model is employed using GEM (Computer modelling group) codes.

To keep same thermodynamic properties of fluids in the model, PR EOS option is selected and some fluids properties are verified against actual binary measurement data from Belsorp unit.

The importance of getting accurate single component isotherms so that accurate parameters can be determined from the model match (using any choice of the models).

The comparison of cases with these different approaches shows some improvement in prediction of gas concentration. However, there is a room for improvement in getting binary adsorption equilibrium and adsorption isotherms using more robust methodology for very low CO2 fields. Present research work laid a good foundation to improve as a reservoir management tool or surveillance tool for CO2 high % production field.

There are new research works similar to current study but none of them is focused on coals and also not intended to prediction of future gas concentration production partly because lack of field data to calibrate the model.

Then it is important to have a good Binary isotherm from the IAS theory or any desired model. These are the input used in the prediction model for gas concentration profiles [47,53,61]

REFERENCES

[1] D.D.C.D. Melo, B.R. Scanlon, Z. Zhang, E. Wendland, L. Yin, Reservoir storage and hydrologic responses to droughts in the Paranï¿½ River basin, south-eastern Brazil, Hydrol. Earth Syst. Sci. 20 (2016) 4673–4688. doi:10.5194/hess-20-4673-2016.

[2] Z. Pan, L.D. Connell, Impact of coal seam as interlayer on CO2 storage in saline aquifers: A reservoir simulation study, Int. J. Greenh. Gas Control. 5 (2011) 99–114. doi:10.1016/j.ijggc.2010.06.012.

[3] N. Ayawei, A.N. Ebelegi, D. Wankasi, Modelling and Interpretation of Adsorption Isotherms, J. Chem. 2017 (2017). doi:10.1155/2017/3039817.

[4] I. Hamawand, T. Yusaf, S.G. Hamawand, Coal seam gas and associated water: A review paper, Renew. Sustain. Energy Rev. 22 (2013) 550–560. doi:10.1016/j.rser.2013.02.030.

[5] R. Barrera, C. Salazar, J.F. Pérez, Thermochemical equilibrium model of synthetic natural gas production from coal gasification using Aspen Plus, Int. J. Chem. Eng. 2014 (2014). doi:10.1155/2014/192057.

[6] M. Mastalerz, A. Drobniak, A. Schimmelmann, Characteristics of Microbial Coalbed Gas during Production; Example from Pennsylvanian Coals in Indiana, USA, Geosciences. 7 (2017) 26. doi:10.3390/geosciences7020026.

[7] P. Guo, Y. Cheng, Permeability prediction in deep coal seam: A case study on the No. 3 coal seam of the southern Qinshui basin in China, Sci. World J. 2013 (2013). doi:10.1155/2013/161457.

[8] J. Drago, The bipore model in solid/liquid extraction: the continuous process, Wärme-Und Stoffübertragung. 20 (1986) 255–261. doi:10.1007/BF01303459.

[9] L. Zhang, J. Selker, A. Qu, A. Velayudhan, Numerical estimation of multicomponent adsorption isotherms in preparative chromatography: Implications of experimental

error, J. Chromatogr. A. 934 (2001) 13–29. doi:10.1016/S0021-9673(01)01297-3.

[10] Y. Zheng, T. Gu, Modified van der Waals equation for the prediction of multicomponent isotherms, J. Colloid Interface Sci. 206 (1998) 457–463. doi:10.1006/jcis.1998.5733.

[11] F.O. Okeola, E.O. Odebunmi, Freundlich and Langmuir isotherms parameters for adsorption of methylene blue by activated carbon derived from Agrowastes, Adv. Nat. Appl. Sci. 4 (2010) 281–288.

[12] M. Belhachemi, F. Addoun, Comparative adsorption isotherms and modeling of methylene blue onto activated carbons, Appl. Water Sci. 1 (2011) 111–117. doi:10.1007/s13201-011-0014-1.

[13] R. Khandanlou, M.B. Ahmad, H.R.F. Masoumi, K. Shameli, M. Basri, K. Kalantari, Rapid adsorption of copper(II) and lead(II) by rice straw/Fe3O4nanocomposite: Optimization, equilibrium isotherms, and adsorption kinetics study, PLoS One. 10 (2015). doi:10.1371/journal.pone.0120264.

[14] F. Mactaggart, L. McDermott, A. Tynan, C.A. Gericke, Exploring the determinants of health and wellbeing in communities living in proximity to coal seam gas developments in regional Queensland, BMC Public Health. 18 (2017). doi:10.1186/s12889-017-4568-1.

[15] P.E. Hardisty, T.S. Clark, R.G. Hynes, Life cycle greenhouse gas emissions from electricity generation: A comparative analysis of australian energy sources, Energies. 5 (2012) 872–897. doi:10.3390/en5040872.

[16] T. Masuda, Peculiar Diffusion Mechanisms within Micropores of Zeolite Catalysts, J. Japan Pet. Inst. 46 (2003) 281–294. doi:10.1627/jpi.46.281.

[17] I.A.W. Tan, B.H. Hameed, Adsorption isotherms, kinetics, thermodynamics and desorption studies of basic dye on activated carbon derived from oil palm empty fruit bunch, J. Appl. Sci. 10 (2010) 2565–2571. doi:10.1016/j.jhazmat.2008.08.025.

[18] H. Cheng, E. Hu, Y. Hu, Impact of mineral micropores on transport and fate of organic contaminants: A review, J. Contam. Hydrol. 129–130 (2012) 80–90. doi:10.1016/j.jconhyd.2011.09.008.

[19] J. Philibert, One and a half century of diffusion: Fick, Einstein, before and beyond, Diffus. Fundam. 4 (2005) 1–19.

[20] J. Busse, J.R. de Dreuzy, S. Galindo Torres, D. Bringemeier, A. Scheuermann, Image processing based characterisation of coal cleat networks, Int. J. Coal Geol. 169 (2017) 1–21. doi:10.1016/j.coal.2016.11.010.

[21] G.K.W. Dawson, J.S. Esterle, Controls on coal cleat spacing, Int. J. Coal Geol. 82 (2010) 213–218. doi:10.1016/j.coal.2009.10.004.

[22] W. Solano-Acosta, M. Mastalerz, A. Schimmelmann, Cleats and their relation to geologic lineaments and coalbed methane potential in Pennsylvanian coals in Indiana, Int. J. Coal Geol. 72 (2007) 187–208. doi:10.1016/j.coal.2007.02.004.

[23] B.P. Muljadi, M.J. Blunt, A.Q. Raeini, B. Bijeljic, The impact of porous media heterogeneity on non-Darcy flow behaviour from pore-scale simulation, Adv. Water Resour. 95 (2016) 329–340. doi:10.1016/j.advwatres.2015.05.019.

[24] J.P. Spivey, K.G. Brown, W.K. Sawyer, J.H. Frantz, Estimating non-Darcy flow coefficient from buildup-test data with wellbore storage, SPE Reserv. Eval. Eng. 7 (2004) 256–269. doi:10.2523/77484-MS.

[25] J.G. Wang, A. Kabir, J. Liu, Z. Chen, Effects of non-Darcy flow on the performance of coal seam gas wells, Int. J. Coal Geol. 93 (2012) 62–74. doi:10.1016/j.coal.2012.01.013.

[26] P.Q. Huy, K. Sasaki, Y. Sugai, S. Ichikawa, Carbon dioxide gas permeability of coal core samples and estimation of fracture aperture width, Int. J. Coal Geol. 83 (2010) 1–10. doi:10.1016/j.coal.2010.03.002.

[27] Z. Ye, D. Chen, J.G. Wang, Evaluation of the non-Darcy effect in coalbed methane production, Fuel. 121 (2014) 1–10. doi:10.1016/j.fuel.2013.12.019.

[28] R. Freij-Ayoub, Opportunities and challenges to coal bed methane production in Australia, J. Pet. Sci. Eng. 88–89 (2012) 1–4. doi:10.1016/j.petrol.2012.05.001.

[29] L. Yuan, Theories and techniques of coal bed methane control in China, J. Rock Mech. Geotech. Eng. 3 (2011) 343–351. doi:10.3724/SP.J.1235.2011.00343.

[30] E.J.P. Jones, M.A. Voytek, M.D. Corum, W.H. Orem, Stimulation of methane generation from nonproductive coal by addition of nutrients or a microbial consortium, Appl. Environ. Microbiol. 76 (2010) 7013–7022. doi:10.1128/AEM.00728-10.

[31] C. Boger, J.S. Marshall, R.C. Pilcher, Worldwide Coal Mine Methane and Coalbed Methane Activities, in: Coal Bed Methane From Prospect to Pipeline, 2014: pp. 351–407. doi:10.1016/B978-0-12-800880-5.00018-8.

[32] C.F. Curtiss, R.B. Bird, Multicomponent Diffusion, Ind. Eng. Chem. Res. 38 (1999) 2515–2522. doi:10.1021/ie9901123.

[33] V. Giovangigli, Multicomponent flow modeling, Sci. China Math. 55 (2012) 285–308. doi:10.1007/s11425-011-4346-y.

[34] N.I.R. Ramzi, S. Shahidan, M.Z. Maarof, N. Ali, Physical and Chemical Properties of Coal Bottom Ash (CBA) from Tanjung Bin Power Plant, in: IOP Conf. Ser. Mater. Sci. Eng., 2016. doi:10.1088/1757-899X/160/1/012056.

[35] W.P. Diamond, S.J. Schatzel, Measuring the gas content of coal: a review, Int. J. Coal Geol. (1998). doi:10.1016/S0166-5162(97)00040-2.

[36] Z. Majewska, G. Ceglarska-Stefańska, S. Majewski, J. Zietek, Binary gas sorption/desorption experiments on a bituminous coal: Simultaneous measurements on sorption kinetics, volumetric strain and acoustic emission, Int. J. Coal Geol. (2009). doi:10.1016/j.coal.2008.09.009.

[37] K. Czerw, Methane and carbon dioxide sorption/desorption on bituminous coal-Experiments on cubicoid sample cut from the primal coal lump, Int. J. Coal Geol. 85 (2011) 72–77. doi:10.1016/j.coal.2010.10.002.

[38] J.C. Pashin, Variable gas saturation in coalbed methane reservoirs of the Black Warrior Basin: Implications for exploration and production, Int. J. Coal Geol. (2010). doi:10.1016/j.coal.2009.10.017.

[39] M. Mastalerz, W. Solano-Acosta, A. Schimmelmann, A. Drobniak, Effects of coal storage in air on physical and chemical properties of coal and on gas adsorption, Int. J. Coal Geol. 79 (2009) 167–174. doi:10.1016/j.coal.2009.07.001.

[40] Y. Jing, R.T. Armstrong, P. Mostaghimi, Digital coal: Generation of fractured cores with microscale features, Fuel. 207 (2017) 93–101. doi:10.1016/j.fuel.2017.06.051.

[41] P.J. Crosdale, B.B. Beamish, M. Valix, Coalbed methane sorption related to coal composition, Int. J. Coal Geol. 35 (1998) 147–158. doi:10.1016/S0166-5162(97)00015-3.

[42] J. Zang, K. Wang, Gas sorption-induced coal swelling kinetics and its effects on coal permeability evolution: Model development and analysis, Fuel. 189 (2017) 164–177. doi:10.1016/j.fuel.2016.10.092.

[43] W.C. Zhu, C.H. Wei, J. Liu, T. Xu, D. Elsworth, Impact of gas adsorption induced coal matrix damage on the evolution of coal permeability, Rock Mech. Rock Eng. 46 (2013) 1353–1366. doi:10.1007/s00603-013-0392-9.

[44] Y. Zhang, M. Lebedev, M. Sarmadivaleh, A. Barifcani, T. Rahman, S. Iglauer, Swelling effect on coal micro structure and associated permeability reduction, Fuel. 182 (2016) 568–576. doi:10.1016/j.fuel.2016.06.026.

[45] P.J.E. Harlick, F.H. Tezel, Adsorption of carbon dioxide, methane, and nitrogen: Pure and binary mixture adsorption by ZSM-5 with SiO2/Al2O3 ratio of 30, Sep. Sci. Technol. 37 (2002) 33–60. doi:10.1081/SS-120000320.

[46] L.F. Gomez, R. Zacharia, P. Bénard, R. Chahine, Multicomponent adsorption of biogas compositions containing CO2, CH4and N2on Maxsorb and Cu-BTC using extended Langmuir and Doong–Yang models, Adsorption. 21 (2015) 433–443. doi:10.1007/s10450-015-9684-6.

[47] A.L. Myers, J.M. Prausnitz, Thermodynamics of mixed-gas adsorption, AIChE J. 11 (1965) 121–127. doi:10.1002/aic.690110125.

[48] J. Chen, L.S. Loo, K. Wang, An ideal absorbed solution theory (IAST) study of adsorption equilibria of binary mixtures of methane and ethane on a templated carbon, J. Chem. Eng. Data. 56 (2011) 1209–1212. doi:10.1021/je101099c.

[49] M. Fechtner, A. Kienle, Efficient simulation and equilibrium theory for adsorption processes with implicit adsorption isotherms – Ideal adsorbed solution theory, Chem. Eng. Sci. 177 (2018) 284–292. doi:10.1016/j.ces.2017.11.028.

[50] A. Seidel, D. Gelbin, On applying the ideal adsorbed solution theory to multicomponent adsorption equilibria of dissolved organic components on activated carbon, Chem. Eng. Sci. 43 (1988) 79–88. doi:10.1016/0009-2509(88)87128-8.

[51] S.J. Allen, G. Mckay, J.F. Porter, Adsorption isotherm models for basic dye adsorption by peat in single and binary component systems, J. Colloid Interface Sci. 280 (2004) 322–333. doi:10.1016/j.jcis.2004.08.078.

[52] K.K.H. Choy, J.F. Porter, G. McKay, Langmuir isotherm models applied to the multicomponent sorption of acid dyes from effluent onto activated carbon, J. Chem. Eng. Data. 45 (2000) 575–584. doi:10.1021/je9902894.

[53] Ji-Quan Shi, S. Durucan, Gas storage and flow in coalbed reservoirs: implementation of a bidisperse pore model for gas diffusion in coal matrix , SPE Reserv. Eval. Eng. 8 (2005) 169–175. doi:10.2118/84342-pa.

[54] D.M. Smith, F.L. Williams, Diffusion models for gas production from coals. Application to methane content determination, Fuel. 63 (1984) 251–255. doi:10.1016/0016-2361(84)90046-2.

[55] W. Zhao, Y. Cheng, H. Jiang, H. Wang, W. Li, Modeling and experiments for transient diffusion coefficients in the desorption of methane through coal powders, Int. J. Heat Mass Transf. 110 (2017) 845–854. doi:10.1016/j.ijheatmasstransfer.2017.03.065.

[56] G. Wang, T. Ren, Q. Qi, L. Zhang, Q. Liu, Prediction of Coalbed Methane (CBM) Production Considering Bidisperse Diffusion: Model Development, Experimental Test, and Numerical Simulation, Energy and Fuels. 31 (2017) 5785–5797. doi:10.1021/acs.energyfuels.6b02500.

[57] M. Pillalamarry, S. Harpalani, S. Liu, International Journal of Coal Geology Gas diffusion behavior of coal and its impact on production from coalbed methane reservoirs, Int. J. Coal Geol. 86 (2011) 342–348. doi:10.1016/j.coal.2011.03.007.

[58] M. Kudasik, N. Skoczylas, A. Pajdak, The repeatability of sorption processes occurring in the coal-methane system during multiple measurement series, Energies. 10 (2017). doi:10.3390/en10050661.

[59] G. Wang, T. Ren, Q. Qi, J. Lin, Q. Liu, J. Zhang, Determining the diffusion coefficient of gas diffusion in coal: Development of numerical solution, Fuel. 196 (2017) 47–58. doi:10.1016/j.fuel.2017.01.077.

[60] C. Qiao, L. Li, R.T. Johns, J. Xu, Compositional Modeling of Dissolution-Induced Injectivity Alteration During CO2 Flooding in Carbonate Reservoirs, SPE J. (2016) 809–826. doi:10.2118/170930-MS.

[61] S.C. Blair, J.G. Berryman, Permeability and Relative Permeability in Rocks, Int. Geophys. 51 (1992) 169–186. doi:10.1016/S0074-6142(08)62822-3.

[62] M. Mastalerz, H. Gluskoter, J. Rupp, Carbon dioxide and methane sorption in high volatile bituminous coals from Indiana, USA, Int. J. Coal Geol. 60 (2004) 43–55. doi:10.1016/j.coal.2004.04.001.

[63] J.E. Warren, P.J. Root, E. Warren, The Behavior of Naturally Fractured Reservoirs, SPE J. 3 (1963) 245–255. doi:10.2118/426-PA.

[64] J.E.E. Warren, The Behavior of Naturally Fractured Reservoirs, Soc. Pet. Eng. J. 3 (1963) 245–255. doi:10.2118/426-PA.

[65] A.J. Jadhav, V.C. Srivastava, Adsorbed solution theory based modeling of binary adsorption of nitrobenzene, aniline and phenol onto granulated activated carbon, Chem. Eng. J. 229 (2013) 450–459. doi:10.1016/j.cej.2013.06.021.

Appendix A

Formula derivation for Bi-pore model accounted for micro-meso pore interactions

Mass Balance in macropore

$$\varepsilon_m \frac{dC_m}{dt} = \frac{1}{r^2}\frac{d}{dr}\left[r^2 D'_{mo}\frac{dC_m}{dr}\right] - \left[\frac{dC_\mu}{dt}\right](1-\varepsilon_m)$$

Assume Instantaneous filling of micropores from macropores

$$\frac{dC_\mu}{dt} = \frac{dC_\mu}{dC_m}\frac{dC_m}{dt} \quad \text{(Chain Rule)}$$

$$\varepsilon_m \frac{dC_m}{dt} + (1-\varepsilon_m)\frac{dC_m}{dt}\frac{dC_\mu}{dC_m} = \frac{1}{r^2}\frac{d}{dr}\left[r^2 D'_{mo}\frac{dC_m}{dr}\right]$$

$$\frac{dC_m}{dt}\left[\varepsilon_m + (1-\varepsilon_m)\frac{dC_\mu}{dC_m}\right] = \frac{1}{r^2}\frac{d}{dr}\left[r^2 D'_{mo}\frac{dC_m}{dr}\right]$$

$$C_\mu = \frac{q_m b C_m}{1 + bC_m}$$

Concentration change btw micropore and macropore can be described

$$\frac{dC_\mu}{dC_m} = q_m b C_m\left[\frac{-b}{(1+bC_m)^2}\right] + \frac{1}{1+bC_m}q_m b$$

$$= \frac{-q_m b^2 C_m + q_m b(1+bC_m)}{(1+bC_m)^2}$$

$$\frac{dC_\mu}{dC_m} = \frac{-q_m b^2 C_m + q_m b + q_m b^2 C_m)}{(1+bC_m)^2} = \frac{q_m b}{(1+bC_m)^2}$$

$$\left[\varepsilon_m + (1-\varepsilon_m)\,\frac{q_m b}{(1+bC_m)^2}\right]\frac{dC_m}{dt} = \frac{1}{r^2}\frac{d}{dr}\left[r^2 D'_{mo}\frac{dC_m}{dr}\right]$$

$$\left[\varepsilon_m + (1-\varepsilon_m)\,\frac{q_m b}{(1+bC_m)^2}\right]\frac{dC_m}{dt} = \frac{D'_{mo}}{r^2}\left[2r\frac{dC_m}{dr} + r^2\frac{d^2C_m}{dr^2}\right]$$

$$\left[\varepsilon_m + (1-\varepsilon_m)\,\frac{q_m b}{(1+bC_m)^2}\right]\frac{dC_m}{dt} = D'_{mo}\frac{d^2C_m}{dr^2} + \frac{2}{r}D'_{mo}\frac{dC_m}{dr}$$

Bulk Equation

$$V_p\frac{dC_b}{dt} = \frac{-3}{R_p}\,\frac{m}{\rho_p}D'_{mo}\frac{dC_m}{dr}\Big|R$$

Boundary conditions

a) Centre of particles

$$\frac{dC_m}{dt} = 0$$

$$\left[\varepsilon_m + (1-\varepsilon_m)\,\frac{q_m b}{(1+bC_m)^2}\right]\frac{dC_m}{dt} = 3D'_{mo}\frac{d^2C_m}{dr^2}$$

b) Surface of particles

$$\frac{dC_m}{dr} = \frac{C_m^* - C_{m-1}}{2\Delta r}$$

$$\frac{d^2C_m}{dr^2} = \frac{C_m^* - 2C_m + C_{m-1}}{2\Delta r^2}$$

Appendix A (continued)

MATLAB Code for Bi-dispersed model

```
% To model bipore diffusion process (micropores and macropores)
% consider the particles contains two types of pores, other conditions are
% same, to assign micro and macro porosity to the particles
% Change the code for unipore model



function Santos_BG2_30deg_bipore

load ASAPexp_BG2_30.dat
t_exp=ASAPexp_BG2_30(:,1);       % time s
ads_exp=ASAPexp_BG2_30(:,2);    % mol/m3 adsorbed gas concentration

load Data_BG2_30.dat

V=Data_BG2_30(1)*1e-6;    % Free space m3
P=Data_BG2_30(2);          % Cell pressure mmHg
Temp=Data_BG2_30(3);          % Temp K
mp=Data_BG2_30(4);         % Mass of sample g
Pold=Data_BG2_30(5);       % Old equilibrium pressure before start of this test
mmHg

% All input parameters

R = 160e-6;    %Particle radius, m
Np= 30;       %A Spherical shaped particle is subdivided into 30 equally
delr = R/Np;  %radius of individual sections, r1, r2, r3,...  r31, m
MolWt= 16;  % MolWt for Methane, g
epsp= 0.3258; %porosity may change to two porosity for micro and macro
rho= 1.5477*1e6*(1-epsp); % 1.0435 g/m^3 particle density

Rgas= 62.363E-3; % Gas Constant value, mmHg K m^3/mol

%%%%%%%%%%%%%%%%%%%%%%%%%%%%%%%%%%%%%%%%%%%%%%%%%%%%%%%%%%%%%%%%%%%%%%%%%%%%

% qAm = 453.8680;   % mol/m^3, Langmuir max conc in micropore
% EAm= 1.8265073+04;  % J/mol Micro
% bm=(3.92053995e-6*exp((-EAm/(Rgas*Temp))));       % m3/mol langmuir pressure
constant micropore
%
% qAmo = 0.628392013;   % mol/m^3, Langmuir max conc mesopore
% EAmo= 85.252602; %J/mol Meso
% bmo=(0.4306331*exp((-EAmo/(Rgas*Temp))));     % m3/mol langmuir pressure
constant mesopore

%new parameters


qAm = 5.563499697365191e+02;   % mol/m^3, Langmuir max conc in micropore
EAm= 1.822936790521974e+04;  % J/mol Micro
bm=(3.038535432771275e-06*exp((-EAm/(Rgas*Temp))));       % m3/mol langmuir
pressure constant micropore

qAmo =  2.220556544435218;   % mol/m^3, Langmuir max conc mesopore
EAmo= 5.582569743563221e+03; %J/mol Meso
bmo=(0.057508199598658*exp((-EAmo/(Rgas*Temp))));     % m3/mol langmuir pressure
constant mesopore
```

```
%micro and macro paramters swap to see the match different??
% qAm =0.628392013;    % mol/m^3, Langmuir max conc in micropore
% EAm= 85.252602; % J/mol Micro
% bm=(0.4306331*exp((-EAm/(Rgas*Temp))));       % m3/mol langmuir pressure
constant micropore
%
% qAmo = 453.8680;    % mol/m^3, Langmuir max conc mesopore
% EAmo=  1.8265073+04; %J/mol Meso
% bmo=(3.92053995e-6*exp((-EAmo/(Rgas*Temp))));     % m3/mol langmuir pressure
constant mesopore

%%%%%%%%%%%%%%%%%%%%%%%%%%%%%%%%%%%%%%%%%%%%%%%%%%%%%%%%%%%%%%%%%%%%%%%%%%%%

r=(0:delr:R);  %arrange radial section from 0; 2.667e-5, 5.333e-5,...

Cbulk_old = Pold/(Rgas*Temp);    %mol/m^3 Bulk Gas conc b4 CH4 dosing
Cbulk_init= P/(Rgas*Temp);  %Bulk Gas conc after CH4 dosing, Initial G conc

%************************************************************************
T = 5000; %intend to run the model ; 3000 sec, this can be altered
delt=10;   % 10 sec interval will be used to advance the simulation

tspan=(0:delt:T);

for i=1:Np+1
    Cinit(i)=qAm*bm*Cbulk_old/(1+bm*Cbulk_old); % Par Ini Con 16.498 mol/m^3
end

for i=Np+2:2*Np+2
    Cinit(i)=qAmo*bmo*Cbulk_old/(1+bmo*Cbulk_old); % Par Ini Con 16.498 mol/m^3
end

Cinit(2*Np+3)= Cbulk_init; %Ini Bulk Gas conc in the tank, mol/m^3


[t,C]=ode15s(@(t,C)CH4biporefun02(t,C,Np,R,mp,rho,epsp,V,qAm,bm,qAmo,bmo),tspan,Ci
nit);

Cg=C(:,2*Np+3);             % Cg is Cbulk at 2*Np+2,(63) (outside)
Cmi=C(:,1:Np+1);            % Cpar is 1=> Np+1; (31) (surface)
Cmo=C(:,Np+2:2*Np+2);       % Cmo, macro conc, i=> Np+2,(32) => 2*Np+2,(62) mol/m^3


%
[t,C]=ode15s(@(t,C)CH4biporefun02(t,C,Np,R,mp,rho,epsp,V,qAm,bm,qAmo,bmo),tspan,Ci
nit);

for i=1:(T/delt+1)           %delt = 100, therefore, starts i=1,101,201..

Molads(i)=V*(Cg(1)-Cg(i));     %Ads amount (mol)= Tank_Vol*(change in Cbulk)

end

Mads=Molads*MolWt;     %Ads amount (mass) in g

Mads_Coal=Mads/mp;      % Amount adsorbed per gram of coal [g CH4/g coal]

for i=1:(T/delt+1)
    N_molads(i)= (Molads(i)-Molads(1))/(Molads(T/delt+1)-Molads(1));
```

```
end
%
% figure(1),plot(t,Cmi(:,1));
% title('CH4 conc in micro centre spherical layer vs time')
% xlabel('time  sec')
% ylabel('CH4 conc mole/m^3')

% figure(2),plot(t,Cmo(:,1));
% title('CH4 conc in macro centre spherical layer vs time')
% xlabel('time  sec')
% ylabel('CH4 conc mole/m^3')

% figure(3),plot(t,Cmi(:,Np+1));
% title('CH4 conc in micro outermost spherical layer vs time')
% xlabel('time  sec')
% ylabel('CH4 conc mole/m^3')

% figure(4),plot(t,Cmo(:,Np+1));
% title('CH4 conc in macro outermost spherical layer vs time')
% xlabel('time  sec')
% ylabel('CH4 conc mole/m^3')

%  figure(5),plot(r,Cmi(301,1:Np+1));
%  title('CH4 conc in micro all layers vs particle interface')
%  xlabel('radius "r"  cm')
%  ylabel('CH4 conc mole/m^3')

%  figure(6),plot(r,Cmo(301,1:Np+1));
%  title('CH4 conc in macro all layers vs particle interface')
%  xlabel('radius "r"  cm')
%  ylabel('CH4 conc mole/m^3')


% figure(7),plot(t,N_molads);
% title('Normalised CH4 adsorbed vs time')
% xlabel('time  sec')
% ylabel('CH4 amt g')
figure (8),plot(t_exp,ads_exp,'.',t,N_molads);
title('CH4 adsorbed per coal mass unit vs time')
xlabel('time  sec')
ylabel('g CH4/g coal expt and model')
figure (9),plot(t_exp,ads_exp_abs,'.',t,Mads_Coal);
title('CH4 adsorbed per unit coal mass (g/g)(Lab data) vs time')
xlabel('time  sec')
ylabel('ads CH4 g/g coal expt and model')

figure(10),surf(r,t,Cmi);
title('CH4 ads amount in all radius, all layers')
end

function dCdt=CH4biporefun02(t,C,Np,R,mp,rho,epsp,V,qAm,bm,qAmo,bmo)

%Data
% Dm = 1.10450e-13;  %Diffusivity coeff for particle micropore size m2/sec
% Dmo = 1.042095e-12;  %Diffusivity coeff for particle macropore size m2/sec
Dmo = 1.10450e-12;  %Diffusivity coeff for particle micropore size m2/sec
Dm = 1.042095e-12;  %Diffusivity coeff for particle macropore size m2/sec
delr=R/Np;      %thickness of radial section (donut section);r2= 2.6667e-6m
r=(0:delr:R);  %arrange radial section from 0; 2.667e-5, 5.333e-5,...

%N=total number of particles;  %total volume/a particle volume
%Volume=sample mass/coal density; % sample volume calcuated, in m^3;
```

```
N= (mp/rho)/(4/3*pi()*R^3);    % number of particles will be obtained from


for i=1:2*Np+3
    if i==1
        d2Cdr2=(2*C(i+1)-2*C(i))/delr^2;  % using Symmetry BC, L'Hospital rule
        dCdr=0;                              % dCdr gives indeterminant (0.0/0.0)
        dCdt(i)=(3*Dm*d2Cdr2);              % lim r=> 0.0 gives (dC/dr)/r =>
d2Cdr2**

    end

    if(1<i)&&(i<Np+1)
        d2Cdr2=(C(i+1)-2*C(i)+C(i-1))/delr^2;
        dCdr=(C(i+1)-C(i-1))/(2*delr);
        dCdt(i)=(Dm*d2Cdr2+2*(Dm/r(i))*dCdr);

    end

    if i==Np+1
        d2Cdr2=((qAm*bm*C(i+1)/(1+bm*C(i+1)))-2*C(i)+C(i-1))/delr^2;
        dCdr=((qAm*bm*C(i+1)/(1+bm*C(i+1)))-C(i-1))/(2*delr);
        dCdt(i)=(Dm*d2Cdr2+2*(Dm/r(i))*dCdr);
    end


    if i==Np+2
        d2Cdr2=(2*C(i+1)-2*C(i))/delr^2;  % using Symmetry BC, L'Hospital rule
        dCdr=0;                              % dCdr gives indeterminant (0.0/0.0)
        dCdt(i)=(3*Dmo*d2Cdr2);             % lim r=> 0.0 gives (dC/dr)/r =>
d2Cdr2**
    end


    if ((Np+2)<i)&&(i<(2*Np+2))
        d2Cdr2=(C(i+1)-2*C(i)+C(i-1))/delr^2;
        dCdr=(C(i+1)-C(i-1))/(2*delr);
        dCdt(i)=(Dmo*d2Cdr2+2*(Dmo/r(i-31)*dCdr));
     end

    if i==2*Np+2
        d2Cdr2=((qAmo*bmo*C(i+1)/(1+bmo*C(i+1)))-2*C(i)+C(i-1))/delr^2;
        dCdr=((qAmo*bmo*C(i+1)/(1+bmo*C(i+1)))-C(i-1))/(2*delr);
        dCdt(i)=(Dmo*d2Cdr2+2*(Dmo/r(i-31))*dCdr);
    end


    if i==2*Np+3
        dCdrmi =(C(Np+1)-C(Np-1))/(2*delr);  % need to do full jump, then 2delr
        dCdrmo =(C(2*Np+2)-C(2*Np))/(2*delr);  %
       % dCdt(i)=-(D/V)*dCdr*4*pi()*(R^2)*epsp*N; % to be consistent with above
all
        dCdt(i)=(-(Dm/V)*dCdrmi*4*pi()*(R^2)*N)+(-(Dmo/V)*dCdrmo*4*pi()*(R^2)*N);
% to be consistent with above all
    end
end
dCdt=dCdt';
end
```

ISOTHERMS DATA AND FITTED PARAMETERS FROM LANGMUIR MODEL

Santos Sample and Data		MATLAB	MATLAB	MATLAB model used
		qAm	bm	
		mmol/g	m3/mol	
Isotherm data	1082			
	30 degC	0.3410	0.0062	LANGMUIR
	50 degC	0.3542	0.0037	
	70 degC	0.5386	0.0017	
Isotherm data	100458			
	30 degC	0.2570	0.0078	LANGMUIR
	50 degC	0.0924	0.0132	
	70 degC	0.0734	0.0142	
BG Samples Isotherms				
Isotherm data	BG2			
	30 degC	0.3693	0.0076	LANGMUIR
	50 degC	0.3112	0.0057	
	70 degC	0.2507	0.0045	
Isotherm data	BG3			
	30 degC	0.2651	0.0059	LANGMUIR
	50 degC	0.0991	0.0084	
	70 degC	0.0598	0.0112	

ISOTHERMS DATA MEASURED IN THE LAB USING ASAP 2020 VOLUMETRIC EQUIPEMENT